

Universidade do Minho  
Escola de Ciências

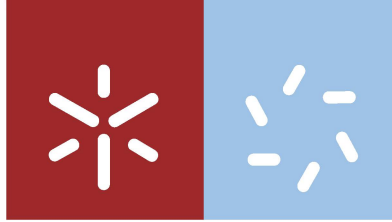
Magda Alexandra Pereira de Barros

**Development of Electrochemical DNA-based sensors and  
Immunoassays for Lipid Transfer Protein Allergen Detection  
in Tomato Seeds**

Magda Alexandra Pereira de Barros  
**Development of Electrochemical DNA-based sensors and Immunoassays  
for Lipid Transfer Protein Allergen Detection in Tomato Seeds**

UMinho | 2018

December 2018



**Universidade do Minho**  
**Escola de Ciências**

Magda Alexandra Pereira de Barros

**Development of Electrochemical DNA-based sensors and  
Immunosensors for Lipid Transfer Protein Allergen Detection  
in Tomato Seeds**

Master thesis

Master in Biophysics and Bionanosystems

Supervisors:

**Doctor João Miguel Ferreira da Rocha**

**Doctor Maria de Fátima de Sá Barroso**

## Declaration

**Name:** Magda Alexandra Pereira de Barros

**E-mail:** [Maguipb.94@gmail.com](mailto:Maguipb.94@gmail.com)

**Citizen card number:** 14956634

**Master's Dissertation Title:**

" Development of Electrochemical Genosensors and Immunosensors for Lipid Transfer Protein Allergen Detection in Tomato Seeds"

**Supervisors:**

Doctor João Miguel Ferreira da Rocha

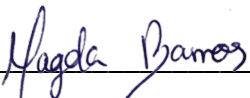
Doctor Maria de Fátima de Sá Barroso

**Conclusion year:** 2018

**Master's Degree:** Biophysics and Bionanosystems

PARTIAL REPRODUCTION OF THIS DISSERTATION IS AUTHORIZED ONLY FOR THE PURPOSES OF INVESTIGATION, BY WRITING DECLARATION OF THE INTERESTED PARTY, WHICH COMMITMENT.

University of Minho, December 18, 2018

**Signature:**  \_\_\_\_\_

## ACKNOWLEDGEMENTS

First of all, I would like to thank to my mother and brother for supporting me in those days with more stress and bad mood. Without them this adventure would never be made.

Thank you to the Grupo de Electroanálisis y (Bio)sensores Electroquímicos (GEBE) group of the Universidad Complutense de Madrid (UCM), Madrid, Spain, for all the unconditional help, knowledge and kindness given. It was a great pleasure to meet you and, above all, to work with all of you. In special to Dr. Susana Campuzano for giving me all the support needed and the chance to work with her research group.

I would also like to thank my supervisor, Dr. Fátima Barroso for all the support and help given during the preparatory advanced training prior the Erasmus +, in this process of writing the thesis and for being always kind to me.

To the “*Amigolas*”, “*Gordas*” and all of my friends for being always there whenever I needed and for the relaxation moments. Cheers to our friendship.

I am also grateful to be the godmother of my “*bicho pequeno*” Miguel, who contributed to my happiness while I was working on the thesis.

I would like to thank the International Relations Office for granting me the Erasmus+ scholarship that allowed me to perform the laboratorial work in the University Complutense of Madrid. Finally, I am very grateful to the Instituto Superior de Engenharia do Porto (ISEP), Porto, Portugal, and, also to the host institution – the Department of Biology (DB) from the University of Minho (UMinho), Braga, Portugal, where the curricular unit of Master’s Project was designed and the dissertation was developed. Also a thanks to the host research centers, the Rede de Química e Tecnologia (REQUIMTE) from ISEP, and the Centro de Biologia Molecular e Ambiental (CBMA) from DB-UMinho.

## **Development of Electrochemical Genosensors and Immunosensors for Lipid Transfer Protein Allergen Detection in Tomato Seeds**

### **ABSTRACT**

In Mediterranean areas tomato allergy has been dramatically increasing and cross-reactive with other fruit allergies because of the similar protein structure between them. Sola I 7 belongs to the non-specific lipid transfer proteins family and is the major allergen in tomato seeds – being one of the key allergens related with several allergic symptoms namely anaphylaxis. To improve food safety, biosensors have become an excellent device for (bio)chemical analysis, specially the electrochemical biosensors which compete with conventional analytical methodologies.

This thesis reports the development of 2 new setups of electrochemical DNA-based sensors for sola I 7 DNA detection, and a new electrochemical immunosensor for sola I 7 protein detection and the implementation of these two procedures in a dual biosensor for simultaneous detection.

Functionalized magnetic beads (MBs) was used as immobilization platform for electrochemical DNA-based sensor (DNA magnetobiosensor) and immunosensor (magnetoimmunosensor). The implementation of screen-printed carbon electrodes (SPCEs) as transducer and MBs makes these approaches more attractive because of the increased sensitivity, reduced time of analysis and minimization of matrix effects.

A limit of detection (LOD) of 0.2 pM was obtained for the DNA magnetobiosensor whereas a LOD of 1.4  $\mu\text{g mL}^{-1}$  was obtained in the magnetoimmunosensor. Both approaches were tested in real food extracts without previous amplification or preconcentration of the genetic/protein material – which makes from them reliable and promising analytical tools for food safety and consumer protection.

**Key-words:** Electrochemical biosensors. Magnetic Beads. Sola I 7. Tomato seeds allergy. Amperometry. Sandwich format. Screen-printed carbon electrodes. Food Safety.

# **Desenvolvimento de Genossensores e Imunossensores Eletroquímicos para a Detecção do Alérgeno Proteínas Transportadoras de Lípidos nas Sementes do Tomate**

## **RESUMO**

Nas áreas mediterrânicas, a alergia ao tomate tem aumentado dramaticamente e é reativa, de forma cruzada, com outras alergias a frutas pela similaridade entre as proteínas. A proteína Sola I 7 pertence à família das proteínas transportadoras de lípidos não específicas e é o principal alérgeno nas sementes do tomate, sendo um dos principais componentes relacionados com vários sintomas alérgicos graves, nomeadamente a anafilaxia. A fim de melhorar a segurança alimentar, os biossensores tornaram-se um excelente dispositivo para análise química e biológica, especialmente os biossensores eletroquímicos que competem com os procedimentos analíticos convencionais.

Esta tese descreve o desenvolvimento de dois novos formatos de sensores eletroquímicos baseados em DNA para a deteção do DNA *sola 7*, um novo imunossensor eletroquímico para deteção da proteína *sola 7* e a implementação destes dois procedimentos num biossensor duplo para determinação simultânea das duas biomoléculas.

As partículas magnéticas funcionalizadas (MB) têm sido utilizadas como plataforma de imobilização no desenvolvimento do sensor eletroquímico de DNA eletroquímico (magnetogenossensor) e imunossensor (magnetoimunossensor). O uso de elétrodos de serigrafados de carbono (SPCEs) como transdutor e de MBs tornam estas abordagens mais atrativas devido à maior sensibilidade, menor tempo de análise e minimização dos efeitos de matriz.

Obteve-se um limite de deteção (LOD) de 0,2 pM no magnetogenossensor, ao passo que no magnetoimunossensor foi de 1,4  $\mu\text{g mL}^{-1}$ . Ambas as abordagens foram testadas em extratos alimentares reais, sem amplificação prévia ou pré-concentração do material genético/proteico, o que confere a estas ferramentas analíticas confiança e serem promissoras para a segurança alimentar e proteção ao consumidor.

**Palavras-chave:** Biossensores eletroquímicos. Partículas Magnéticas. Sola I 7. Alergia a sementes de tomate. Amperometria. Formato sanduíche. Elétrodos de carbono impressos em tela. Segurança alimentar.

# TABLE OF CONTENTS

<b>ACKNOWLEDGEMENTS</b> .....	<b>III</b>
<b>ABSTRACT</b> .....	<b>IV</b>
<b>RESUMO</b> .....	<b>V</b>
<b>ABBREVIATIONS</b> .....	<b>VIII</b>
<b>INDEX OF TABLES</b> .....	<b>IX</b>
<b>INDEX OF FIGURES</b> .....	<b>X</b>
<b>1 Scope of the thesis</b> .....	<b>14</b>
1.1 Aims of the thesis.....	15
1.2 Outline of the thesis.....	15
<b>2 Literature review</b> .....	<b>17</b>
2.1 Introduction.....	17
2.2 Food Safety.....	18
2.2.1 Food allergy .....	18
2.2.2 Lipid transfer proteins .....	20
2.2.3 Conventional methods for allergens analysis .....	21
2.3 Biosensors .....	22
2.3.1 Immobilization strategies.....	25
2.3.2 Electrochemical DNA magnetobiosensors .....	29
2.3.3 Electrochemical magnetoimmunosensors .....	29
2.4 Amplification strategies for electrochemical biosensors.....	30
2.4.1 Amplification strategies based on a rational design of the electrode surface.....	30
2.4.2 Amplification strategies based on the use of nanomaterials .....	34
2.4.3 Nucleic acid-based amplification strategies .....	36
2.4.4 Enzyme-based electrochemical strategies .....	37
2.4.5 Quantum dots-based electrochemical strategies.....	39
<b>3 Development of an electrochemical DNA biosensor for <i>Sola I 7</i> determination</b> .....	<b>42</b>
3.1 Introduction.....	42
3.2 Material and Methods.....	44
3.2.1 Apparatus and electrodes .....	44
3.2.2 Chemicals and solutions.....	45
3.2.3 Construction of the amperometric DNA sensor.....	46
3.2.4 Amperometric measurements .....	47
3.3 Results and Discussion.....	48
3.3.1 Selection of oligonucleotide sequences for the DNA sensor construction.....	48
3.3.2 Optimizations of the Experimental Conditions.....	49
3.3.3 Analytical characteristics of the electrochemical DNA sensor .....	56
3.3.4 Application of the DNA sensor genosensor to detect <i>Sola I 7</i> in tomato samples .....	60
3.3. Conclusions .....	61
<b>4 Development of a magnetoimmunosensor and dual magnetobiosensor for <i>Sola I 7</i> determination</b> <b>63</b>	
4.1 Introduction.....	63
4.2 Material and Methods.....	65
4.2.1 Apparatus and electrodes .....	65
4.2.2 Chemicals and solutions.....	66

4.2.3	Construction of the amperometric immunosensor .....	67
4.2.4	Amperometry measurements .....	68
4.3	Results and Discussion.....	68
4.4	Optimizations of the experimental conditions.....	69
4.4.1	Analytical characteristics of the immunosensor .....	73
4.4.2	Application of immunosensor to detect Sola I 7 in tomato seeds samples .....	76
4.5	Dual magnetobiosensor for simultaneous determination of Sola I 7 protein and <i>sola</i> / 7 DNA .....	77
4.6	Conclusions .....	80
<b>5</b>	<b>General conclusions and future prospective .....</b>	<b>81</b>
5.1	General conclusions .....	81
5.2	Future prospective.....	81
<b>6</b>	<b>References .....</b>	<b>83</b>



## ABBREVIATIONS

**aM:** Attomolar

**AN:** Acupuncture needle

**anti-solal7-HRP:** Antibody-HRP complex for solal7 recognition

**AuNPs:** Gold nanoparticles

**BQ:** Benzoquinone

**CP:** Coat proteins

**cp-anti-solal7:** Capture antibody for solal7 recognition

**CTAB:** Hexadecyl trimethyl-ammonium bromide

**DNA:** deoxynucleic acid

**DOX:** Doxorubicin

**DPV:** Differential pulse voltammetry

**EAST:** Enzyme allegrosorbent test

**ECL:** Electrochemiluminescence

**EDC:** Carbodiimide

**ELISA:** Enzyme-linked immunosorbent assay

**fM:** femto molar

**GMO:** Genetically modified organism

**GO:** Graphene oxide

**GOD:** glucose oxidase

**GR:** Graphene

**HDA:** Helicase-dependent isothermal amplification

**HQ:** hydroquinone

**HRC:** Hybridization chain reaction

**HRM:** High-resolution melting analysis

**HRP:** Horseradish peroxidase

**Ig:** Immunoglobulin

**IUPAC:** International Union of Pure and Applied Chemistry

**kDa:** kilodalton

**LOD:** Limit of detection

**LOQ:** Limit of quantification

**LR:** Linear range

**LTP:** Lipid transfer protein

**MBs:** Magnetic beads

**MNP:** Magnetic nanoparticle

**MPN:** Mesoporous Pt nanospheres

**MWCNT:** Multi-walled carbon nanotube

**NHS:** N-hydroxysuccinimide

**nM:** Nanomolar

**NP:** Nanoparticle

**NR:** Nanorod

**nsLTP:** Non-specific lipid transfer protein

**PCR:** Polymerase chain reaction

**pM:** Pico-molar

**PR:** Pathogenesis-related protein

**ProtA:** Protein A

**QD:** Quantum dot

**RAST:** Radioallergosorbent test

**RNA:** Ribonucleic acid

**RNA-bCp:** Biotinylated RNA capture probe

**RNA-bDp:** Biotinylated RNA detector probe

**S/B:** Signal to blank ratio

**SAM:** Self-assembled monolayer

**SDS:** sodium dodecyl sulphate

**SPCE:** Screen-printed carbon electrode

**SPE:** Screen-printed electrode

**ssDNA:** single-strand deoxynucleic acid

**Strep-:** Streptavidine

**TMB:** 3,3',5,5'-tetramethylbenzidine

**UV:** Ultra violet

## INDEX OF TABLES

<b>Table 1.</b> Some relevant families of allergens in food [18–20].	19
<b>Table 2.</b> Advantages and drawbacks of the five basic immobilization methods. Adapted from Salazar (2016) [70]	26
<b>Table 3.</b> Examples of amplification strategies based on a rational design and enzymatic label [105], [107], [108], [109], [110], see in the table	33
<b>Table 4.</b> Examples of electrochemical transduction strategies using nanomaterials [123], [127], [108], [128], [124]	41
<b>Table 5.</b> Oligonucleotides used for the electrochemical DNA sensor development	46
<b>Table 6.</b> Optimization of the experimental variable	57
<b>Table 7.</b> Analytical characteristics obtained for the determination of LTPs using ProtA-HRP or AntiIgG-HRP as enzymatic label	58
<b>Table 8.</b> Optimization of the experimental variables involved in the magnetoimmunosensor to <i>sola</i> I 7 developed	70
<b>Table 9.</b> Mixtures containing the immunoassay and the genoassay for <i>Sola</i> I 7 protein and <i>sola</i> I 7 DNA simultaneous determination.	79

## INDEX OF FIGURES

<b>Figure 1.</b> Schematic representation of the activation reaction using carbodiimide (EDC) and N-hydroxysulfosuccinimide (sulfo-NHS). Source Esteban Fernández de Ávila (2014) [80] .....	27
<b>Figure 2.</b> Examples of magnetic beads (MBs) modified with different recognition elements for several applications. Modified image from Ávila, E.F. (2014) [80]. .....	29
<b>Figure 3.</b> Schematic strategy based on a rational design of the electrode surface using DNA tetrahedral nanostructures as capture probe. Scheme based on Dong et al. (2015) [105]. .....	32
<b>Figure 4.</b> Nucleic-acid amplification strategies (PCR and HDA) for electrochemical DNA-based sensors. Scheme based on Barreda-Garcia <i>et al.</i> (2016) [117] and Moura-Melo <i>et al.</i> , 2015 [109]. .....	37
<b>Figure 5.</b> Schematic representation of the electrochemical transduction and amperometric response of the genosensor showing the procedure steps and the redox reaction on the SPCE. ....	47
<b>Figure 6.</b> Oligonucleotides structures (data from <a href="http://www.ncbi.nlm.nih.gov/blast">www.ncbi.nlm.nih.gov/blast</a> ) [153]. .....	49
<b>Figure 7.</b> Influence of the RNA-bCp concentration (0.0; 0.05; 0.10; 0.25 and 0.50 $\mu\text{M}$ ) immobilized onto MBs (using 60 min of RNA-bCP incubation time) <b>(A)</b> . Influence of the RNA-bCp (0.25 $\mu\text{M}$ ) incubation time (15; 30; 45 and 60 min) in the MBs <b>(B)</b> on the amperometric responses obtained in the DNA sensor optimization steps. Analytical features: 30 minutes for each incubation time of the DNA target and RNA-bDp (0.1 $\mu\text{M}$ ), antibody-RNA-DNA (1/500) plus protein A-HRP (1/500) (labeling mixture without pre-incubation). Blank=B, gray bars, and 0.1 nM of synthetic DNA target (signal, S, orange bars) and the corresponding S/B ratio values (in red) error bars estimated as the standard deviation of three replicates. ....	50
<b>Figure 8.</b> Schematic representation of the number of steps used on the hybridization protocol optimization: RNA-bCp 0.25 $\mu\text{M}$ ; DNA target 0.1 nM, RNA-bDp 0.1 $\mu\text{M}$ , anti-DNA-RNA-ProtA-HRP (1/500), incubation time (each steps) 30 minutes. ....	51
<b>Figure 9.</b> Influence of the number of steps used on the laboratorial protocol on the amperometric current. Analytical features: incubation time 30 minutes. (for each step); 0.1 $\mu\text{M}$ of RNA-bDp, antibody-RNA-DNA (diluted 1/500) and protein A-HRP (1/500) (mixture preincubated 60 minutes; (blank, B, grey bars); 0.1 nM of synthetic DNA target (signal, S, orange bars); and the corresponding S/B ratio values (in red). Error bars estimated as the standard deviation of three replicates. ....	52
<b>Figure 10.</b> Influence of the RNA-bDp concentration (A) and the incubation time (B) on the amperometric current. Blank 0 nM of DNA target (B, gray bars), 0.1 nM of synthetic DNA target (signal, S, orange bars) and the corresponding S/B ratio values (in red). Error bars estimated as the standard deviation of three replicates. ....	53
<b>Figure 11.</b> Influence of the Anti-DNA-RNA concentration of the amperometric current. Blank, B, gray bars and 0.1 nM of synthetic DNA target (signal, S, orange bars) and the corresponding S/B ratio values (in red). Error bars estimated as the standard deviation of three replicates. ....	54

<b>Figure 12.</b> 1st format: 1st electrochemical signal amplification format. 2nd format: 2nd electrochemical signal amplification format. ....	55
<b>Figure 13.</b> Amperometric currents obtained on the electrochemical signal amplification optimization. Blank, B, gray bars, 0.1 nM of synthetic DNA target (signal, S, orange bars) and the corresponding S/B ratio values (in red). Error bars estimated as the standard deviation of three replicates.....	55
<b>Figure 14.</b> Calibration plot obtained for the synthetic DNA target with the developed DNA sensor using the ProtA-HRP and AntilgG-HRP as enzymatic label.....	57
<b>Figure 15.</b> Storage stability. S/B ratio values of 0.01 nM of DNA synthetic target. Error bars estimated as the standard deviation of three replicates. ....	58
<b>Figure 16.</b> Amperometric responses measured when a complementary, mismatched DNA target and non-complementary DNA ( <i>cor a 9</i> ) to the RNA capture and detector probe was used. Error bars estimated as triple of the standard deviation of three replicates. ....	60
<b>Figure 17.</b> Microcarrier structure holding the schematic biorecognition display of the immunosensor without transducer. ....	69
<b>Figure 18.</b> Amperometric responses obtained in the optimization of the capture antibody concentrations where 5 $\mu\text{g mL}^{-1}$ was the optimal concentration(A) and incubation time of the cp-anti-solaI7 where 15 minutes was the optimal incubation time(B). Error bars estimated as the standard deviation of three replicates.....	71
<b>Figure 19.</b> Amperometric responses obtained in the optimization of the number of steps. In the one step, the target (10 $\mu\text{g mL}^{-1}$ ) and det-Ab-HRP (1/50) were incubated at the same time for 30 minutes, whereas in the two steps, 10 $\mu\text{g mL}^{-1}$ of Sola I 7 was incubated firstly in 30 minutes and then 1/50 of anti-solaI7-HRP 30 minutes. Error bars estimated as the standard deviation of three replicates.....	72
<b>Figure 20.</b> Amperometric response obtained in the optimization of the det-Ab-HRP dilutions where 1:50 was the optimal concentration (A) and incubation time of the det-Ab-HRP where 30 minutes was the optimal incubation time (B). Error bars estimated as the standard deviation of three replicates. ....	73
<b>Figure 21.</b> Calibration plot designed for sola I 7 (incubation of 25 $\mu\text{L}$ in 0, 1, 2.5, 5 and 10 $\mu\text{g mL}^{-1}$ prepared in PBS, pH 7.5). Error bars estimated as the standard deviation of three replicates. ....	74
<b>Figure 22.</b> Control graph to stability evaluation of cp-anti-solaI7-MBs stored at 4 °C in 50 $\mu\text{L}$ of filtrated PBS. Values of amperometric current of signal to blank ratio are represented to 5 $\mu\text{g mL}^{-1}$ of sola I 7 standard. Error bars estimated as the standard deviation of three replicates. ....	75
<b>Figure 23.</b> Selectivity of the magnetoimmunosensor for sola I 7 detection. Amperometric current values achieved to standards of 5 $\mu\text{L mL}^{-1}$ Sola I 7, Sina 1, Sina 3, Sola I 3, Sola I 6, Prup 3. Error bars estimated as the standard deviation of three replicates.....	76
<b>Figure 24.</b> Amperometric responses of 9 extracted samples (green) and the Sola I 7 standard (orange). Error bars estimated as the standard deviation of three replicates. ....	77

**Figure 25.** Schematic display of the disposable dual magnetobiosensor for the simultaneous determination of Sola I7 protein and *so/a* / 7 DNA **A**); picture showing the SPdCE and the homemade magnet holding block **B**) and the modified MBs on the SPdCE assembled on the magnet holding block and in the specific cable connector emerged in the electrochemical cell **C**). Relative sizes of the components are not drawn on real scale [162] .....78

**Figure 26.** Simultaneous amperometric responses measured with the dual magnetobiosensor for mixtures containing different concentrations of Sola I 7 protein and the *so/a* / 7DNA represented in the **Table 9**.  $E_{app} = -0.20$  V vs. Ag pseudo-reference electrode. Error bars were calculated as the standard deviation of three replicates. ....79



## 1 Scope of the thesis

Food allergy is an emerging public health problem where 1-2 % of the total human population suffers from clinically proven food allergies. Hidden ingredients in food are in the origin of accidental contamination, thus a great concern arises both to producers and allergic consumers [1]. Moreover, their vestigial presence in food are usually enough to have an allergic reaction, thus their detection in foodstuffs can be a very hard task in addition to the natural interference of the whole food matrix [2].

A number of analytical methods described in the literature have been successfully applied to evaluate the presence of allergens in foods. Most of the methods for allergens detection are mainly divided in two great groups: the immunological and the DNA-based assays. In general, the immunological methodologies are based on specific binding between epitopes on the target molecule (*i.e.* a known allergen or a specific protein present in the allergenic food) and an immunoglobulin specifically raised against the target [3]. Alternatively to the immunological methods, the DNA based assays involve the extraction of a specific allergen (or marker protein) encoding-DNA fragment [4].

While still not very used for routine analysis, novel biosensors such as the electrochemical genosensors and immunosensors provide unique features that can make them excellent analytical tools, *e.g.* sensitive, selective, less expensive, in some cases able for real-time measurements, environmentally friendly, reusable and fast (especially when automated and/or miniaturized), and able to effectively replace the classical methodologies [2].

The basis of functioning of electrochemical genosensors lies on the electrochemical detection of the hybridization reaction of two complementary DNA strands. The construction of genosensors involves several steps, that can be briefly summarized in the immobilization of an oligonucleotide probe onto the electrode surface and subsequent detection of the complementary strand (the target) by hybridization. Conversely, electrochemical immunosensors depend on a specific non-covalent binding between antibodies (commonly used as analyte-specific probes) and antigens (analytes). The enzyme-linked immunosorbent assay (ELISA) approaches – which falls into two major formats, the sandwich and competitive – represent the most popular technology for the implementation of immunoassays offering low detection limits. As a matter of fact, the complexity of the assay workflow, the use of costly reagents, the bulky ELISA readers, and the time-consuming operation are a few limitations in ELISA assays [5].

This master's thesis dissertation was focused on the development of (1) two new designs of electrochemical magnetogenosensors and (2) a magnetoimmunosensor format for LTP allergen of tomato seeds detection, as well as the implementation of (3) a dual electrochemical immuno-DNA-magnetobiosensor. The format of the developed electrochemical magnetobiosensors was based on different design constructions through the use of screen-printed carbon electrodes (SPCE), as electrochemical platforms, and MBs as immobilization platform, for the biotin RNA capture probe and specific capture antibody.

## 1.1 Aims of the thesis

The main propose of this research work was to develop new fast selective and sensitive designs for the construction of electrochemical biosensors for the tomato seeds allergen detection. The specific aims include:

- 1- Development of an electrochemical magnetogenosensor for *sola* / 7 DNA sequence detection;
- 2- Development of an electrochemical magnetoimmunosensor for Sola I 7 protein detection;
- 3- Optimization, characterization and evaluation of the experimental variables in the DNA-based and immuno-based devices; and
- 4- Development of a multidetector electrochemical biosensor for Sola I 7 protein and *sola* / 7 DNA determination.

## 1.2 Outline of the thesis

The research work described in this thesis was performed in a multidisciplinary research group, the "Grupo de Electroanálisis y (Bio)sensores Electroquímicos" (GEBE) from the University Complutense of Madrid (UCM) and integrated on the scope of an Erasmus + placement.

This thesis was structured in **six chapters**, covering the research aims stated above:

**Chapter 1:** Describe the context of the present work, aims and the thesis outline.

**Chapter 2:** Presents a literature review of some earliest biosensors with new electrochemical amplification technics. Furthermore, this chapter describes the definition of food allergy, lipid transfer proteins and biosensors.



The experimental results are presented in the following chapters, namely the Chapter 3 and 4. In these chapters a brief introduction, materials and methods, results and discussion and conclusions are provided.

**Chapter 3:** The content of this chapter is related to the development of two different formats of DNA-based biosensors for *sola* / 7 detection, as well as the optimization of analytical variables, characterization of the bioplatfrom and its application in food matrixes. This electrochemical biosensor described the use of MBs as immobilization platform, sandwich DNA-RNA heteroduplex format, anti-DNA-RNA as recognition element, protA-HRP/antiIgG-HRP as enzyme/antibody-label complex and screen-printed carbon electrode as transducer.

**Chapter 4:** Describes the development of a magnetoimmunosensor using a sandwich format, MBs as immobilization platform and screen-printed carbon electrode as transducer. The optimization steps, and characterization and application needed prior to biosensor validation is described. Also, this chapter demonstrates the application of a dual magnetobiosensor for Sola I 7 protein and *sola* / 7 DNA sequence detection using a screen-printed dual carbon electrode.

**Chapter 5:** Contains the general conclusions and perspectives for future research on this topics.

**Chapter 6:** All the bibliographic references are listed.

## 2 Literature review

### 2.1 Introduction

Foodborne illnesses compromise negatively the world's economy in terms of medical costs, lost productivity and food wastes. The foodborne illnesses are caused by contaminants present in food. Such contaminants are classified as biological – if they are pathogenic bacteria, parasites or viruses – chemical – if they are natural toxins or pesticides, and allergens – mainly proteins [6].

Eating is an enjoyable human experience but for many people suffering from food allergies and sensitivities, such a joy of eating is drastically diminished by their constant concerns with the potential adverse reactions to the food consumed. In the USA about 36 million cases of illness occurs annually as a result of foodborne contaminants [7].

Therefore, it is of first importance for such consumers with food allergies to have access to the full information about food ingredient composition and safety, so as helping to prevent cross-contaminations and possible foodborne illnesses [2, 8]. To guarantee food safety, the food industry must provide analysis of the food product and for to that purpose the methodologies for contaminant detection must be fast, with extreme sensitive and selective and of low-cost. Biosensors fit such requirements and, therefore, has become useful devices for chemical analysis, competing with conventional analytical devices like chromatographs or spectrophotometers. Their compact design, user-friendly measurement protocols and low-cost are key elements for the success in a large set of applications related to the food industry [9].

Biosensors can be generally defined as analytical devices that transforms the biological responses by incorporating biorecognition elements (*e.g.* antibodies, enzymes, nucleic acids, aptamers, bacteriophages, organelles, microorganisms, *etc*) and biological materials (*e.g.* antibodies, enzymes, nucleic acids, cell-receptors, tissues, organelles, microorganisms, *etc*) with a physical transducer (optical, electrochemical or mass-based) to generate a measurable signal. The technique for biorecognition element immobilization is essential for fabrication of useful biosensors. These techniques may include adsorption, microencapsulation, entrapment on the sensor surface, covalent attachment and crosslinking methods [10].

Biosensors are classified in terms of specificity, sensitivity, assay time, detection limit, robustness, reproducibility, validation and accuracy [10]. Aiming at improving their characteristics,

amplification and transduction technics are employed. Particularly, the enzyme labels are of special interest: the catalytic conversion of the substrate amplifies the signal and increases the sensitivity of the analyte detection by several orders of the concentration magnitude. Moreover, the use of nanomaterials extends substantially the operational and analytical characteristics of the DNA biosensors. Similar results are obtained by a combination of the DNA probes and aptamers with antibodies employed for the direct linking of the label, *e.g.* ferrocene or enzyme [9].

## **2.2 Food Safety**

### **2.2.1 Food allergy**

Food allergy is an adverse immune response to food proteins. The allergy reaction can be induced by mediated-immunoglobulin E (IgE), non-mediated-IgE- or the combination of both, *i.e.* mediated and non-mediated reactions. IgE-mediated reactions are a result from cross-linking of allergen-specific IgE on mast cell and basophils. The allergic-reaction occurs after 20 minutes to no more than 2 hours from ingestion and the symptoms typically appears within 4 to 12 hours. These reactions cause diseases as anaphylaxis, oral allergy syndrome, and acute urticaria. Non-mediated-IgE reactions are related to the action of T cells and brings disease problems as food protein-induced enterocolitis syndrome, celiac disease and contact dermatitis. Atopic dermatitis, eosinophilic esophagitis and eosinophilic gastroenteritis are a cause of both mediated- and non-mediated-IgE reactions [11].

As a result of the dramatic rise of food allergy in the population over the past two decades, investigations on this subject are progressively increasing. Studies have shown a loss of oral tolerance related to the day time, variation to the dietary exposures and, more recently, external environmental factors – such as insufficient sunlight, endocrine disrupting chemicals and pesticides – were correlated with food allergies [12, 13]. Variations in environmental conditions may enhance the expression of allergenic proteins, thus potentially increasing the allergen effects of different plants. For example, LTPs from pepper and peach were differentially activated by biotic and abiotic environmental stresses [14].

There are about 150 million people spread worldwide with allergy to one or more food. In the USA 90 % of allergic reactions in food are estimated to be linked with the allergens present in 8 groups of food: milk, egg, peanuts, tree nuts, wheat, soy, fish and shellfish [15]. Additionally, the most prevalent food allergy worldwide among adults is the peanut allergy [16, 17].

More than 65% of plant food allergens are members of only four protein families/super families, *viz.* the prolamin, cupin, Bet v 1 and profilin family. Animal derived food allergens belong mainly to three protein families, *viz.* the tropomyosins, parvalbumins and caseins (**Table 1**). Pollen-food syndrome is a term describing associations between inhalant pollen allergies and allergic manifestations on ingestion of particular fruits, vegetables and spices. Many of these proteins are widely distributed throughout the plant kingdom and may consequently be involved in extensive IgE cross-reactivity between antigens from taxonomically unrelated plant species. Families such as profilins, pathogenesis-related proteins (PRs) and LTPs are involved in pollen-food syndrome [18–20].

**Table 1.** Some relevant families of allergens in food [18–20].

	<b>Allergen Families</b>	<b>Examples of protein allergens</b>	<b>Food group</b>	<b>Function</b>
<b>Animal source</b>	Tropomyosins	Pen a 1	Shellfish (shrimp, crab, lobster, abalone, mussels, squid, octopus)	Regulate contraction in both muscle and non-muscle cells
	Parvalbumins	$\beta$ -parvalbumins (Lit v 4.0101, Gad c1)	Cod, salmon, tuna, mackerel	Regulating free intracellular calcium levels
	Caseins	Bos d 8	Milk	Comprises a heterogeneous mixture of structurally mobile proteins known
<b>Plant source</b>	Prolamins	2S albumins (Ara h 2–6-7, Jug r 1, Ana o 3, Ric c 1–3, Sin a 1, Bra j 1, Ber e 1); nsLTP (Pru p 3, Jug r 3, Cor a 8, Mal d 3); $\alpha$ -amylase inh (rice); Prolamins of cereals (Tri a 19, Sec c 20)	Wheat, Barley, Rice, maize, soybean, sunflower, sesame, apple, peach, corn, peanut.	Seeds storage proteins, plant protection, seeds storage globins.
	Cupins	Vicilins (Ara h 1, Ses l 3, Jug r 2, Ana o 1, Cor a 11); Legumins (Ara h 3–4, Jug r 4, Ana o 2, Cor a 9)	Peanut, soybean, hazelnut, cashew nut	Sucrose-binding activities and enzymatic activities in germinins
	Bet v 1 homologs	Mal d 1, Pru av 1, Pru p 1, Act d 8, Api g 1, Dau c 1	Birch pollen, apple, cherry, peach, kiwi, celery, carrot	Plant protection, acting as a steroid carrier
	Profilins	Api g 4, Mal d 4, Ara h 5	Flowering plants	Regulate actin polymerization

### 2.2.2 Lipid transfer proteins

In Mediterranean areas, LTPs are the most frequent cause of food allergy in adults with several anaphylactic reactions and pollen-food allergy syndromes [19, 21, 22]. Widely distributed in the plant kingdom (especially in the Rosaceae family), these members of the prolamin superfamily (PR-14) are located in the skin, pulp and seeds of numerous fruits and vegetables – such as apple, peach, corn, tomato, olive, kiwi, carrot, among others. LTPs are characterized by the low molecular weight (7-30 kDa) and a compact structure in a conserved pattern of 6-8 cysteines – forming three to four disulfide bridges – as well as by their function of non-specific and reversible binding and lipid transportation between cell membranes – which occurs during fruit ripening and as a defense mechanism against fungal and bacterium infections [14, 19, 23].

These proteins are divided into two subclasses – LTP1 and LTP2 – generally differing in the molecular weight, number of amino-acids, spatial structure, disulfide bond arrangement, localization, potential function and a few other features. Family 1 LTPs has 9-10 kDa and 90-95 amino-acids, usually localized in cutin-coated organs (leaves, stems, flowers) of the plant. Furthermore, they possess a cutin biosynthesis function, the sterol-binding ability is absent, and the LTP1 allergens are present in 42 plants. Family 2 LTPs has 6-7 kDa and 65-70 amino-acids, localized in suberin-coated organs (subterraneous organs) in the plant. It possesses the suberin biosynthesis function and the sterol-binding ability. The LTPs allergens are listed in tomato, celery and peanut [23, 24].

Due to their high resistance to thermal and proteolytic treatments, this class I of allergens are considered genuine food allergens [25]. Such features allow the allergens to maintain their immunogenetic and allergenic capabilities and, thus, to interact with the immune system associated with the gastrointestinal epithelia. This interactions induces both sensitization and systemic symptoms, though their stability is pH dependent [26].

Non-specific LTPs are involved in general vital functions of the plant defense and, therefore, is widely spread among a varied number of plants. Those non-specific LTPs are closely related in terms of functionality, share a highly conserved sequence regions and homologous three-dimensional structures. Such similarity causes cross-recognition for IgE – thus resulting in cross-reactivity and multiple allergenicity for individuals [27]. A study in USA [28] identified a high number of protein allergens recognized by IgE and IgG4 in peanut allergy patients which ones was peanuts

(Arah h 9), walnuts (*Jug r 3*), peaches (*Pru p 3*) and tomatoes (*Lyc e 3.0101* and *Lyc e LTP3MAC*) more often indicating that they represent a conserved an possible cross-reactive regions.

This research work will focus in tomato allergens particularly the tomato seed allergen *Sola l 7*. This allergen is a non-specific LTP with an important function in seed storage and protection against plant pathogens. In the Mediterranean, tomato allergy is increasing and a cross-reactive with other fruit allergies are being reported, especially with peach allergy – the most allergenic fruit allergy in this region [29–31]. An electrochemical genosensor and immunosensor will be developed to detect tomato seed allergen in food samples.

### **2.2.3 Conventional methods for allergens analysis**

Ideally, the analytical methods for allergens detection must be rapid, efficient, sensitive, selective and cost-effective. In recent years, portable kits and automated procedures has been developed including the protein-based approach, DNA-based approach and in silico methods [32].

ELISA is the most common protein-based method [33]. Two distinct strategies may occur in ELISA. In the so-called direct method, the antigen of interest is directly immobilized on a solid surface, in which a primary antibody-enzyme conjugated is attached. On the other hand, in the indirect method the capture antibody is firstly attached to the antigen of interest and then the enzyme-conjugated secondary antibody recognizes the complex capture antibody-antigen. Finally, ELISA detect antigens by the mean of two distinct formats, the sandwich [34] and the competitive [35]. Other immunoassay-based methods for food allergen detection include Enzyme Allergosorbent Test (EAST) and the Radioallergosorbent Test (RAST), which detect IgE-specific binding in biological samples using allergens bound to a solid phase in microplates [36].

DNA-based detection tools have the principle of amplifying specific genes that encodes the protein allergen using Polymerase Chain Reaction (PCR). PCR consists on a short oligonucleotide sequence (primer) that binds selectively to a complementary DNA strand that, in turn, flanks the DNA sequence of interest – i.e. the DNA sequence to be extended and amplified by the DNA polymerase. The resulting DNA fragments can be further separated by agarose gel electrophoresis detected in a transilluminator. There are mainly 3 types of PRC: the conventional PCR, PCR coupled to ELISA and real-time PCR – the latter the most common for semiquantitative or quantitative determination of food allergens [37].

The silico approach uses bioinformatic tools and online databases to evaluate the similarity between protein structures of known and potential allergens, predicting allergenicity in food proteins. This method was recommended by Food and Agriculture Organization (FAO) and World Health Organization (WHO), from the United Nations (UN), for the prediction of novel allergens [38, 39].

### **2.3 Biosensors**

A device which provides information of biological, physical or chemical properties in a given system is defined as sensor. According to the definition of IUPAC "*a chemical sensor is a device that transforms chemical information, ranging from the concentration of a specific sample component to total composition analysis, into an analytically useful signal. The chemical information, mentioned above, may originate from a chemical reaction of the analyte or from a physical property of the system investigated*" [40].

The growing interest in sensor applications has enhanced its use in food analysis. The main advantages in the use of sensors in food analysis lies in the typical requirements, *viz.* the need to (1) measure in real time, (2) simplify the processes of analysis and increase its efficiency, (3) design miniaturized devices, (4) simultaneously detect different analytes, and (5) develop cost-effective analytical tools.

In turn, a biosensor is generally defined as an analytical device which converts a biological response into a quantifiable and processable signal [9] and are classified according to two main characteristics, *viz.* the (1) format of the assay and (2) physic nature of the transducer.

In direct biosensors, the format of the assay is such that the reaction between the analyte and the element of recognition is detected by direct measurement of the physic changes that have taken place. Conversely, in indirect biosensors, an additional reaction is needed to produce the detection. The additional reaction uses labeled reagents such as enzymatic, electroactive and fluorescent compounds. Moreover, indirect biosensors can be developed in two distinct formats: competitive and noncompetitive. In the competitive format, the analyte competes with an analyte marked by certain anchorage sites to a specific bioreceptor, whereas in the noncompetitive format, the signal is directly proportional to the analyte concentration [41–43].

The physic nature of transducer can be grouped into piezoelectric biosensors (mass and/or micro viscosity alterations of wave propagation) [44], thermoelectric biosensors (temperature

change or heat release) [45], magnetic biosensors (exposure of a magnetically labelled biomolecule to a magnetic field) [46], optical biosensors (absorption or emission of electromagnetic radiation) [47] and electrochemical biosensors (electron tunneling, ion mobility, diffusion of electroactive or changed species) [48, 49].

Focusing on electrochemical biosensors, the given definition is “*a self-contained integrated device, which is capable of providing specific quantitative or semi-quantitative analytical information using a biological recognition element (biochemical receptor) which is retained in direct spatial contact with an electrochemical transduction element*” [48].

Electrochemical sensing usually requires a reference electrode (RE), a counter or auxiliary electrode (AE) and a working electrode (WE) – the latter also known as the sensing or redox electrode. The RE – commonly made from Ag/AgCl – is kept at a distance from the reaction site so as to maintain a known and stable potential. The WE serve as the transduction element in the biochemical reaction, while the AE establishes a connection to the electrolytic solution so that a current can be applied to the WE. These electrodes should be both conductive and chemically stable. Therefore, depending on the analyte, platinum, gold, carbon (*e.g.* graphite) and silicon compounds are commonly used [50–53].

The transduction of the signal requires devices based on electrochemical techniques. Electrochemical biosensors usually use amperometric, potentiometric and conductometric devices [54–56] but other techniques are also available such as impedimetric and field-effect [57, 58].

Amperometric devices are those of greater interest because of their ability to monitor the faradaic currents resulting from the electronic exchange between the biological recognition element and the working electrode maintained at an appropriate constant potential. The direct relationship between the current intensity ( $i_d$ ) generated when a certain electroactive species is oxidized or reduced, and the concentration of those species can be expressed according to the following expression:

$$i_d = n \cdot d \cdot C_s = k \cdot C_s \quad (I)$$

where  $n$  is the number of total electrons exchanged in the electrochemical reaction,  $d$  is the product between the Faraday constant, the electrode area and the constant of mass transfer rate,  $C_s$  is the analyte concentration in solution and  $k$  is the coefficient constant of the proportionality between  $i_d$  and  $C_s$ , which takes different values according to the type of the electrode used.



Amperometric detection of the biological reaction needs the use of labeling – which are ultimately oxidoreductase enzymes. The detection of the reaction between the biological system and the antigen can be carried out by amperometric measurements of the product or the substrate of the enzymatic reaction whenever these compounds are electroactive. Interferences by other electroactive molecules of the samples are likely to occur in this type of systems. Such phenomena can be avoided by searching substrates or products of the enzymatic reaction with higher or lower potentials than the interfering elements. Another way to overcome this problem is using alternative strategies, such as the amperometric measurement of the electron exchange that takes place in the active center of the enzyme and the surface of the electrode. The electron exchange can be directly measured if the enzyme active center orientation and the distance to the electrode are suitable or by using a non-physiologic electron exchanger named as mediator. Mediators are usually molecules with a low molecular weight capable to transfer electrons between the active center of the enzyme and the electrode. They can be adsorbed in the electrode surface, mixed in a carbon paste, attached near to the enzyme in a conductive polymer onto the electrode surface, covalently bound or used instead in solution.

The combination of knowledge between biological responses and electrochemistry demonstrated to be very used, offering the possibility to design a new generation of highly specific, sensitive, selective and reliable micro (bio-)chemical sensors and sensor arrays, to be employed in important sectors such as in medical devices (disease's detection) or food safety [6, 8, 59–62].

Biosensors can also be classified according to the nature of the biological element of recognition. Catalytic biosensors are based on enzymes, tissues and microorganisms. The enzymatic biosensors are the most among those. They are based on proteins that catalyse enzymatic reactions and are recognized by its high efficiency and extreme selectivity. The progress of enzymatic reactions is related to the concentration of the analyte – which, in turn, can be measured by monitoring the rate of formation of a product, the disappearance of a reactant, or the inhibition of the reaction. Affinity biosensors are based on the binding event between the target molecule and the bioreceptor, for instance an antibody, a nucleic acid, or a hormone receptor – which are the origin of a physicochemical change that will be further measured by the transducer. Immunosensors, genosensors and aptasensors are examples of affinity biosensors.

### 2.3.1 Immobilization strategies

The basic requirement of a biosensor is that the biological material should bring the physicochemical changes near to the transducer. In this way, immobilization technologies have played a major role upon the design of biosensors. Immobilization not only helps in forming the required closeness between the biomaterial and the transducer, but also helps in stabilizing the biosensor for reuse. The biological material has been immobilized directly on the transducer or, in most cases, in membranes that can be subsequently mounted on the transducer. Biomaterials can be immobilized either through adsorption, entrapment, covalent binding, cross-linking, affinity or a combination of all these techniques [63, 64] – which are summarized in **Table 2**.

Immobilization by adsorption is accepted as the simplest method of physical immobilization. For a fixed period of time the enzymes are dissolved in solution and the solid support must be in contact with the enzymatic solution. In such procedure part of the initial enzymes do not adsorb to the surface and have to be removed by washing in a buffer. Despite being the simplest method, the immobilization by adsorption is the weakest as a result of the weak bonds involved, such as Van der Waal's forces and electrostatic and/or hydrophobic interactions.

Since the enzymes are poorly bound to the support, the desorption is facilitated by changes in temperature, pH and ionic strength of the medium. Under the influence of these factors, the biosensors present poor operational and storage stability as well as non-specific adsorptions [65].

Adsorption methods can be attained by physical adsorption or electrostatic interactions. The Physical adsorption [66] consists in the simple deposition of an enzyme onto a surface. In the electrostatic interactions, the enzymes are electrostatically immobilized onto a charged surface by the means of different techniques such as layer-by-layer deposition [67] – based on alternate layers of polyelectrolyte and enzyme with opposite charges – and electrochemical doping [68] – based on the fact that controlling the pH, the negatively or positively charged enzymes can be doped into the conductive polymer film during its oxidation or reduction process, respectively. Pre-immobilization on ion-exchanger beads allows to avoid enzyme leakage from the porous immobilization matrix. Retention in a lipid microenvironment by the Langmuir-Blodgett technic offers the possibility to prepare ultrathin layers based on the self-assembly properties of amphiphilic biomolecules at the interface air/water and suitable for enzyme immobilization [69].

**Table 2.** Advantages and drawbacks of the five basic immobilization methods. Adapted from Salazar (2016) [70]

<b>Strategies</b>	<b>Binding nature</b>	<b>Advantages</b>	<b>Drawbacks</b>
<b>Adsorption</b>	Weak bonds: hydrophobic, Van der Waals or ionic interactions	Simple and easy Cheap Limited loss of enzyme activity	Desorption Nonspecific adsorption
<b>Entrapment</b>	Incorporation of biomolecules within a gel or polymeric network	Wide applicability Several types of enzymes may be simultaneously immobilized	Diffusion barrier Enzyme leakage High concentrations of monomer and enzyme
<b>Cross-linking</b>	Enzymes molecules are cross-linked by a functional reactant (e.g. di-aldehyde)	Biocatalyst stabilization Simple	High biomolecule activity loss Diffusion barrier
<b>Covalent binding</b>	Chemical binding between functional groups of the biomolecule and support	No diffusion barrier Short time response Stable	Coupling with toxic product Matrix and biomolecule cannot be regenerated
<b>Affinity</b>	Affinity bonds between two affinity partners (e.g. avidin/biotin)	Controlled and oriented immobilization Remarkable selectivity	Need specific functional groups High cost

In the recent years, NPs has gained popularity because of its success in increasing the adsorption properties. Particularly the use of oxide and metallic nanoparticles as electrode modifiers provide a similar natural environmental for enzymes immobilization, increasing the active surface of the electrode [71]. Moreover, carbon nanotubes and graphene provides to the biosensors a huge conductivity, high surface area and strong adsorption capacity [71, 72].

Immobilization by entrapment is the incorporation of the enzyme in three-dimensional matrices such as electropolymerized films amphiphilic network, silica gel, and carbon paste. Electropolymerization is a simple method in which the enzyme is immobilized onto the electrode surface soaked in an aqueous solution with the enzyme and monomeric molecules and applying a potential current to the transducer. Electropolymers are associated with nanomaterials that act as intermediates between the redox center of the enzyme and the electrode, facilitating electron transfer [74]. Entrapment in an amphiphilic network is composed by an hydrophobic and an hydrophilic phase and the principle is based on the swelling properties of the polymers used [75]. Silica gel process involves hydrolysis of alkoxide precursors under acidic (or alkaline) conditions,

followed by condensation of the hydroxylated units – leading to the formation of a porous gel [76]. Entrapment in a carbon paste – which is a binder and carbon powder mixture and used as electrode material – is effective for biological components incorporation. This matrix allows a fast electron transfer with a versatile, stable and good reproducibility of the modified electrode [77].

Immobilization by covalent binding stands out mainly due to the contribution of the stability in biosensors – among many other advantages on the immobilization of the biological materials. The binding of biomolecules such as enzymes or antibodies is carried out by an initial activation of the surface using multifunctional reagents [glutaraldehyde, carbodiimide (EDC), N-hydroxysuccinimide (NHS)] that activates carboxylic and amino groups. Biomolecules can be immobilized by covalent binding on functionalized nanotubes existing on the electrode surface, as well as in the self-assemble monolayers (SAM) using EDC to activate and promote the binding [77, 78]. The activation reaction is schematically represented in the **Figure 1**.

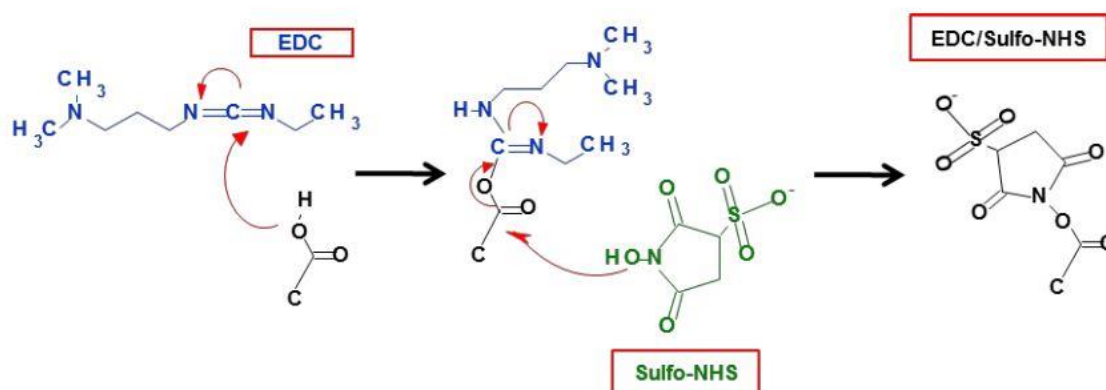


**Figure 1.** Schematic representation of the activation reaction using carbodiimide (EDC) and N-hydroxysulfosuccinimide (sulfo-NHS). Source Esteban Fernández de Ávila (2014) [80]

Immobilization by cross-linking is based on intramolecular cross-linked between bifunctional agents (biomolecules and polymers) and can be carried out by copolymerization with another inert protein or by adsorbing biomolecules onto an adsorbent where the cross-linkage is further undertaken. This method is attractive due to its simplicity and the strong chemical binding achieved between biomolecules. The main drawback is the possibility of activity losses due to the distortion of the active enzyme conformation and the chemical alterations of the active site during cross-linking [65].

Immobilization by affinity is an excellent strategy to obtain the correct orientation of the biomaterials – specially antibodies for immunosensors development. There are several methods to create bioaffinity bonds between an activated support and a specific group of protein sequence such as protein A (ProtA) and protein G [79, 80] – both with good affinity to the Fc region of antibodies – and biotin-(strept)avidin – which has a great potential to be used with enzymes, antibodies or DNA [83].

Magnetobiosensors are another classification for biosensors using MBs – ranging from nanometres to a few micrometres – as immobilization platform strategy. MBs consist of a paramagnetic or superparamagnetic core, mainly based on different iron oxide forms such as magnetite ( $\text{Fe}_3\text{O}_4$ ) and maghemite ( $\gamma\text{-Fe}_2\text{O}_3$ , ferrimagnetic) – which are covered with suitable outer layers such as of agarose, cellulose, silica, silicone, porous glass, mica or polystyrene to protect them against the formation of aggregations [5]. They are biomolecules transporters, separators and concentrators of different analytes, as well as to control electrochemical proceedings on the electrode surface. The use of MBs has demonstrated to be a useful tool to improve the sensitivity, to reduce the time of analysis and to minimize matrix effects in the preparation of electrochemical biosensors [84]. Additionally, the easy manipulation of MBs for samples analysis can be achieved without any pre-enrichment, purification or pretreatment steps instead of the normal standard methods. MBs have many advantages as an immobilization platform strategy. One of the most important advantages is the capacity to improve the performance of immunological reactions. Such improvement comes from the increased surface area and faster assay kinetics, which, in turn, is a result of the analyte being suspension with no need to migrate too far to meet the ligand [85]. **Figure 2** summarizes different types of commercial MBs modified with streptavidin, protein A or G, carboxylic groups, oligonucleotides or antibodies and their corresponding applications.

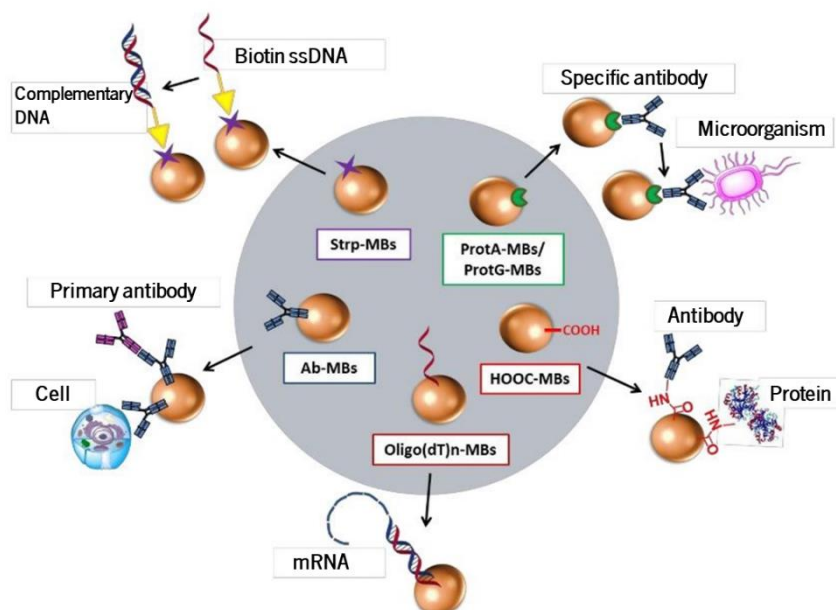


**Figure 2.** Examples of magnetic beads (MBs) modified with different recognition elements for several applications. Modified image from Ávila, E.F. (2014) [80].

### 2.3.2 Electrochemical DNA magnetobiosensors

In the last decade, DNA has become more interesting to develop several procedures and applications in order to obtain simple and portable devices for the DNA detection. Electrochemical genosensors are capable to achieve selectivity and sensibility on the hybridization reaction and presents important features such as the possibility of miniaturization, portability and relative low-cost. A DNA biosensor consists in a single DNA strand immobilized in a surface, which will be further hybridized by its complementary DNA strand [86]. The main advantage in using DNA in electrochemical biosensors lies in its high physicochemical stability in addition to other advantages such as detection speed, high performance, aptitude for automation and disposable character. Nevertheless, hybridization interferences occurs frequently in this type of biosensors and the use of MBs as immobilization platform is a good choice to overcome such a limitation [87]. DNA magnetobiosensors have been studied in the detection of allergens such as hazelnut [1], gluten [88], peanut [89] and lysozyme [90].

### 2.3.3 Electrochemical magnetoimmunosensors

The magnetoimmunosensors encompass the integration of the immunosensor in MBs with different linking groups to immobilize the immunoreactive. The use of MBs in immunosensors offer many advantages, as well as in magnetogenosensors, the target analyte is preconcentrated on the

surface of the MBs using a simple magnetic manipulation by an external magnet that allows the separation of the MB-analyte complex from the matrix sample increasing the selectivity, reduction of the size, cost and analysis time per assay [91].

Electrochemical magnetoimmunosensors are widely employed in food, environmental and clinical analysis. The most common use of magnetoimmunoassay structures involves enzymatic-labelled assays on MBs. Briefly, such assays are based in the immobilization of a specific capture antibody into the MBs, incubation with the sample containing the target analyte and, finally, a labelling step using HRP- or ALP-labelled reporting antibodies (sandwich type). Magnetoimmunosensors can be found for detection of allergens, such as peanut, Arah 1 and Arah 2 [60, 90],  $\beta$ -lactoglobulin and  $\alpha$ -lactalbumin in milk [91, [92] and ovalbumin [95].

## **2.4 Amplification strategies for electrochemical biosensors**

This section describes new techniques related to the electrode surface design in terms of the amplification of the transduction signal. Different strategies based either on a rational design of the electrode surface or in the use of electroactive label are described (**Tables 3** and **4**).

### **2.4.1 Amplification strategies based on a rational design of the electrode surface**

Recently, miniaturization of the solid electrodes is being used to get several fundamental and practical advantages including a dramatic reduction of the sample volume, the portability and the cost effectiveness. Moreover, the fabrication of these printed devices on bendable substrates has enabled the development of a wide range of new electrode systems. In this way, the screen-printing technology is a well-established technique for the fabrication of cheap, portable and disposable electrode systems. The whole electrode system, including reference, counter and working electrodes (usually made on gold, silver or carbon) can be printed on the same substrate surface [94–96].

Although screen-printed electrodes (SPE) are routinely used for laboratorial purposes, Niu and collaborators (2017) [99] developed a new device made of a traditional stainless-steel acupuncture needle as electrode substrate. In this work, a nanosensing electrode was constructed using gold nanoparticles (AuNPs) and graphene (GR) as modifiers of a stainless-steel acupuncture needle as substrate electrode. Using this new device a limit of detection (LOD) of  $2.5 \times 10^{-8}$  mol L<sup>-1</sup> was achieved [99].

The working electrode surface modification can be performed by using different approaches, namely using DNA nanostructures. As the name says, DNA nanostructures are composed by nanoscale structures made of DNA, which acts both as a structural and functional element. DNA nanostructures can serve as scaffolds for the formation of more complex structures [100]. DNA nanostructures find numerous applications in food safety, targeted drug delivery, studies of DNA-mediated electron transfer (ET), sensing, and operating as biological sensor and actuator system [101].

Special attention must be given to the formation of self-assembled monolayers (SAMs) in the electrode surface [102]. The presence of SAM into the working electrode provides well-ordered assemblies on the electrode substrates because they have sensitivity and selectivity for the development of SAM-based DNA sensors. A 3D-DNA tetrahedral nanostructures for the molecules identification was developed by Abi and co-authors (2014) [103]. Aiming at increasing the molecular recognition at the biosensing interface, a convenient method for controlling the biomolecule-confined surface was provided [103]. Briefly, a DNA tetrahedron represents a rigid and stable 3D nanostructure formed by self-assembly of four DNA strands. The shape of the tetrahedron can be modified by mechanical reconfiguration of the DNA strand at the edge of the tetrahedron in response to an external stimulation [104]. The DNA tetrahedra developed by Abi (2014) [103] was assembled by annealing four DNA strands, which were immobilized in a gold surface via thiol linkers existing in the extremes of its three DNA strands. One of three (not parallel to the surface tetrahedron edges) contained a partially self-complementary region with a stem-loop hairpin structure, reconfigurable upon hybridization to a complementary DNA sequence. A non-intercalative ferrocene (Fc) redox label was attached to the reconfigurable tetrahedron edge in such a way that reconfiguration of this edge changed the distance between the electrode and Fc [103].

In other work, Dong (2015) [105] also developed a DNA sensor based on DNA tetrahedral nanostructure for the detection of avian influenza A (H7N9) virus through recognizing of a fragment from hemagglutinin gene sequence, using amperometric techniques (**Table 3**). The DNA tetrahedral probe was immobilized in a gold electrode surface based on self-assembly between three thiolated nucleotide sequences and a longer nucleotide sequence containing complementary DNA to hybridize with the target single-strand (ss)DNA (**Figure 3**). The captured target sequence was hybridized with a biotinylated-ssDNA oligonucleotide as a detection probe to form a sandwich-type arrangement, and thereafter avidin horseradish peroxidase (HRP) was introduced to produce



an amperometric signal through the interaction with 3,3',5,5'-tetramethylbenzidine (TMB) substrate [105].

A more sophisticated electrochemical DNA-based sensor was produced by Zeng and co-authors (2015) [106] based on double tetrahedral nanostructures for the sensitive DNA detection. The DNA-based sensor design was based on the utilization of thiolated and biotinated modified DNA tetrahedral nanostructures as captures and probes, respectively. The biotin-tagged three dimensional DNA tetrahedral nanostructures were employed for efficient signal amplification by capturing multiple catalytic enzymes. Using such a strategy, the developed DNA biosensor presented a LOD of 1fM DNA target. Moreover single base mismatch was discriminated [106].

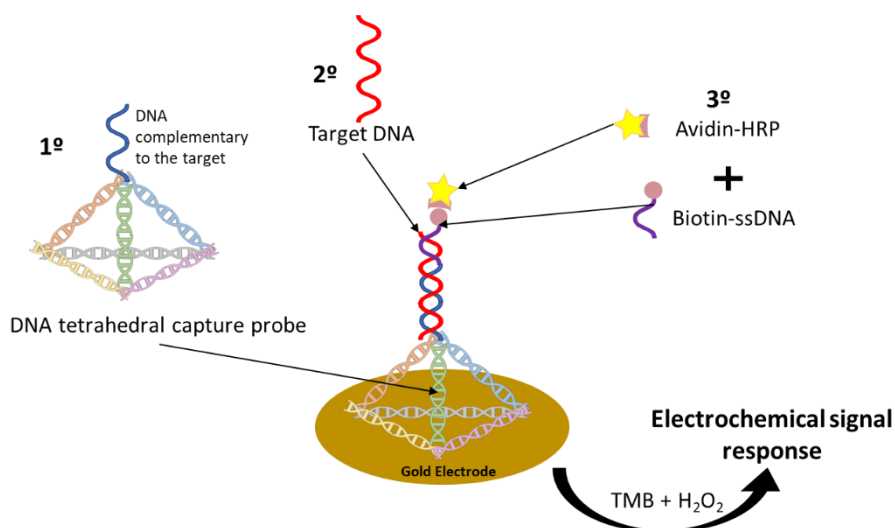


**Figure 3.** Schematic strategy based on a rational design of the electrode surface using DNA tetrahedral nanostructures as capture probe. Scheme based on Dong et al. (2015) [105].

**Table 3.** Examples of amplification strategies based on a rational design and enzymatic label [105], [107], [108], [109], [110].

Target	Sample/ Applicability	Immobilization Procedure/Type of Hybridization Assay	Amplification Scheme	Electrode	Electrochemical Technique	LR	LOD	Ref.
Gene fragment from H7N9 virus	Clinical samples	Thiolated DNA tetrahedral probe (SH-ssDNA) immobilized onto AuE surface	Enzymatic: Avidin-HRP	AuE	Amperometry	1 pM-2.5 nM	0.75 pM	[105]
MicroRNA	—	miRNA target triggers HCR of 2 DNA hairpin probes resulting a multiple G-quadruplex-incorporated long duplex DNA chains.	Signal drop of MB intercalated into duplex DNA	ITO electro	DPV	1–800 pM	1 pM	[107]
Cor a 9 (Hazelnut) DNA	Denatured PCR amplified samples	Biotin DNA probe immobilized onto strep-MBs / Sandwich hybridization format	Enzymatic: Strep-HRP	SPCE placed on Magnetic holding block	Amperometry	0.0024 - 0.75 nM	0.72 pM	[108]
Cauliflower Mosaic Virus 35S Promoter DNA	Genetically modified organisms (GMOs)	Thiolated P35S DNA capture probe immobilization on AuE/ Sandwich hybridization format	Enzymatic: anti-FITC Fab- POD	Gold film	Chronoamperometry	0.1 - 3.0 nM	100 pM	[109]
rpoB gene of Mycobacterium tuberculosis	—	Thiolated MB-DNA1 and DWs immobilized onto AuE electrode /Electrochemical biosensing based on nicking endonuclease assisted by DNA walking strategy	MB-hairpin probes	AuE	CV	1 fM - 100 nM	0.6 fM	[110]

**AuE** – Gold electrode; **DPV** – Differential pulse voltammetry; **DW** – Double tetrahedral nanostructures; **ITO** – Indium tin oxide; **MBs** – Magnetic beads; **NPs** – Nanoparticles; **SPGE** – Screen printed gold electrode;

**SWV** – Square wave voltammetry; **LR** – Linear range; **LOD** – Limit of detection.

#### 2.4.2 Amplification strategies based on the use of nanomaterials

The application of nanomaterials as a strategy for the electrochemical signal amplification has been increasingly applied in biosensors due to their physicochemical properties. Electrochemical generation strategies developed on nanostructured surfaces using graphene, graphene oxide, mesoporous nanomaterials, AuNRs and MWCNTs and/or using bioconjugates of AuNPs with multiple bioreactors as signaling carriers [111] provide remarkable progress in nanotechnology and bioconjugation techniques some of them are described in the **Table 4**.

Mesoporous Pt nanospheres (MPNs) have received special concerns due to their high pore volume, large surface area, high loading capacity, distinct electrical conductivity, easy functionalization, and superior catalytic activity. Introducing MPNs in electrochemical sensors could efficiently increase the specific biosensing surface and deliver amounts of signal molecules – which could clearly enhance the performance of the sensor. Recently, Pu and collaborators (2017) [110] developed a sensitive and universal ratiometric electrochemical biosensing platform for the ultrasensitive detection of several bioanalytes. This ratiometric electrochemical device employed MPNs as nanocarriers for electroactive signal reporter (DOX) and thiol-functionalized DNA. This proposed universal ratiometric electrochemical biosensor exhibited high sensitivity with a broad detection range to different biomolecules – including small molecules, nucleic acids, and proteins. This biosensor also performed well-accepted signal response in identifying serum samples, thus resulting in a wide prospect for bioanalysis and clinical diagnosis [110].

MNPs  $\text{Fe}_3\text{O}_4$  NPs, have received an increasing attention by the scientific community due to their potential applications in several fields (*e.g.* biomedicine, environment and food) and, particularly, in biosensors. Such interest results from their good stability and biocompatibility, high surface area, low toxicity and easy preparation and separation [112]. Zhang *et al.* (2017) [113], reported the chemical synthesis and functionalization of gold-coated MNPs ( $\text{Fe}_3\text{O}_4@Au$  MNPs) and the thiolated single stranded DNA (ssDNA) immobilization onto the  $\text{Fe}_3\text{O}_4@Au$  MNPs. In the presence of silver ions ( $\text{Ag}^+$ ) cytosine DNA oligonucleotide hybridized with the thiolated ssDNA to form an intramolecular duplex, in which  $\text{Ag}^+$  can selectively bind to cytosine–cytosine mismatches forming C– $\text{Ag}^+$ –C complex. The exposed stem of the C– $\text{Ag}^+$ –C complex opened two alternating ferrocene-labeled DNA hairpins in turn and triggered HCR to form a super sandwich DNA structure on the surface of  $\text{Fe}_3\text{O}_4$  at Au NPs. The HCR products modified  $\text{Fe}_3\text{O}_4$  at Au NPs were brought to the surface of magnetic gold electrode for direct electrochemical measurements. The proposed

strategy led to a LOD of 0.5 fM and a wide dynamic range of 1 fM–100 pM for Ag<sup>+</sup> target. The developed biosensor was highly selective and its practical applicability in tap water and lake water samples was also investigated with a great result [113].

A recent and innovative application of nanomaterials in electrochemical biosensors as electrode modifiers is the use of AuNPs and graphene both electrodeposited in a traditional stainless steel acupuncture needle (AN) [99]. The advantage of using AuNPs on AN surface was to increase the surface area, which provided a roughness interface that was suitable for the following graphene modification. With GR formed on the surface of AuPNs/AN by electrodeposition of GO suspension, a thin and wrinkled GR layers could be found in the gaps between AuNPs – which resulted in a specific large electrode interface.

Tobacco mosaic virus (TMV) is a new approach for the development of electrochemical biosensors using TMV nanotubes or coat proteins (CP) aggregates as enzyme nanocarriers [114]. TMV can be chemically and/or genetically modified with functional groups to facilitate biochemical reactions and, consequently, to achieve a high selectivity toward the respective analyte. Finally, TMV nanotubes can be integrated in receptor layers and transducers, through conventional analytical techniques, to develop highly selective and sensitive sensors and systems. In this research work, Bäcker (2017) [114], employed for the first time in amperometric detection of glucose as model system sensor, chips combining Pt electrodes loaded with glucose oxidase (GOD)-modified TMV nanotubes or CP aggregates as enzyme nanocarriers, respectively. At present, glucose biosensors are widely utilized as clinical indicator of diabetes and in food industry for quality control [114].

Dendrimers such as PAMAN G4 and polymers (PPy, PANI) were also used as electrode modifiers to improve the performance of such electrochemical generators for the determination of circulating biomarkers. Besides, these approaches were developed using integrated formats and coupling conveniently modified MBs with SPEs or conventional magnetic electrodes. Electrochemical DNA-based sensors recently developed have detected proteins and DNA in the ranges 0.5 pM-1 nM and 1 aM-3.09 nM, respectively, depending on each application. By analyzing actual samples, all sensors have been found to be suitable for practical purposes [111].

The MB-based genosensing approaches perform the hybridization and transduction steps on different surfaces which eliminates the major problems associated with nonspecific adsorptions of non-target sample components, enhancing considerably the assay specificity and sensitivity [111]. Montiel and co-authors (2017) [1] developed an electrochemical DNA magnetobiosensor

for any variety of hazelnut tracers in food determination [1]. This assay consisted on sandwich hybridization format using MBs as modifier surface – where the DNA capture probe was immobilized and the hybridization with the target occurred. For electrochemical transduction, the modified MBs must be magnetically captured on the working electrode surface and then measured by amperometry in stirred solutions. The reduction current from the benzoquinone formed in the Strep-HRP catalyzed oxidation of HQ.

### **2.4.3 Nucleic acid–based amplification strategies**

The gold standard strategy used for nucleic acid-based amplification is the polymerase chain reaction (PCR) technique to amplify million times the DNA chains so as to have more quality of the signaling. Basically, if there are more DNA probes in the DNA-based sensor, an increased electrochemical signal will be achieved. Nowadays, other alternatives are available with better analytical performance than PCR, namely the end-point PCR, PCR-ELISA, qPCR, multiplex PCR, qPCR, and, more recently, qPCR combined with high-resolution melting analysis (HRM) [115].

Hybridization chain reaction (HCR) is another technique for nucleic acid-based amplification strategy based on an enzyme-free methodology in which the laboratorial protocol is made at room temperature and with a low time consumption [116]. HCR is a kinetics-controlled reaction where a cascade of hybridization events between two species of metastable DNA hairpin probes is triggered to form a long dsDNA structure [113]. Although has been used for Ag<sup>+</sup> detection, this technique brings additional interest for signal amplification. In addition, its usefulness has been showed for the detection of miRNAs described by Hou (2015) [107], in which the presence of the target miRNA (let-7a, a tumor suppressor in breast cancer) triggers the HCR of two species of metastable DNA hairpin probes, resulting in the formation of multiple G-quadruplex-incorporated long duplex DNA chains in solution [107]. Using a “signal-off” mode approach was based on monitoring the decrease in the electrochemical response of methylene blue measured by differential pulse voltammetry (DPV) at indium tin oxide (ITO) electrodes after intercalation into the duplex and the generated multiple G-quadruplexes. A linear relationship between the DPV peak current and the logarithm of the let-7a concentration was obtained in the 1–800 pM range achieving a LOD of 1 pM [116].

Although all the controversy, the development of genetically modified organisms (GMOs) and their use for food and feed purposes still rising. Moura-Melo *et al.* (2015) [109], have experimentally characterized the helicase-dependent isothermal amplification (HDA) and sequence-specific detection of a transgene from the Cauliflower Mosaic Virus 35S Promoter (CaMV35S). HDA

is one of the most appealing isothermal schemes developed in recent years, because of its exponential nature and its simple reaction scheme, as schematized in **Figure 4**. In HDA, three enzymes – polymerase, helicase and single-stranded binding protein (SSB)– act together under the same reaction conditions, along with two primers to accomplish amplification. Using chemical energy from ATP hydrolysis, helicase disrupts hydrogen bonds between complementary DNA strands, thus generating single-stranded templates for primers hybridization and subsequent elongation. SSB acts as an assistant, stabilizing the unwound DNA. This work [109] reports guidelines to help the design of DNA-based sensors for detecting HDA amplicons – which can be employed in the development of effective genetic detection tools for a wide range of applications, such as food safety control, environmental monitoring and clinical diagnosis [109].

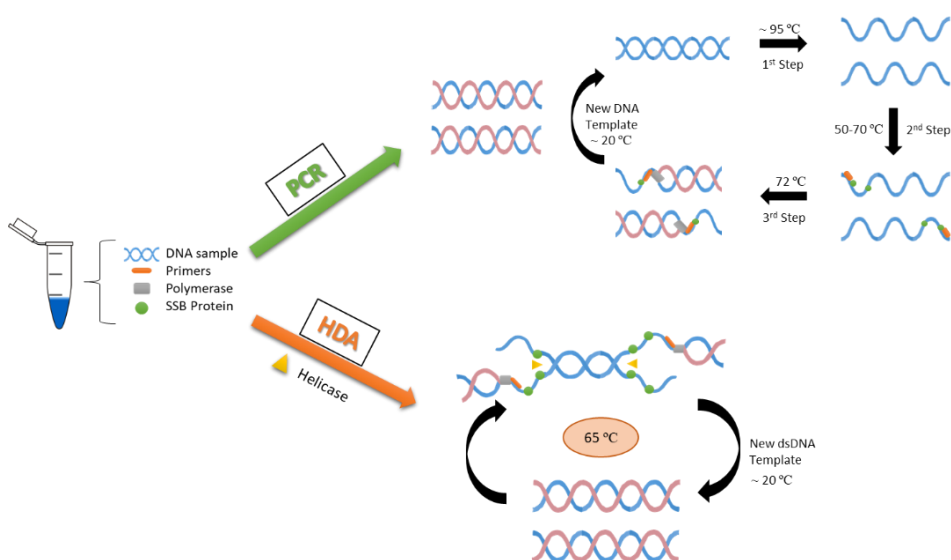


**Figure 4.** Nucleic-acid amplification strategies (PCR and HDA) for electrochemical DNA-based sensors. Scheme based on Barreda-García *et al.* (2016) [117] and Moura-Melo *et al.*, 2015 [109].

#### 2.4.4 Enzyme-based electrochemical strategies

Enzymes are commonly used as label to amplify the electrochemical signal in biosensors. Enzymatic reactions have been combined with an additional amplification process (*i.e.* redox cycling [118]), or using multienzyme labels per detection probe [119]. Redox cycling is a process that can repetitively generate or consume signalling species (molecules or electrons) in the presence of reversible redox species [120]. The two reactions (oxidation and reduction) in redox cycling can be obtained either enzymatically, chemically, or electrochemically. Multienzyme-based

branched DNA assays have been used in the ultrasensitive detection of DNA and RNA [121]. Although the assays can be automated, the detection procedures are quite complicated, which is unsuitable as a universal platform technology for ultrasensitive biosensors [122].

The enzymatic label used in *Salmonella* sp. amperometric detection [123] was the horseradish peroxidase (HRP) linked to an antibody antiDIG. The 3' terminal of the DNA probe was labelled with digoxigenin and when the direct hybridization occurred, an antiDIG-HRP solution is added to the electrode. Using this enzymatic label, a LOD of 60 pM was calculated. Still in terms of enzymatic strategies, another method to detect GMOs with electrochemical genosensors (**Table 3**) is the employment of enzymatic labeling with anti-FITC Fab-POD on the DNA target. The immobilized POD activity, just related to the hybridized target, was determined by immersion of the working surface into 450  $\mu$ L of enzyme substrates solution (TMB + H<sub>2</sub>O<sub>2</sub>) followed by chronoamperometric detection of the oxidized TMB [109].

Mycotoxins are a type of secondary toxic metabolites produced by fungi and are closely related with severe food poisonings. Long Wu et al. (2017) [124], employed ferrocene (Fc) anchored to an AFB1 aptamer probe and combined with methylene blue (MB) attached to a complementary DNA – thus acting as dual signals. The recognition method was determined by the release of MB-cDNA from the electrode surface and the Fc tag of the aptamer sequences came close to the electrode surface due to their conformational change by AFB1 recognition. Electrochemical signal of MB exhibited a decrement and, in turn, Fc showed an increment [124].

The adulteration of meat products is another problem in the food industry, affecting the public health and simultaneously contributing to an unfair competition in the meat market. DNA-based assays have also been used for the accurate detection of meat adulteration. An electrochemical biosensing platform for the detection of horsemeat by targeting a 40-mer fragment of mitochondrial DNA D-loop region of horse was developed by Montiel (2017) [108]. The proposed assay involves direct hybridization of the target mitochondrial DNA fragment with a specific RNA capture probe immobilized in streptavidin-functionalized magnetic beads (Strep-MBs). For recognition of the captured DNA/RNA heteroduplexes, a commercial antibody labeled to a bacterial protein conjugated with a horseradish peroxidase homopolymer (ProtA-HRP40) was used. The variation in the cathodic current – measured using the H<sub>2</sub>O<sub>2</sub>/HQ system after magnetic capture of the modified MBs in SPCE – could be correlated with the presence of the target DNA in the analyzed sample [108]. The LOD achieved in this essay was 0.12 pM.

#### 2.4.5 Quantum dots-based electrochemical strategies

One of the most active trends in the analytical field is the application of QDs in electrochemical and biological sensing, due to their high surface-to-volume ratio, high reactivity and small size. Slight changes in the external environment lead to significant changes in particle valence and electron transfer. Based on these significant changes, QDs can be used to construct electrochemical biosensors with biological macromolecules – which are generally characterized by high sensitivity, rapid response and high selectivity. Some QD-based electrochemical biosensors are tabulated in **Table 4** [125].

In a work described by Long Wu *et al.* (2017) [124], develop an electrochemical genosensor for the AFB1 mycotoxin detection applying electrochemiluminescence (ECL) system. ECL signals were produced from CdTe/CdS/ZnS quantum dots (QDs) and luminol. Here, horseradish peroxidase-modified gold nanorods (HRP/Au NRs) acted as the quencher/enhancer and quenched the ECL signal of the QDs and simultaneously catalyzed H<sub>2</sub>O<sub>2</sub> to enhance the ECL intensity of luminol. In the absence of AFB1, both the ECL signal of the QDs and luminol appeared as the cDNA hybridized with the aptamer. In the presence of the target, the AFB1 aptamers hybridized with the target and released the cDNA sequence, which leads to the increment of the QD ECL signal and the decrease of the luminol signal. The ratio of the ECL intensity (QDs/luminol) exhibited a good linearity and high sensitivity for AFB1 detection [124]. Although this protocol does not fit with an electrochemical biosensor, the basis of the sensor construction is exclusively founded on electrochemical system.

An magnetochemical support was tested in a more complex biosensor for the determination of anti-transglutaminase IgA antibodies, a celiac disease biomarker. In this work [126], a methodology for the detection of cadmium on SPEs using a portable magnetochemical support was developed – which enhances the mass transfer of the analytes due to the forced convection by the magnetohydrodynamic (MHD) effect. This methodology was applied to the detection of QDs at low concentrations and, afterwards, to the detection of QDs employed as labels for electrochemical biosensors using SPEs. Such assay was based on the protein detection but, could be easily transferred to any kind of biosensing systems (*e.g.* electrochemical genosensor) [126].

Kokkinos (2015) [127], developed a disposable quantum dot-based DNA biosensor, on a screen-printed graphite surface with embedded bismuth citrate as a bismuth precursor (**Table 4**).



Proof of applicability was demonstrated for the ASV-QD assay of the C634R mutation of the RET gene [related to Multiple Endocrine Neoplasia Type 2 (MEN2)]. The operationalization of these electrochemical biosensors was based on (i) the DNA assay in their surfaces – involving hybridization of the biotinylated target oligonucleotide with the surface-immobilized complementary probe – and its labeling with streptavidin-conjugated PbS-QDs, and (ii) the anodic stripping voltammetry (ASV) detect the Pb(II) released from QDs by acidic dissolution. The accumulation of Pb on the sensor surface, the embedded Bi citrate was converted in situ to Bi-NPs enabling ultra-trace Pb determination. This method achieve a limit of detection of  $0.03 \text{ pmol L}^{-1}$ . [127].. The design of this assay can be easily employed for food safety purposes by choosing proper oligonucleotides.

In a recent study [128], a novel electrochemical biosensor for detecting streptavidin was developed (**Table 4**). The probe comprised biotin, sig-DNA strand with an amino group, CdSe QDs, and its substrate strand (capturing DNA strand) with a thiol group. Hybridization of the sig-DNA strand and capturing DNA strand (cap-DNA) was impeded in the presence of streptavidin due to steric hindrance, thus the amount of CdSe QDs on the surface of a gold electrode was decreased. The amount of CdSe QDs in the surface of the gold electrode was detected by differential pulse anodic stripping voltammetry. Under optimal conditions, the detection limit of streptavidin was  $0.65 \text{ pg mL}^{-1}$  [128].

**Table 4.** Examples of electrochemical transduction strategies using nanomaterials [123], [127], [108], [128], [124].

Target	Sample/ Applicability	Immobilization Procedure/ Type of Hybridization Assay	Electrode	Electrochemical Technique	Linear range	Limit of detection	Ref.
<i>DNA probe Salmonella sp.</i>	Pathogenic genome of <i>Salmonella</i> performed by PCR	Immobilization of thiolated DNA probe onto gold/ Direct hybridization	Gold nanocomposite with graphite epoxy composite (nano-AuGEC)- modified SPGE	Amperometry	60 pM - 300 pM	60 pM	[123]
C634R DNA mutation	—	Complementary BSA-oligonucleotide conjugate probe immobilized onto WE/ Direct hybridization	SPCs graphite electrode Bi citrate modified	DPV	0.1 pM - 10 nM	0.03 pM	[127]
mt-DNA D-loop region	Raw beef and horsemeat	RNA probe immobilized onto strep-MBs / Direct hybridization	SPCE placed on Magnetic holding block	Amperometry	0.39 - 75 pM	0.12 pM	[108]
Streptavidin	—	DNA immobilized on the electrode surface/ Hybridization with CdSe QDs	GCE	DPASV	1.96 pg mL <sup>-1</sup> - 1.96 µg mL <sup>-1</sup>	0.65 pg mL <sup>-1</sup>	[128]
Aflatoxin B1 (AFB1)	Peanut; maize; wheat	Thiolated DNA onto AuE /Hybridization with the aptamer and the complementary DNA (cdNA)	GCE modified with AuNPs and graphene	CV, SWV and EIS	1.0 pM - 50 nM and 5.0 pM - 10 nM	0.43 pM and 0.12 pM	[124]

**AuNPs**- gold nanoparticles; **CV** - cyclic voltammetry; **DPASV** - differential pulse anodic stripping voltammetry; **DPV** - differential pulse voltammetry; **EIS** - electrochemical impedance spectroscopy, **GCE**- glassy carbon electrode; **MBs** - magnetic beads; **QDs** - Quantum dots; **SPCE** - screen printed carbon electrode; **SWE** - square wave electrode; **WE** - working electrode.

### **3 Development of an electrochemical DNA biosensor for *sola* I 7 determination**

#### **3.1 Introduction**

Tomato (*Solanum lycopersium*), a plant widely cultivated, is the second fruit most consumed worldwide, both as fresh and processed food [31]. The consumption of tomato provides well-established health benefits, which rely on its composition in vitamins and phytonutrients (lycopene,  $\beta$ -carotene, ascorbate and polyphenols) as well in minerals (potassium, calcium, phosphorus, magnesium) [129], [130].

Despite the health benefits, tomatoes contain some proteins that may cause allergies [132]. Indeed, tomato has been reported as one of the most prevalent plant-derived food sensitizers [133], [134] [133], [134]. Tomato allergenic frequency ranged between 1.5 and 20.0 % in different populations of patients with specific IgE [135]. Furthermore, 6.5 % of this allergic population are from Spanish Mediterranean region [133], [136], although 80 % of those still tolerating its consumption [137].

Several specific allergenic proteins have been already identified in tomato fruit [138], such as Sola I 1 (profilin), Sola I 2 ( $\beta$ -fructofuranosidase), Sola I 3 (nsLTP), Sola I 4 (Bet v 1-like), Sola I 5 (cicophilin), Sola I 6 (nsLTP) and Sola I 7 (nsLTP) [31], [139]–[142].

A number of these proteins (Sola I 3 and Sola I 6-7) are members of the nsLTPs. nsLTP plant family are a cross-reacting plant pan-allergens of 9-10 kDa molecular mass, and widespread in the plant kingdom. It has been reported that nsLTPs are predominantly present in the peel of fruits, but members of this family have been also identified in tomato seeds [33], [143].

Regarding Sola I 7, this protein belongs to class 1 of nsLTPs and has been identified in large concentrations in tomato seeds – being one of the key allergens related with several allergic symptoms, namely anaphylaxis (71.4% of the patients with anaphylaxis presented a positive response to the protein Sola I 6 and Sola I 7). Besides that, it was demonstrated that Sola I 7 is structurally similar to other protein families, namely the Act d 10 (53% of similarity), Pru p 3 (41%), and Ara h 9 (51%). These allergens are present in sunflower seeds, peach, apple and peanut – thus, demonstrating the existence of cross-reactive allergy to these fruits [31].

Since tomato and/or their sauce are a common ingredient widely used in homemade food preparation and industrial food processing, its presence in food is a major concern for both the

food industry and food-allergic consumers. Therefore, analytical methods with high specificity and sensitivity, able to detect even traces of allergens in a rapid, robust, reliable, end-user friendly and cost-effective are of first interest in sectors such as food safety [1].

Currently, the analytical methods are mainly focused on testing allergic proteins – *viz.*, SDS-PAGE, immunoblotting, ELISA – and genes of residual allergens. Unfortunately, industrial production of processed food involves heat and high-pressure treatments, which often denatures partially or totally food proteins and, consequently interfering with their detection [1], [144]. Therefore, DNA-detection technology has been developed as an alternative for such purposes [145]. Moreover, the DNA amplification by PCR guarantees the required sensitivity levels [108].

Different methods using PCR have been described for tomato allergen *sola 1 7* DNA detection [141], [146], [147]. Even though PCR has been considered the gold standard methodology for the DNA detection, this biological technique is relatively time-consuming and costly. Hence, the development of analytical methodologies using electrochemical DNA biosensing approaches are likely to become convenient, low-cost and flexible instrumental alternatives. Such strategies combine the high selectivity of the DNA-based methods with the advantages of the electrochemical sensors [108]. Moreover, the use of disposable SPEs, as sensor, and MBs, as suitable platforms for the development of electrochemical sensors, make these approaches more attractive because of the increased sensitivity, reduced analysis time and minimization of matrix effects [148]. Although some electrochemical DNA-based sensors have been developed to detect DNA/RNA – allowing the food allergen identification, namely peanut (*ARA h 2*) [145], hazelnut (*cor a 9*) [1] and gluten ( *$\alpha$ 2-gliadin*) [149] – no electrochemical sensors for tomato detection has been reported so far.

This original work presents the development of a novel electrochemical DNA magnetobiosensor approach for the sensitive and selective detection of a 60 mer DNA sequence, encoding part of the allergenic protein *sola 1 7* DNA from tomato. The DNA sensor design is based on the electrochemical detection of a sandwich hybridization format between RNA-DNA complementary sequences. To that purpose, selective biotinylated RNA capture probes (complementary to DNA *sola 1 7* target) were immobilized into commercial streptavidin-functionalized MBs, and a RNA-DNA sandwich assay was further performed. The electrochemical signal amplification was made by using anti-DNA-RNA heteroduplex antibody conjugated with an HRP (ProtA-HRP) or antiIgG-HRP as enzymatic label. The electrochemical transduction strategy involved SPCEs using hydroquinone (HQ) as electron transfer mediator and H<sub>2</sub>O<sub>2</sub> as HRP substrate.

The LOD is a term widely used to describe the smallest concentration of a measurement that can be reliably measured by an analytical procedure, in this case by the electrochemical DNA sensor. It is important to characterize the analytical performance of the DNA sensor in order to understand its capability and detection limits, as well as to compare its performance with other assays – so as to determine which is “fit for propose”. To calculate the LOD a slope of a calibration plot ( $m$ ) and the standard deviation ( $sd$ ) of 10 measurements of the blank (without target) must be determined to use the expression  $3 \times sd/m$ , in molarity. In this assay a LOD of  $1.1 \times 10^{-12}$  M (1st format) and  $0.2 \times 10^{-12}$  M (2nd format) was achieved.

Aiming at confirmation of the selectivity of the DNA sensor, 3 single strands was designed with the *sola / 7* DNA target as reference – where each of which a specific amino acid or amino acids was changed, and named as mismatch (1 mismatch, 2 mismatch and 3 mismatch). Theoretically, the more mismatches are in the DNA used as target the more similar will be with the blank of the sensor, which represent the absence of target. Also, a non-complementary DNA target was used as control to confirm that if a DNA target which is not complementary with the probes is used, then the amperometric signal of these ones will be equal to the blank. Finally, and to complete the characterization of the electrochemical DNA sensor, an assay using real samples of DNA extracted from tomato seeds and peel were used. By this mean, the DNA sensor can be thus employed as an analytical procedure to identify the *sola / 7* allergen in real foods samples.

## **3.2 Material and Methods**

### **3.2.1 Apparatus and electrodes**

Amperometric measurements were performed using a CH Instruments (Austin, TX) model 812B potentiostat controlled by software CHI812B. SPCEs (DRP-110, DropSens, Spain), consisting of a 4 mm diameter carbon working electrode, a carbon counter electrode, and an Ag pseudoreference electrode, were used as electrochemical transducers in conjunction with a specific cable connector (DRP-CAC, DropSens). All measurements were performed at room temperature.

Intended for magnetically capture, the modified Strep-MBs onto the SPCEs surface a neodymium magnet (AIMAN GZ) embedded in a homemade Teflon casing was used.

A Raypa steam sterilizer, a biological safety cabinet Telstar Biostar, a thermocycler (SensoQuest LabCycler, Progen Scientific Ltd), an incubator shaker Optic Iyymen System (Comecta S.A., Sharlab), a Bunsen AGT-9 Vortex to homogenize the solutions the solutions, a magnetic

particle concentrator DynaMag-2 (123.21D, Invitrogen Dynal AS), and the centrifuges Heraeus Multifuge 3 SR plus (Thermo Scientific) and 5424 (Eppendorf) were also employed during the experiments.

### 3.2.2 Chemicals and solutions

Strep-MBs beads (2.8  $\mu\text{m}$ - $\emptyset$ , 10 mg mL<sup>-1</sup>, Dynabeads M280 Streptavidin, 11206D) were purchased from Dynal Biotech ASA. Sodium di-hydrogen phosphate (NaH<sub>2</sub>PO<sub>4</sub>), di-sodium hydrogen phosphate (Na<sub>2</sub>HPO<sub>4</sub>), tris(hydroxymethyl)aminomethane (Tris)-hydrochloride (Tris-HCl), sodium chloride (NaCl) and potassium chloride (KCl) were purchased from Scharlab. The horseradish peroxidase homopolymer (ProtA-HRP) conjugate, hydroquinone (HQ) and H<sub>2</sub>O<sub>2</sub> (30%, w/v) were purchased from Sigma-Aldrich. Anti-mouse Immunoglobulin G-HRP conjugate (antiIgG-HRP) was purchased from Abcam. RNA-DNA hybrid antibody (clone: D5H6) (anti-DNA-RNA) was purchased from Covalab. Commercial blocker casein solution "BB" (a ready-to-use, PBS solution of 1% w/v purified casein) was purchased from Thermo Scientific.

Buffer saline solutions were prepared in water obtained from a Millipore Milli-Q purification system (18.2 M  $\Omega$  cm): phosphate-buffered saline solution (PBS) consisting of: (i) 0.01 M phosphate buffer solution containing 0.137 M NaCl and 0.0027 M KCl, pH 7.5; (ii) 0.05 M phosphate buffer, pH 6.0 (for the amperometric measurements); and (iii) Binding and Washing (B&W) buffer consisting of 10 mM Tris-HCl solution containing 1 mM EDTA and 2 M NaCl, pH 7.5.

The specific oligonucleotide sequences: biotinylated RNA capture probe (RNA-bCp), biotinylated detector RNA probe (RNA-bDp) and DNA target (**Table 5**) were obtained as lyophilized desalted salts from Sigma-Aldrich. Upon reception, they were reconstituted in nuclease-free water to a final concentration of 100  $\mu\text{M}$ , divided into small aliquots, and stored at  $-80^\circ\text{C}$ .

**Table 5.** Oligonucleotides used for the electrochemical DNA sensor development

Oligonucleotide name	Sequence 5´-3´	pb
Biotinylated RNA capture probe (RNA-bCp)	Biotin-CUACAGCAUGCUGCACCCGGGCUCGCCACCC	30
biotinylated detector RNA probe (RNA-bDp)	UGUGUCAGGAACGGGACACAGGGUGCCAAG-Biotin	30
DNA target (Target)	CTTGGCACCTGTGTCCCGTTCCTGACACAGGGTGGCGAGCCC GGTGCAGCATGCTGTAG	60
DNA target 1-mismatch	CTTGGCACCTGTGTCCCGTTCCTGACACAGGGTGGCGAGCCC GGCGCAGCATGCTGTAG	60
DNA target 2-mismatch	CTTGGCACCTGTGGCCCGTTCCTGACACAGGGTGGCGAGCCC GGCGCAGCATGCTGTAG	60
DNA target 3-mismatch	CTTGGCACCTGTGGCCCGTTCCTGACACAGGGTGGTGTAGCCC GGTGCAGCATACTGTAG	60

### 3.2.3 Construction of the amperometric DNA sensor

Strep-MBs were used as magnetic electrochemical platform for the biosensor construction. For that, 5 µL aliquot of the commercial microbeads were added in 1.5 ml Eppendorf tubes and washed twice with 50 µL of B&W buffer (pH 7.5). After each washing step, Strep-MBs were magnetically concentrated and the supernatant discarded. Then, 25 µL of 0.25 µM RNA-bCp-30 mer, prepared in B&W buffer (pH 7.5), was incubated in the Strep-MBs for 30 minutes at 37° C and 950 rpm. The prepared RNA-bCp-Strep-MBs were washed two times with 50 µL of a commercial blocker casein solution. After that the sandwich hybridization reaction between the RNA-DNA heteroduplexes was promoted by incubating the modified MBs in a solution containing 25 µL of the detector RNA probe at 0.1 µM (RNA-bDp-30 mer) and the desired DNA target (60 mer) at 0.01 nM (both prepared in blocker casein solution (BB)) for 30 minutes, at 37° C and 950 rpm. In order to enzymatically label the DNA sensor, the MBs functionalized with the RNA-DNA heteroduplex were resuspended in anti-DNA-RNA (1µg ml<sup>-1</sup>) and 40 µg ml<sup>-1</sup> of anti-mouse IgG-HRP or Protein A-HRP (2 enzymatic format labelling was tested) for 60 min at room temperature in a laminar flow cabinet. Finally, two washes with 50 µL of blocker casein solution were performed.

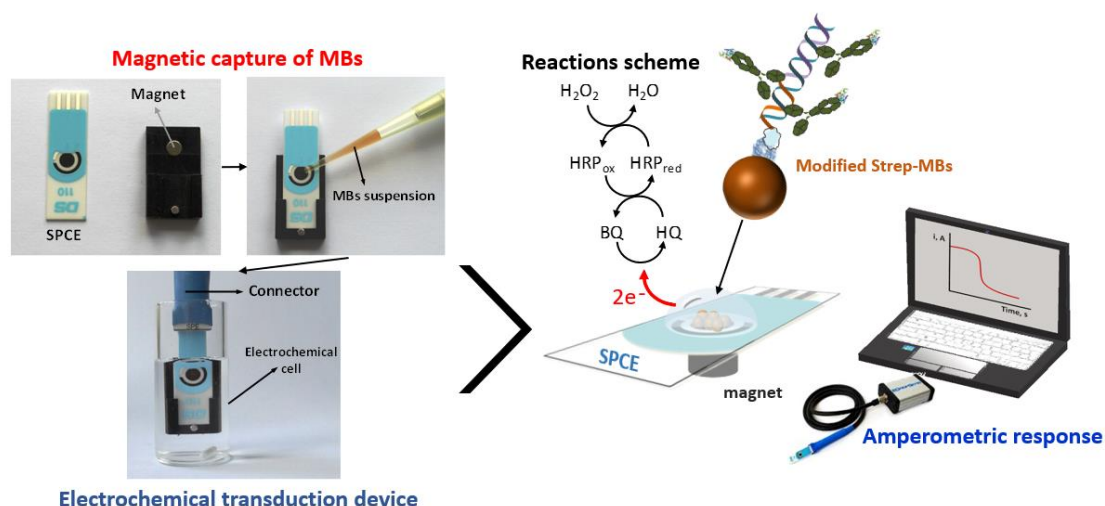


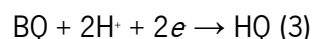
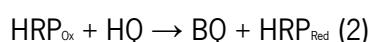
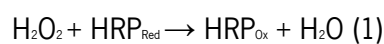
**Figure 5.** Schematic representation of the electrochemical transduction and amperometric response of the genosensor showing the procedure steps and the redox reaction on the SPCE.

### 3.2.4 Amperometric measurements

Amperometric measurements were performed in stirred solutions by immersing the SPCE/magnet holding block ensemble into an electrochemical cell containing 10 mL of 0.05 M sodium phosphate buffer solution (pH 6.0) and 1.0 mM HQ (recent preparation, *i.e.* just before performing the electrochemical measurement) and applying a detection potential of -0.20 V against the Ag pseudo-reference electrode of the SPCE. Once the baseline was stabilized, 50  $\mu$ L of a  $\text{H}_2\text{O}_2$  solution (0.1 M) was added, and the electrochemical current was recorded until a steady state was achieved. The magnitude of the measured cathodic current was directly proportional to the DNA target concentration.

In this research work, the HQ is used as an electroactive mediator of shuttling electrons from the electrode surface to the redox center of HRP (HRP was coupled to the RNA-DNA heteroduplex). Accordingly, the catalytic reduction mechanism of  $\text{H}_2\text{O}_2$  by the immobilized HRP can be described as: (i)  $\text{H}_2\text{O}_2$  substrate was reduced to  $\text{H}_2\text{O}$  by the immobilized HRP in reduced state ( $\text{HRP}_{\text{red}}$ ), and  $\text{HRP}_{\text{red}}$  itself will turn into its oxidized state  $\text{HRP}_{\text{ox}}$  (**Equation 1**); then, (ii) HQ can reverse  $\text{HRP}_{\text{ox}}$  back into  $\text{HRP}_{\text{red}}$  and be oxidized into benzoquinone (BQ) (**Equation 2**); and (iii) BQ can engage in electron exchange with the electrode and itself turns back into HQ (**Equation 3**). Therefore, HQ recycles in the system causing the amplification of the reduction current [150]. The reaction mechanism of the catalytic process can be expressed as follows:





### 3.3 Results and Discussion

**Figure 5** shows an outline of the fundamental concepts used to develop the electrochemical DNA sensor for the *sola / 7* detection. This sensor was based on the utilization of antibodies able to specifically bind, with a high degree of affinity, to DNA-RNA heterohybrids in a nucleotide sequence-independent manner for the nucleic acid determination. Briefly, Strep-MBs used as microplatform were modified with a specific RNA-bCp and used to selectively capture the synthetic DNA target. The sandwich hybridization assay was performed by incubating the RNA-bCp-MBs with the RNA-bDp and the DNA target in solution. The resulting heteroduplexes immobilized on the MBs were labelled with a specific DNA-RNA antibody previously labelled with a Protein A (ProtA) conjugated with HRP (ProtA-HRP). Then, the prepared MBs – bearing the HRP-labelled sandwich hybrids – were magnetically captured on the SPCE working electrode surface previously placed on a custom-fabricated magnetic holding block. The extent of the hybridization reactions was monitored by measuring the reduction current arising from the BQ formed in the HRP catalysed oxidation of HQ upon addition of a  $\text{H}_2\text{O}_2$  solution using amperometry in stirred solutions.

#### 3.3.1 Selection of oligonucleotide sequences for the DNA sensor construction

The design of a DNA sensor for the *sola / 7* specific detection requires the selection of a DNA and RNA sequence specific of the tomato seeds.

In this research, a 60-mer fragment of the tomato endogenous gene was amplified by using a pair of specific primers (mail-F/Mail-R) (**Table 5**) for the *sola / 7* identification. This sequence (DNA target) possesses a secondary structure with a Gibbs energy ( $\Delta G$ ) of  $-11.17 \text{ kcal mol}^{-1}$  under the assay conditions – *viz.*  $T = 37 \text{ }^\circ\text{C}$  and  $[\text{Na}^+] = 0.5 \text{ mol L}^{-1}$  – calculated using online tools [151] and suitable for DNA sensing. The capture and detector RNA probes were also designed to minimize secondary structures, while forming a perfect duplex structure after hybridization on the MBs [152]. The most stable RNA structures have a Gibbs energy of  $-4.0 \text{ kcal mol}^{-1}$  and  $-7.10 \text{ kcal mol}^{-1}$  for a 30 mer RNA capture probe and a 30 mer RNA detector probe, respectively. This

facilitates surface hybridization. All sequences are shown in **Table 5** and their structures are drawn in the **Figure 6**.

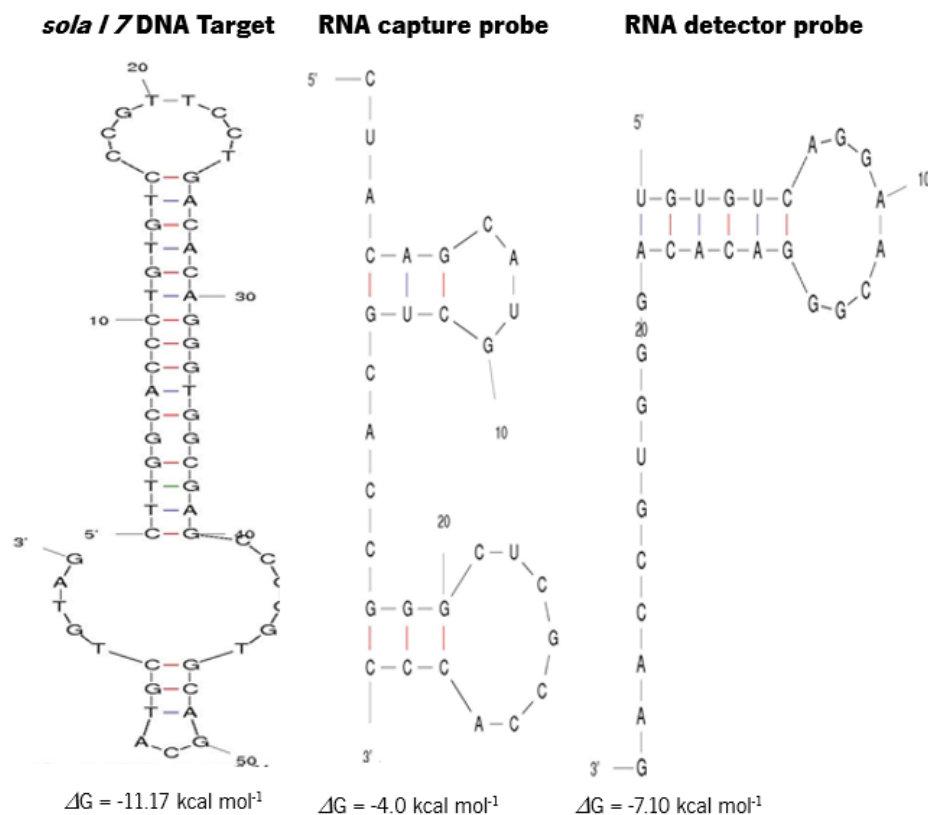


**Figure 6.** Oligonucleotides structures (data from [www.ncbi.nlm.nih.gov/blast](http://www.ncbi.nlm.nih.gov/blast)) [153].

### 3.3.2 Optimizations of the Experimental Conditions

In order to achieve the highest sensitivity and specific detection of *sola* / 7 DNA, all the experimental variables (*i.e.* concentration and incubation time of RNA-bCp, RNA-bDp, Prot A-HRP, IgG-HRP and anti-RNA/DNA, and the number of steps used to perform hybridization assay) involved in this electrochemical biosensing scheme were optimized by taking as criterion of selection the largest ratio between the amperometric responses measured at  $-0.20 \text{ V}$  for 0.0 (blank, B) and 1.00 or 0.01 nM for the synthetic DNA target (signal, S) (signal-to-blank, S/B, ratio) depending of the assay format on use.

It should be emphasized that the immobilization of oligonucleotide probes on the MBs to recognize its complementary DNA target via hybridization was the crucial step in the construction of electrochemical genosensors [154]. In this sense, a good DNA or RNA probe immobilization will promote a high reactivity and good orientation of the immobilized nucleic acid probe to hybridize with its complementary target [155].

The influence of the RNA capture probe concentration immobilized on the Strep-MBs and its incubation time was evaluated. **Figure 7** shows the amperometric responses obtained when a range of RNA-bCp concentrations between 0 and 0.5  $\mu\text{M}$  was employed. The highest ratio between signal and blank was obtained when RNA-bCp concentration of 0.25  $\mu\text{M}$  (**Figure 7 A**) was applied. The amperometric signal obtained for the blank assays (*i.e.* in the absence of DNA target) fluctuated (in the range between 600 and 1600 nA) relatively to the RNA-bCp concentrations (from 0 to 0.5  $\mu\text{M}$ ) because higher concentrations of capture probe promote non-specific bindings, thus increasing the amperometric signal. As a result, the RNA-bCp concentration of 0.25  $\mu\text{M}$  was used for further optimization steps.

Regarding the RNA-bCp incubation time in the Strep-MBs, the best ratio between signal and blank was obtained when the RNA-bCp was in contact with the MBs for 30 minutes (**Figure 7 B**). In this case, the blank signal was 1000 nA – and similar value in all the assays – because it was used the same oligonucleotide concentrations.

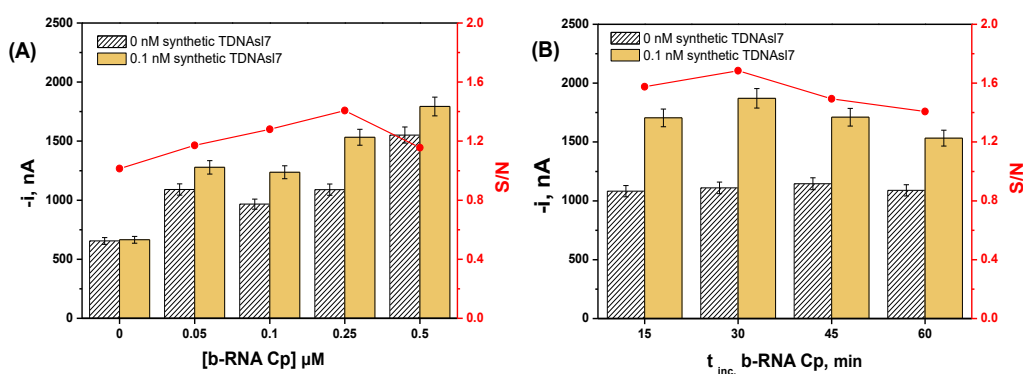


**Figure 7.** Influence of the RNA-bCp concentration (0.0; 0.05; 0.10; 0.25 and 0.50  $\mu\text{M}$ ) immobilized onto MBs (using 60 min of RNA-bCp incubation time) (**A**). Influence of the RNA-bCp (0.25  $\mu\text{M}$ ) incubation time (15; 30; 45 and 60 min) in the MBs (**B**) on the amperometric responses obtained in the DNA sensor optimization steps. Analytical features: 30 minutes for each incubation time of the DNA target and RNA-bDp (0.1  $\mu\text{M}$ ), antibody-RNA-DNA (1/500) plus protein A-HRP (1/500) (labeling mixture without pre-incubation). Blank=B, gray bars, and 0.1 nM of synthetic DNA target (signal, S, orange bars) and the corresponding S/B ratio values (in red) error bars estimated as the standard deviation of three replicates.

Aiming at attaining an easy and fast DNA sensor the number of steps used to perform the hybridization assay was also optimized. **Figure 8** shows a schematic display of the different protocols used. In the 1-step protocol (i), all the assay was performed in single assay. To such purpose, a mixture solution containing DNA target (0.1 nM), RNA-bDP (0.1  $\mu\text{M}$ ) and antiDNA-RNA-

ProtA-HRP (preincubated for 60 minutes) (1/500) was incubated in the RNA-bCp-MBs for 30 minutes. In the 2-step protocol, two distinct options were carried out. In the path (iiA), the RNA-bCp-MBs were incubated, for 30 minutes, in a solution containing 0.1 nM of DNA target and 0.1  $\mu$ M of RNA-bDp. Afterwards, the heteroduplex-MBs were mix with 1/500 antiDNA-RNA-ProtA-HRP for 30 minutes. On the other hand, in the other strategy (iiB) the 2-step protocol was done by incubating the RNA-bCp-MBs (30 minutes in each step), firstly only with the DNA target (0.1 nM) and then with a solution containing RNA-bDp (0.1  $\mu$ M) and an anti-DNA-RNA-ProtA-HRP (1/500). Finally, in the 3-step protocol (iii), the RNA-bCp-MBs were firstly incubated with the DNA target, then with the RNA-bDp and thenafter with the anti-DNA-RNA-ProtA-HRP.

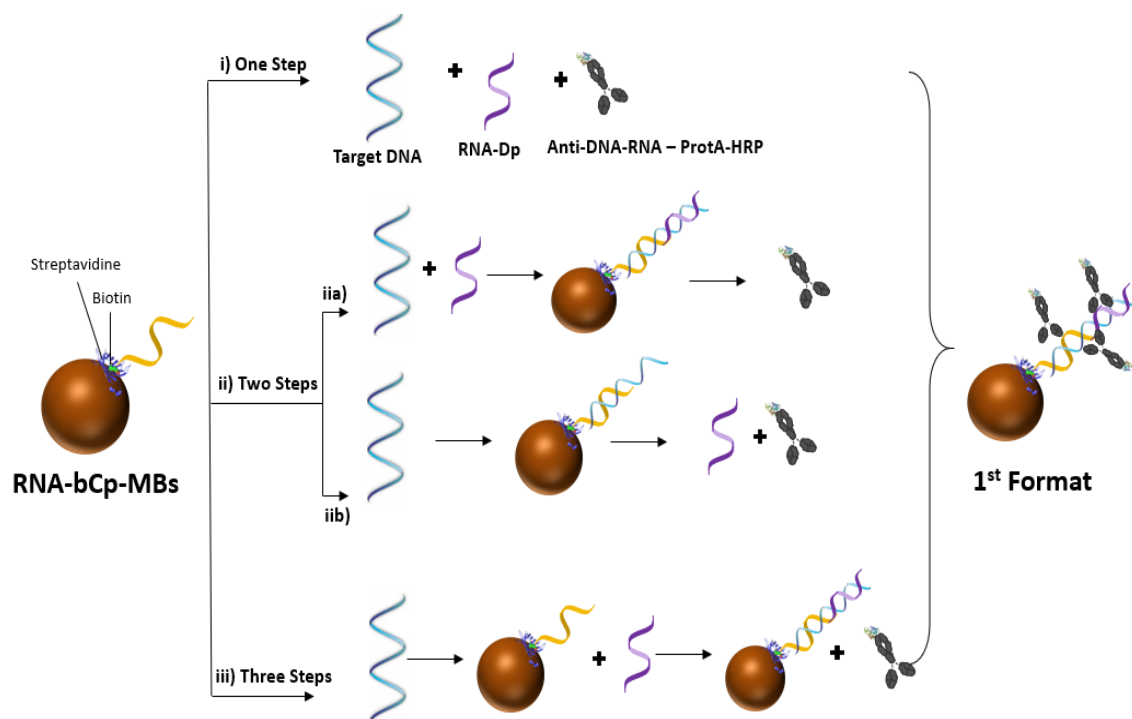


**Figure 8.** Schematic representation of the number of steps used on the hybridization protocol optimization: RNA-bCp 0.25  $\mu$ M; DNA target 0.1 nM, RNA-bDp 0.1  $\mu$ M, anti-DNA-RNA-ProtA-HRP (1/500), incubation time (each steps) 30 minutes.

The amperometric currents obtained for the blank assay and 0.1 nM of DNA target, as well the corresponding signal-to-blank (S/B) ratios for each protocol are presented in **Figure 9**. As observed, the hybridization assay allowed the discrimination between the blank and the DNA target signal in every protocol employed – thus, indicating that the hybridization reaction occurred. However, the largest S/B (2.0) was obtained when a two steps protocol (iia) was used. Indeed, the highest amperometric signal was measured when a mixture of DNA target and RNA-bDp was incubated with the modified MBs and after in the anti-DNA-RNA-ProtA-HRP. As reported by Montiel

and collaborators [108], such behavior can be attributed to the better recognition of the anti-DNA-RNA-ProtA-HRP for the formed heteroduplexes in the Strp-MBs.

Based on above, a two-step protocol involving the heterohybridization of the DNA target and RNA-bDp in the RNA-bCp-MBs and further the labelling of the heteroduplex-MBs with anti-DNA-RNA-ProtA-HRP was used in the next optimization assays.

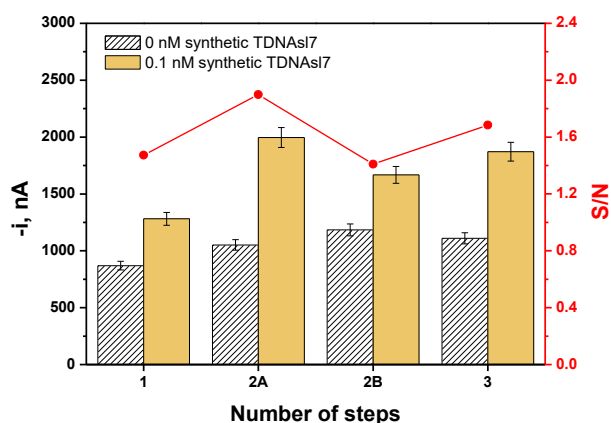


**Figure 9.** Influence of the number of steps used on the laboratorial protocol on the amperometric current. Analytical features: incubation time 30 minutes. (for each step); 0.1  $\mu\text{M}$  of RNA-bDp, antibody-RNA-DNA (diluted 1/500) and protein A-HRP (1/500) (mixture preincubated 60 minutes; (blank, B, grey bars); 0.1 nM of synthetic DNA target (signal, S, orange bars); and the corresponding S/B ratio values (in red). Error bars estimated as the standard deviation of three replicates.

The influence of the RNA-bDp concentration and the incubation time of detector probe and the target with RNA-Cp-MBs mixture was also scrutinized and optimized. The performance of the DNA sensor was evaluated using an RNA-bDp concentration range from 0 to 0.5  $\mu\text{M}$  (**Figure 10 A**) and an RNA-bDP incubation time between 15 to 60 minutes.

Regarding the correlation between the sensitivity with the length of the formed heteroduplex, a higher sensitivity was achieved when comparing a 30 mer heterohybrid (0  $\mu\text{M}$  RNA-bDp, in **Figure 10 A**) with a 60 mer heterohybrid (corresponding to the sandwich hybridization format) – the  $(S/B)_{60\text{ bp}} / (S/B)_{30\text{ bp}}$  ratio for the optimized RNA-bDp concentration was 3.3 (3.6/1.1). As expected, as longer the heterohybrid as larger the number of anti-DNA-RNA is able to label the DNA-RNA heteroduplex – thus, leading to a better recognition and, consequently, increasing the electrochemical signal and the sensitivity.

As depicted by **Figure 10 A**, the best S/B ratio was obtained when a concentration of 0.10  $\mu\text{M}$  of RNA-bDp was used. Regarding the incubation time of the DNA target and RNA-bDp with the RNA-bCp-MBs, the best analytical response was measured an incubation time of 30 min was employed.

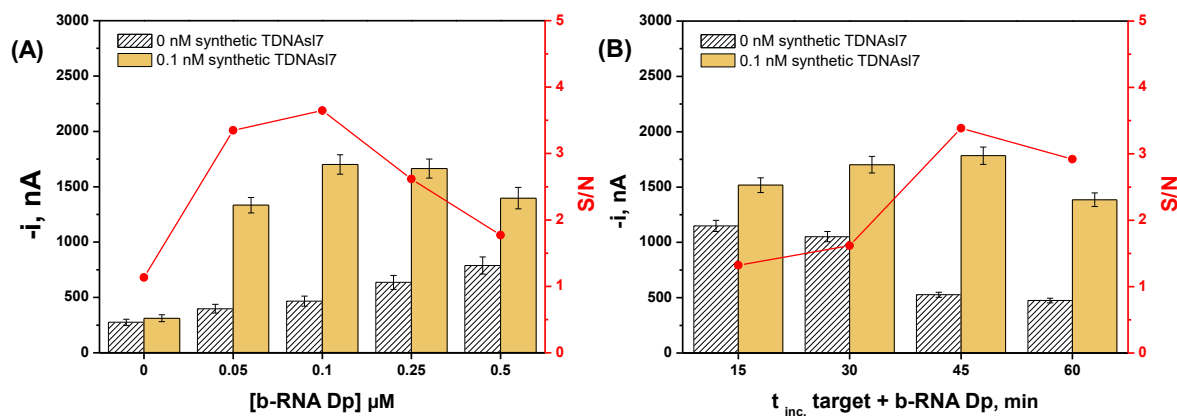


**Figure 10.** Influence of the RNA-bDp concentration (A) and the incubation time (B) on the amperometric current. Blank 0 nM of DNA target (B, gray bars), 0.1 nM of synthetic DNA target (signal, S, orange bars) and the corresponding S/B ratio values (in red). Error bars estimated as the standard deviation of three replicates.

Aiming at increasing the yield of antibody recognizing DNA-RNA hybrids, the concentration of the antibody-RNA-DNA – who is in charge to recognize heteroduplex formed by RNA-bCp + RNA-bDp + DNA target – was also inspected and optimized. **Figure 11** evidences that the optimal value for signal to blank ratio ( $S/B = 14.6$ ) comparatively to the other dilutions was achieved by using an Anti-DNA-RNA dilution of 1/1000.

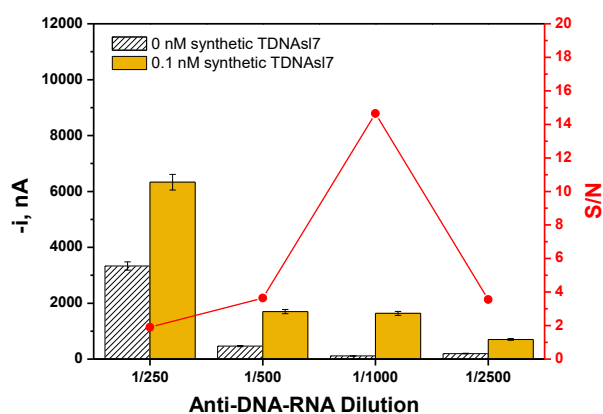


**Figure 11.** Influence of the Anti-DNA-RNA concentration of the amperometric current. Blank, B, gray bars and 0.1 nM of synthetic DNA target (signal, S, orange bars) and the corresponding S/B ratio values (in red). Error bars estimated as the standard deviation of three replicates.

The electrochemical signal amplification measured in the DNA sensor was performed using enzymatic label. To obtain the maximum amperometric current on the DNA detection, two different signal amplification formats strategies were employed. For that purpose, two enzymatic labels were tested, namely a bacterial protein conjugated with horseradish peroxidase (ProtA-HRP) and an anti-mouse immunoglobulin G conjugated with horseradish peroxidase (antiligG-HRP). **Figure 12** represents a succinct schematic representation of the electrochemical signal amplification promoted by enzymatic labels. The labels ProtA-HRP (1<sup>st</sup> format) or AntiligG-HRP (2<sup>nd</sup> format) were conjugated with the anti-DNA-RNA, which selectively recognized the formed heteroduplex.

The influence of the concentration of the enzymatic label and its incubation time in the antiDNA-RNA-heteroduplex-MBs on the amperometric signal was studied (**Figure 13**). As clearly noticed (**Figure 13 A** and **B**), the use of the ProtA conjugated with the HRP amplified significantly the amperometric signal. Indeed, the highest S/B ratio value (S/B = 14,6) was calculated for the dilution of 1/250 of ProtA-HRP. In what concerns the ProtA-HRP or AntiligG-HRP incubation time in the Anti-DNA-RNA-hybrid-MBs, the best S/B ratio value (S/B = 34,1) was obtained when the ProtA-HRP was incubated during 45 minutes in the heteroduplex-MBs.

Although the best analytical results were obtained when the ProtA-HRP was used as label, the analytical study of sensitivity was performed by using these two strategies.

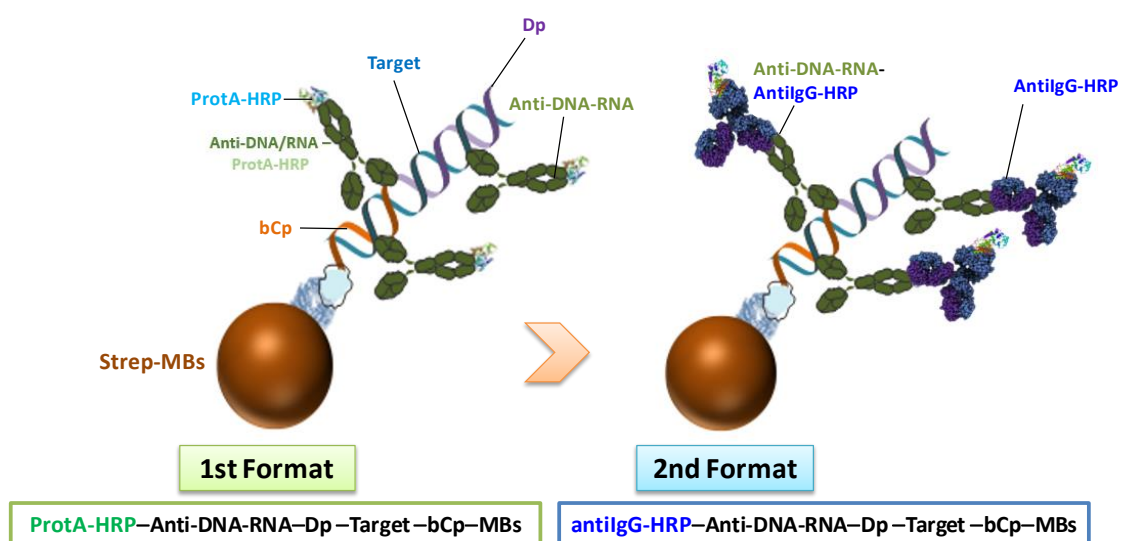


**Figure 12.** 1st format: 1st electrochemical signal amplification format. 2nd format: 2nd electrochemical signal amplification format.

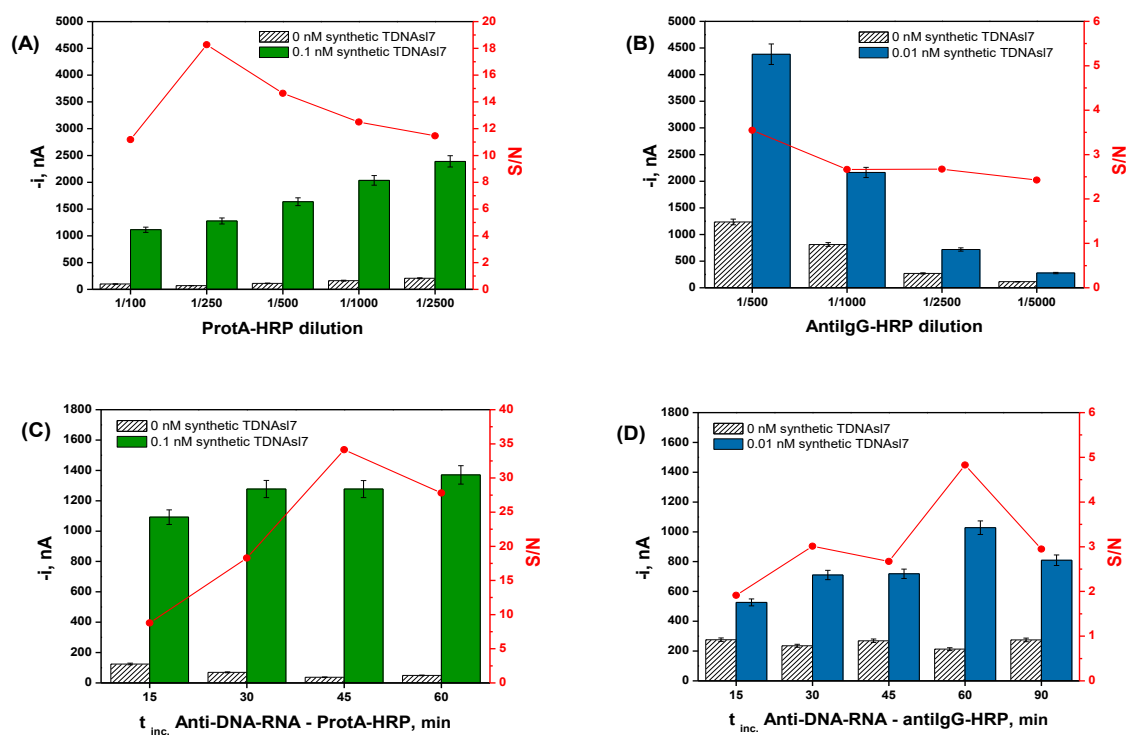


**Figure 13.** Amperometric currents obtained on the electrochemical signal amplification optimization. Blank, B, gray bars, 0.1 nM of synthetic DNA target (signal, S, orange bars) and the corresponding S/B ratio values (in red). Error bars estimated as the standard deviation of three replicates.



### 3.3.3 Analytical characteristics of the electrochemical DNA sensor

Under the optimized experimental conditions (**Table 6**), the influence of increasing the synthetic *soja* / 7 DNA target concentration on the analytical signal was assessed by measuring the amperometric current from 0.8 to 100 pM (**Figure 14**). When the ProtA-HRP as enzymatic label was used, a linear correlation ( $r = 0.9992$ ) between the amperometric intensity and the *soja* / 7 DNA target was found within the range of 3.7 to 100 pM, with a slope and intercept values of 13936 nA nM<sup>-1</sup> and 89 nA, respectively.

$$3 \times sb/m \quad (4)$$

$$10 \times sb/m \quad (5)$$

LOD and LQ were calculated according to the expression **4** and **5** criteria, respectively, and where  $m$  is the slope of the linear calibration plot and  $sb$  was estimated as the standard deviation of ten amperometric measurements obtained in the absence of target DNA. Using this enzymatic amplification format, a LOD of 1.1 pM (corresponding to a detectable absolute amount of 27.5 attomoles) and a LOQ of 3.7 pM were achieved.

These characteristics were compared with those obtained by preparing the electrochemical genosensor using the AntilgG-HRP as enzymatic label (**Table 7**). In this enzymatic format, a calibration curve for synthetic DNA *soja* / 7 (**Figure 14**) target exhibited a linear dependence ( $r = 0.9997$ ) for DNA concentrations between 0.8 to 50 pM. Using these conditions, a slope of 74678 nA. nM<sup>-1</sup> and an intercept of 256 nA was calculated. The LOD and the LOQ were 0.2 pM and 0.8 pM, respectively. The achieved LOD (0.2 pM) corresponds to a detectable absolute amount of 5 attomoles of DNA with no need for using any amplification technique (considering that the sample volume required per analysis is 25  $\mu$ l). As shown in **Table 7**, the use of the AntilgG-HRP label improved the sensitivity of the DNA sensor by 5.8 times with respect to the ProtA-HRP (74678 nA nM<sup>-1</sup> vs 13936 nA nM<sup>-1</sup>) and a LOD lower 1.38 times (3.7 pM vs 0.2 pM). These results highlighted the potential of the developed methodology for the detection of *soja* / 7 DNA in food samples.

**Table 6.** Optimization of the experimental variable

Variables	Tested range	Selected value
RNA-bCp, $\mu\text{M}$	0.0 – 0.5	0.25
Incubation time RNA-bCp, min	15 - 60	30
Incubation number steps	1 - 3	2
RNA-bDp, $\mu\text{M}$	0.0 – 0.5	0.1
Incubation time RNA-bDp, min	15 - 60	30
Anti-DNA-RNA concentration (dilution)	1/250 – 1/2500	1 / 1000
ProtA-HRP concentration (dilution)	1/100 – 1/2500	1/250
Incubation time Anti-DNA-RNA-ProtA-HRP, min	15 - 60	45
AntilgG-HRP concentration (dilution)	1/500 – 1/5000	1/500
Incubation time Anti-DNA-RNA-ProtA-HRP, min	15 - 90	60

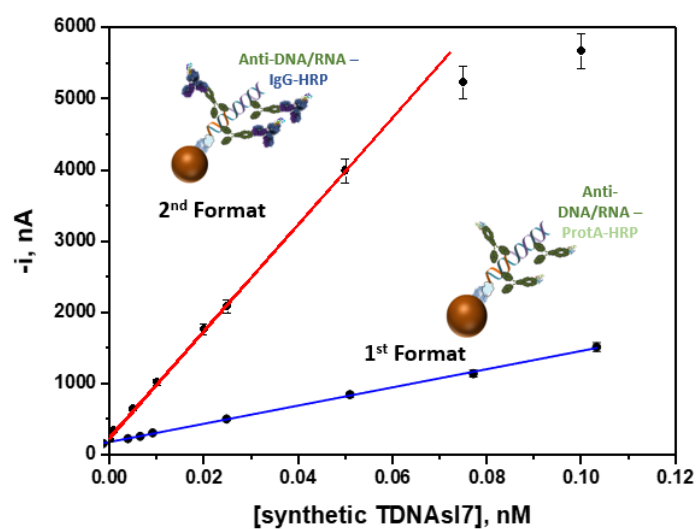


**Figure 14.** Calibration plot obtained for the synthetic DNA target with the developed DNA sensor using the ProtA-HRP and AntilgG-HRP as enzymatic label.

**Table 7.** Analytical characteristics obtained for the determination of LTPs using ProtA-HRP or AntilgG-HRP as enzymatic label

Parameters	ProtA-HRP-Hybrid-MBs	AntilgG-HRP-Hybrid-MBs
r	0.9992	0.9997
Slope, nA, nM <sup>-1</sup>	13936 ± 149	74678 ± 740
Intercept, nA	89 ± 7	256 ± 17
LR, pM	3.7 - 100	0.8 - 50
LOD, pM	1.1	0.2
LQ, pM	3.7	0.8

The reliability of the genosensor was evaluated by calculating the relative standard deviation (RSD) value for the amperometric current for 0.05 nM (1<sup>st</sup> format) and 0.025 nM (2<sup>nd</sup> format) of synthetic DNA target provided by 8 different genosensors prepared in the same manner. The calculated RSD was 4.4 % (in both enzymatic amplification scheme) demonstrated a good reproducibility of the whole procedure including the genosensor fabrication (MBs modification, hybridization reaction and magnetic capture on the SPE surface) and the amperometric transduction.

The storage stability of the heteroduplex-MBs was evaluated by storing the DNA sensor at 4 °C in eppendorf tubes containing 50 µl of buffer solution. No significant differences in the S/B ratio of the amperometric measurements with 0.01 nM of synthetic DNA target were obtained for

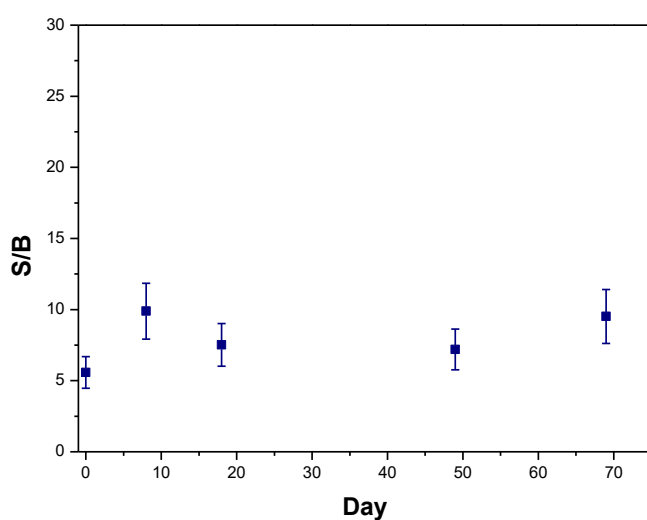


**Figure 15.** Storage stability. S/B ratio values of 0.01 nM of DNA synthetic target. Error bars estimated as the standard deviation of three replicates.

a period of 69 days indicating great stability of the RNA-bCp-MBs, and allowing their preparation and storage in advance until the amperometric measurements until it has to be analyzed (**Figure 15**).

The selectivity of the developed DNA biosensor was studied through heteroduplex hybridization of the RNA-bCp and RNA-bDp with complementary DNA target, single-base mismatched DNA (1-m), two-base mismatched DNA (2-m) and three-base mismatched DNA (3-m) and noncomplementary DNA target. When the noncomplementary DNA sequence were used on the hybridization assay, the current intensities were similar to the blank assay (no DNA target), suggesting that the hybridization reaction did not occurred. Observing the **Figure 16**, it is possible to see that the amperometric answer displayed discrimination between the complementary and the mismatched DNA target. In fact, a decrease of 23%, 40% and 50 % (when compared with the complementary DNA) on the analytical answer were find when the 1-m, 2-m and 3-m was used, respectively. These results suggested that the developed DNA sensor presents good selectivity and specificity and have a great potential for the DNA polymorphism analysis.

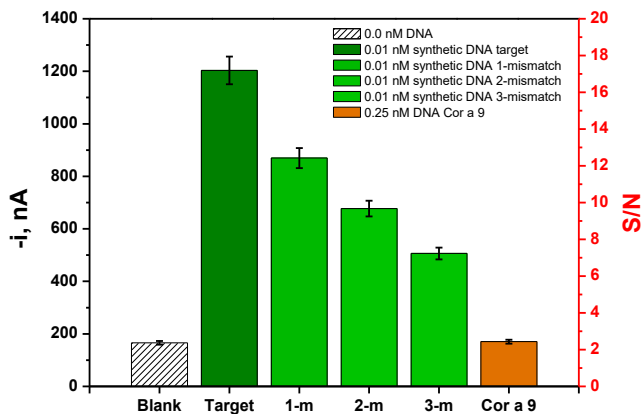


**Figure 16.** Amperometric responses measured when a complementary, mismatched DNA target and non-complementary DNA (*cor a 9*) to the RNA capture and detector probe was used. Error bars estimated as triple of the standard deviation of three replicates.

### 3.3.4 Application of the DNA sensor genosensor to detect *Sola I 7* in tomato samples

The proposed amperometric DNA sensor was applied to detect the *sola I 7* DNA endogenous gene in the whole genomic DNA extracted from tomato seeds and tomato peel. Two different extraction methods were applied to extract genomic DNA from the tomato (seeds and peel), namely the (Hexadecyl trimethyl-ammonium bromide (CTAB) and the sodium dodecyl sulfate (SDS)). In both cases, the amount of extracted DNA analyzed was 100 ng (taking into account the high sensitivity of the developed biosensor, able to detect only 5 attomoles of the synthetic *sola I 7* DNA). Similarly, to synthetic oligonucleotide, 25  $\mu$ L of the extracted DNA were mixed to the solution containing RNA-bDp and incubated with the RNA-bCp-MBs for 30 min. The signal was recorded after the generation of the heteroduplex (for 30 min, at 37° C and 950 rpm) and labelling the amperometric.

As depicted in **Figure 17**, a noticeable amperometric current discrimination between tomato and maize was attained. Indeed, the analytical current obtained for the DNA extracted from the tomato seeds was clearly distinguished from the blank measurement, indicating undoubtedly the presence of *sola I 7* in the seeds. Moreover, best analytical results were found when the DNA

was extracted with the CTBA reagent, therefore indicating that this procedure was more effective on the DNA extraction.

Furthermore, the electrochemical current obtained when it was used the DNA extracted from the tomato peel was lower 4,1 times than those obtained from the DNA extracted from the seeds. As reported by Martín-Pedraza (2016) [31], such behavior was expected to be observed since the tomato peel contains very small amounts of *sola* / 7 [31].

As a negative control, DNA extracted from maize was also subjected to the same experimental procedure and afterwards similarly evaluated with the DNA sensor.

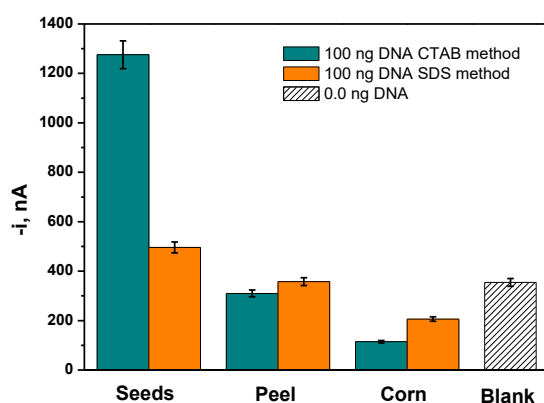


**Figure 17** the obtained analytical current was smaller than the blank signal, thus confirming the selectivity of the methodology.

### 3.3. Conclusions

This research effort presents a novel disposable electrochemical DNA sensor combining the use of selective RNA capture probes with magnetic microbeads technology for the unambiguous identification and detection of the allergen *sola* / 7 in tomato seeds. Two distinct approaches were studied and compared: the first approach use protA-HRP and the second antilgG-HRP as enzymatic label, corresponding to the so-called first and second format, respectively (**Figure 14**). Both approaches demonstrated excellent analytical characteristics for the sensitive detection of the DNA target without previous amplification or preconcentration of the genetic material, but the format based on the labelling with the antilgG-HRP provided a sensitivity 5.4 times higher and a LOD 5.5

times lower. Therefore, it is a rather stable and really specific probe and the main function of this first aim was achieved, resulting in a sensitive limit of *so/a / 7* DNA detection (5 attomoles of target).

In conclusion, this research resulted successfully in a new electroanalytical platform for the selective, sensitive, accurate, reliable and reproducible determination of *so/a / 7* gene in fruits without genetic material amplification or preconcentration necessary. The methodology also demonstrated to be easily translated towards the determination of other analytes of interest in decentralized applications. Besides the use of specific RNA capture and detector probes and of a commercial antibody with high affinity for RNA-DNA heteroduplexes achieved great selectivity methodology and, in general, it showed to be advantageous when compared with others commonly used in terms of simplicity, cost-effectiveness, assay time-consuming and portability of the required instrumentation – which makes them reliable and promising analytical tools for food quality and safety and, ultimately an important contribution to the consumer's protection.

## **4 Development of a magnetoimmunosensor and dual magnetobiosensor for *Sola I 7* determination**

### **4.1 Introduction**

Tomato allergic reactions are very relevant in Mediterranean areas where this vegetable fruit is deeply implemented in the diet of these populations. As an example, approximately 6.5 % among patients attending allergy clinics in the Mediterranean coast of Spain exhibit tomato sensitization, and 0.3 % self-reported worldwide exhibits allergy to the tomato [133] Sola I 7 – and belongs to class 1 in the family member of nsLTPS according to molecular mass of 9KDa. This allergen was identified in large concentration on tomato seeds and it is one of the key allergens related with several symptoms in individuals with tomato allergy [31].

Antibodies, also called immunoglobulins (Ig), are a large family of glycoproteins capable of recognizing antigens with high specificity. They are composed of one or more copies of a characteristic unit that can be visualized by its ‘Y’ shape. Many analytical devices explore these affinity interactions between antibody and antigen complex for detection and measurement in a wide range of applications, for instance in environmental analysis and food safety.

Indeed, immunoassays (antibodies or antigens detection) are presently the method of choice for detection and identification of food allergens. In addition, the most widely immunoassay used is ELISA, offering as low detection limits as around  $10^{-12}$  to  $10^{-9}$  M. In contrast, ELISA present important disadvantages, such as the complexity of the work flow assay, the use of expensive reagents, the bulky ELISA readers and time-consuming operation [156].

In turn, electrochemical immunosensors are affinity biosensors in which selective and high affinity antibodies bind to their antigens (analytes) to produce a measurable electrochemical signal and form a stable complex [6]. Because of the strong binding forces between these biomolecules, immunosensors present high selectivity and sensitivity, and the utilization of electrochemical detection confers specificity, simplicity, portability, generally disposable and can carry out *in situ* or automated detection, thus making from them very attractive tools for a number of applications in different scientific fields – especially in food allergen analysis, such as milk allergens, peanut, hazelnut [157].



Heating and other processing treatments modify (among others) protein structure and, consequently, the results which use proteins as analytes. For transgenic proteins – where there is a lack of antibodies – and for allergenic proteins – whose sequence is conserved among different species, hampering the discrimination ability of the antibodies. Consequently, since the introduction of the PCR technique, DNA has been the target of choice due to its relatively high stability in processed products. In this sense, genosensors are DNA biosensors that rely on a hybridization recognition reaction between two complementary strands, *viz.* the target and the recognition element called probe. Electrochemical DNA sensors can provide low detection limits [1], [2], [106], but it is worth to mention that electrochemical immunosensors are more friendly user.

Alves *et al.* (2015) [158], reported the detection of Ara h 1 and Ara h 6 by using two electrochemical immunosensors based on modified gold nanoparticle-coated screen-printed carbon electrodes. In both cases, two monoclonal antibodies were used in a sandwich-type immunoassay and the antibody-antigen interaction was electrochemically detected through stripping analysis of enzymatically (alkaline phosphatase) deposited silver. The developed immunosensors allowed the quantification of Ara h in the range of  $\text{ng mL}^{-1}$ , and with a LOD of 3.8 and  $0.27 \text{ ng mL}^{-1}$  for Ara h 1 and for Ara h 6, respectively. The immunosensors were successfully applied to Ara h detection in complex food matrices, such as cookies and chocolate.

Pingarron's group reported several immunosensors for the detection of different allergens [60], [92], [93]. The concept used in this work is the same used in their previous works, which involves the use of selective capture and detector antibodies implemented on carboxylic acid-modified magnetic beads – captured magnetically under the surface of a disposable screen-printed carbon electrode for amperometric detection using the hydroquinone (HQ)/ $\text{H}_2\text{O}_2$  system. The magnetic beads (MBs)-based sandwich immunosensor displays the covalent binding of the primary antibody onto the COOH-MBs surface via amidic groups. Prior to use, the COOH-MBs were activated with EDC/sulfo-NHS solution and after the primary antibody incubation step. By adding an ethanolamine solution, the unreacted activated groups on the MBs were blocked. The anti-solal7-MBs were further incubated with different target concentration solutions, followed by the affinity reaction with the HRP-labelled secondary antibody. The MBs bearing the sandwich immune-complexes were captured magnetically on the electrode surface by placing SPCEs on a custom-fabricated magnetic holding block, and the biorecognition event was monitored by amperometric

measurement of the reduction current generated with the HQ/H<sub>2</sub>O<sub>2</sub> system. Milk allergens, such as  $\alpha$ -lactalbumin ( $\alpha$ -LA) and  $\beta$ -lactoglobulin ( $\beta$ -LG), were specifically determined from standard solutions recovering a LOD of 11.0  $\mu\text{g mL}^{-1}$  and 0.8  $\text{ng mL}^{-1}$  for  $\alpha$ -LA and  $\beta$ -LG, respectively [60], [92], [93].

In the present work, novel magnetoimmunosensor to detect Sola I 7 protein and a dual magnetobiosensor to detect Sola I 7 protein and *sola* / 7 DNA sequence are developed and described. The magnetoimmunosensor developed uses a sandwich format employing HOOC-MBs as immobilization platform and SPCEs as transduction platform. A specific capture mouse polyclonal antibody for Sola I 7 recognition was immobilized onto HOOC-MBs surface previously activated with EDC/sulfo-NHS. After blocking the un-reacted activated groups of the HOOC-MBs with ethanolamine, the target protein was sandwiched with the complex detector HRP antibody.

In the case of the dual magnetobiosensor construction, the procedure of immobilization was similar as those described in **Chapter 3** for the DNA sequence detection (genoassay) and the same construction method for the immunoassay as described (in this chapter) for *sola* I 7 protein determination.

Both, the magnetoimmunosensor and dual magnetobiosensor, carried out the amperometric detection at SPCEs or SPdCEs using the HQ/HRP/H<sub>2</sub>O<sub>2</sub> system – which has shown to be very efficient in amperometric detection for enzyme-labeled biosensing devices. The sensitivity of the magnetoimmunosensor reached a LOD of 1.4  $\mu\text{g mL}^{-1}$ . The selectivity of the sensor was also studied by using 5 different standard allergens from different fruits and a high selectivity was attained. Furthermore, to complete the characterization of the magnetoimmunosensor an assay using real samples of Sola I 7 extracted from tomato seeds and peel was used. As a result, it was concluded that the biosensor can be employed as an analytical procedure to identify the Sola I 7 allergen in real food matrixes.

## **4.2 Material and Methods**

### **4.2.1 Apparatus and electrodes**

Amperometric measurements were performed with a CHI812B potentiostat (CH Instruments) controlled by software CHI812B. The electrochemical transducers employed were screen-printed carbon electrodes (SPCEs) (DRP-110, DropSens, Spain) for the magnetoimmunosensor consisting of a 4-mm diameter carbon working electrode and a screen-

printed dual carbon electrodes (DRP-C1110, Dropsens) composed of two elliptic carbon working electrodes (6.3 mm<sup>2</sup> each). For the dual, a carbon counter electrode and an Ag pseudo-reference electrode were employed as transducers. Specific cable connectors ref. DRP-CAC or ref. DRP-BICAC (also from DropSens) were used, both acting as interface between the SPCEs/SPdCEs and the potentiostat. All measurements were carried out at room temperature.

A Bunsen AGT-9 Vortex was used for the homogenization of the solutions. A Thermomixer MT100 constant temperature shaking incubator (Universal Labortechnik,) and a magnetic separator Dynal MPC-S (product no. 120.20, Dynal Biotech ASA, were also employed. Capture of the modified-MBs in the SPCE surface was controlled by a neodymium magnet (AIMAN GZ embedded in a homemade casing of Teflon.

#### **4.2.2 Chemicals and solutions**

All the reagents were of highest available grade. Sodium di-hydrogen phosphate (H<sub>2</sub>NaO<sub>4</sub>P.2H<sub>2</sub>O), di-sodium hydrogen phosphate (Na<sub>2</sub>HPO<sub>4</sub>), Tris-HCl [Tris-HCl, tris(hydroxymethyl)aminomethane hydrochloride, NH<sub>2</sub>C(CH<sub>2</sub>OH)<sub>3</sub>.HCl], sodium chloride (NaCl) and potassium chloride (KCl) were purchased from Scharlab Tween®20, N-(3-dimethylaminopropyl)-N'-ethylcarbodiimide (EDC), N-hydroxysulfosuccinimide (sulfo-NHS), ethanolamine (C<sub>2</sub>H<sub>7</sub>NO), hydroquinone (HQ, benzene-1,4-diol or quinol, C<sub>6</sub>H<sub>6</sub>O<sub>2</sub>), hydrogen peroxide (H<sub>2</sub>O<sub>2</sub>) 30% (w/v) and albumin from chicken egg white (OVA) were purchased from Sigma Aldrich. 2(N-Morpholino) ethanesulfonic acid (MES, C<sub>6</sub>H<sub>13</sub>NO<sub>4</sub>S) and commercial blocker casein solution [ready-to-use, Phosphate-buffered saline (PBS) 1% (w/v) solution of purified casein) was purchased from Thermo Scientific. Carboxylic acid-modified MBs (HOOC-MBs, 2.7 µm Ø, 10 mg mL<sup>-1</sup>, Dynabeads® M-270 Carboxylic Acid) were purchased from Dynal Biotech ASA.

All buffer solutions were prepared with water from Millipore Milli-Q purification system (18.2 MΩ cm). PBS consisted in 0.01 M phosphate buffer solution containing 137 mM NaCl and 2.7 mM KCl. Phosphate-buffered saline (PBS) consisted in 0.01 M phosphate buffer solution containing 0.137 M NaCl and 0.0027 M KCl, pH 7.5. 0.05 M phosphate buffer (pH 6.0); 0.1 M phosphate buffer, pH 8.0; 0.025 M MES buffer, pH 5.0 and 0.1 M Tris-HCl buffer, pH 7.2. Activation of the HOOC-MBs was carried out with an EDC/sulfo-NHS mixture solution (50 mg mL<sup>-1</sup> each in MES buffer, pH 5.0). The blocking step was accomplished with a 1 M ethanolamine solution prepared in a 0.1 M phosphate buffer solution at pH 8.0.

Polyclonal mouse capture antibody and polyclonal mouse HRP conjugated antibody were used for Sola I 7 determination was developed.

#### **4.2.3 Construction of the amperometric immunosensor**

The whole experimental procedures were performed at room temperature and without biosafety cabinet. HOOC-MBs were used as magnetic electrochemical platform for the biosensor construction. First, an aliquot of 3  $\mu\text{L}$  of a well dissolved HOOC-MBs was deposited in 1.5  $\mu\text{L}$  eppendorf. Two washes were then carried out with 50  $\mu\text{L}$  of filtrated MES during 10 minutes at 950 rpm. Each clean step was followed by the magnetic separation of the MBs-suspension in 4 minutes and the supernatant was discarded.

The carboxylic groups of MBs were activated by incubation during 35 minutes in 25  $\mu\text{L}$  of the EDC/sulfo-NHS mixture solution. The typical procedure for ligand coupling is the formation of an amide bond between a primary amino group of the ligand and the carboxylic groups on the surface of the HOOC-MBs, mediated by EDC. The intermediate product of the reaction between the carboxylic acid and the carbodiimide is very labile and hydrolyses quickly. Alternatively, the activated HOOC-MBs can be captured as a less labile intermediate, such as an N-hydroxyl succinimide ester (NHS), and then react with the ligand over a longer period.

The activated MBs were washed twice with 50  $\mu\text{L}$  of MES buffer and re-suspended in 25  $\mu\text{L}$  of a 5  $\mu\text{g mL}^{-1}$  cp-anti-solaI7, prepared in MES buffer and, afterwards, incubated during 15 min at room temperature and 950 rpm. Two washes with 50  $\mu\text{L}$  of MES buffer was carried out before the blocking step. The unreacted activated groups on the MBs were blocked by adding 25  $\mu\text{L}$  of the 1 M ethanolamine solution in 0.1 M phosphate buffer pH 8.0, and incubating the suspension under continuous stirring (950 rpm) for 60 min at room temperature.

Later on, the blocked MBs was washed once with 50  $\mu\text{L}$  of TRIS-HCl 0.1 M pH 7.2 and repeated twice with 50  $\mu\text{L}$  of PBS. Subsequently, 25  $\mu\text{L}$  of sola I 7 target (or the sample under scrutiny) prepared in PBS pH 7.5, then incubated during 30 minutes at room temperature and 950 rpm. Then it was followed by two washing procedures with 50  $\mu\text{L}$  of blocking buffer (PBS solution of 1% w/v purified casein). The final incubation of the target-cp-anti-solaI7-MBs occurred during 30 min (25  $^{\circ}\text{C}$ , 950 rpm) with 25  $\mu\text{L}$  of anti-solaI7-HRP complex (1:50 dilution factor) in the blocking buffer and washed again twice with blocking buffer. The modified-MBs were re-suspended

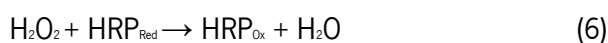
in 45  $\mu\text{L}$  of 0.05 M sodium phosphate buffer solution (pH 6.0) to perform the amperometric detection.

#### 4.2.4 Amperometry measurements

Amperometric measurements of the solutions were performed under stirring – by immersing the SPCE/magnet holding block ensemble into an electrochemical cell containing 10 mL of 0.05 M sodium phosphate buffer solution (pH 6.0) and 1.0 mM HQ (prepared just before performing the electrochemical measurement) – and applying a detection potential of  $-0.20\text{ V}$  vs the Ag pseudo reference electrode of the SPCE. Once the baseline was stabilized, 50  $\mu\text{L}$  of a  $\text{H}_2\text{O}_2$  solution (0.1 M) was added, and the electrochemical current was recorded until a steady-state was achieved. The magnitude of the measured cathodic current was directly proportional to the Sola I 7 target concentration.

The procedure and devices employed for carrying out the amperometric measurements are those shown in **Chapter 3**.

In the current research work, the HQ was used as an electroactive mediator of shuttling electrons from the electrode surface to the redox center of HRP (HRP was coupled to the detector antibody). Consequently, the catalytic reduction mechanism of  $\text{H}_2\text{O}_2$  by the immobilized HRP can be described as follows. First, the (i)  $\text{H}_2\text{O}_2$  substrate was reduced to  $\text{H}_2\text{O}$  by the immobilized HRP in reduced state ( $\text{HRP}_{\text{Red}}$ ), and  $\text{HRP}_{\text{Red}}$  itself turns into its oxidized state  $\text{HRP}_{\text{Ox}}$  (Equation 1). Then, the (ii) HQ can reverse  $\text{HRP}_{\text{Ox}}$  back into  $\text{HRP}_{\text{Red}}$  and be oxidized into benzoquinone (BQ) (**Equation 6**). The (iii) BQ can engage in electron exchange with the electrode and itself turns back into HQ (**Equation 8**). Therefore, HQ recycles in the system causing the amplification of the reduction current [150]. The reaction mechanism of the catalytic process can be expressed as:



### 4.3 Results and Discussion

**Figure 18** gives the schematic representation of the immunosensor biorecognition display. The capture antibody was the affinity to detect Sola I 7 protein as well as the detection

antibody – which is the one who reported the chemical signal through redox reaction of HRP-complex.

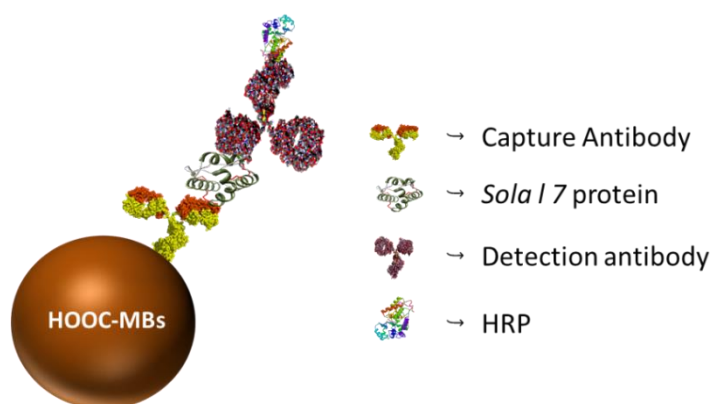


**Figure 17.** Microcarrier structure holding the schematic biorecognition display of the immunosensor without transducer.

#### 4.4 Optimizations of the experimental conditions

The capture antibody and the detection antibody were optimized in terms of concentrations and incubation time. It was also useful to optimize the number of steps needed in the experimental procedure, so as to reduce the time assay. All the variables studied were summarized in **Table 8**, where the selected experimental values of each variable is also given. In the case of the HOOC-MB's, the selected incubation and washing buffers' volumes, and the detection potential used were previously optimized and may be found in Gamella M. *et al.* [159] and Ávila *et al.* [160], as well as the selection of the commercial blocking buffer – which has been proven to be highly effective for minimization of non-specific adsorptions [60], [92][60], [92]. The selection criterion for each variable was the magnitude of the ratio between the amperometric responses measured at -0.20 V in the presence (signal, S) of  $5.0 \mu\text{g mL}^{-1}$  Sola I 7 and in the absence of target protein (blank, B) (S/B ratio).

**Table 8.** Optimization of the experimental variables involved in the magnetoimmunosensor to sola I 7 developed.

<b>Variables</b>	<b>Tested range</b>	<b>Selected value</b>
Cp-anti-solaI7, $\mu\text{g mL}^{-1}$	0 – 50	5
Incubation time cp-anti-solaI7, min	15 – 60	15
Incubation number steps	1 – 2	2
anti-solaI7-HRP concentration, dilution	1:5 – 1:100	1:50
Incubation time anti-solaI7-HRP, min	15 – 60	30

The influence of the cp-anti-solaI7 concentration in the amperometric signals were investigated in the range from 0  $\mu\text{g mL}^{-1}$  to 50  $\mu\text{g mL}^{-1}$ . As observed in **Figure 19 A**, the intensity current of the blank increases in direct proportion to the cp-anti-solaI7 concentration until 25  $\mu\text{g mL}^{-1}$ . Furthermore, above such concentration the current intensity S/B decreases – probably as a consequence of a steric hindrance that hinders the formation of the antigen-antibody complexes for high concentrations of immobilized capture antibody. The optimal concentration was found to be of 5  $\mu\text{g mL}^{-1}$ , once the highest S/B value of 2.5 was obtained. After the cp-anti-solaI7 concentration optimization, the incubation time was performed during the time periods of 15, 30 and 60 minutes with 10  $\mu\text{g mL}^{-1}$  of Sola I 7 and a dilution of 1:5 anti-solaI7-HRP (**Figure 19 B**). The results of the amperometric responses demonstrated a ratio of 4.2 signal to blank (S/B) as the optimum value selected – which corresponds to the 15 minutes of cp-anti-solaI7 incubation time.

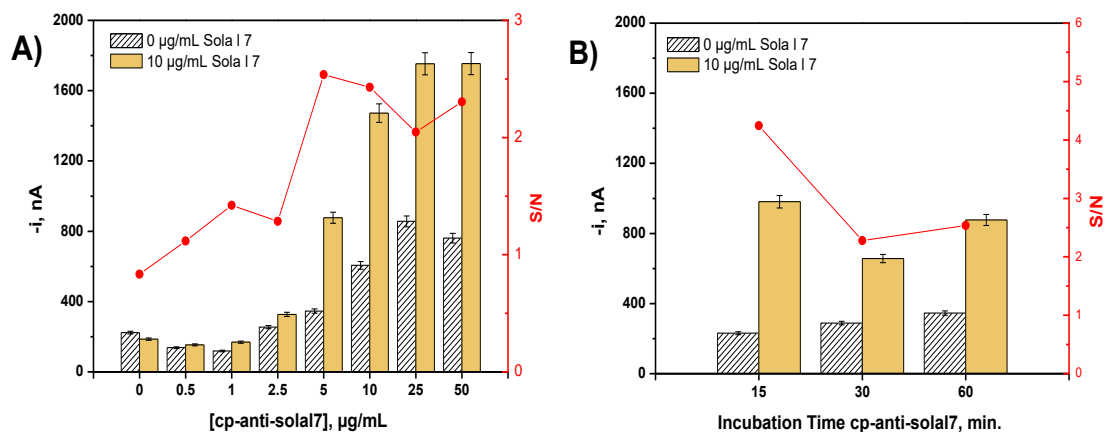


**Figure 18.** Amperometric responses obtained in the optimization of the capture antibody concentrations where  $5 \mu\text{g mL}^{-1}$  was the optimal concentration (A) and incubation time of the cp-anti-solal7 where 15 minutes was the optimal incubation time (B). Error bars estimated as the standard deviation of three replicates

Moreover, with the aim at decreasing the analysis time, the number of steps to be used into the magnetoimmunosensor was evaluated. In **Figure 20** were represented the amperometric responses for  $10 \mu\text{g mL}^{-1}$  of antigen when (i) a mixture of Sola I 7, cp-anti-solal7 and anti-solal7-HRP was incubated in a single step and only for 30 minutes, and in (ii) two steps – *i.e.* incubated with the target Sola I 7 30 minutes prior to the anti-solal7-HRP 30 minutes incubation. The inspection of the **Figure 20** shows that the one step (30 minutes) protocol was faster than the two steps (30 + 30 minutes). However, the obtained blank signal in the step 1 protocol was higher than the blank intensity obtained with two steps. As a result, the ratio S/B increases with the 2 step procedure and, therefore, the best amperometric response was obtained under these conditions – with a ratio S/B of 1.6. It is worth to mention that the current measured without Sola I 7 (blank signal) and adding the antigen and the anti-solal7-HRP at the same time proved to harmonize with non-specific bindings, thus increasing the amperometric response – as shown in the results in one step protocol. In the case of two steps, a lower probability of non-specific binding suited with the blocking buffer washing process after Sola I 7 target incubation procedure which increase the ratio S/B.



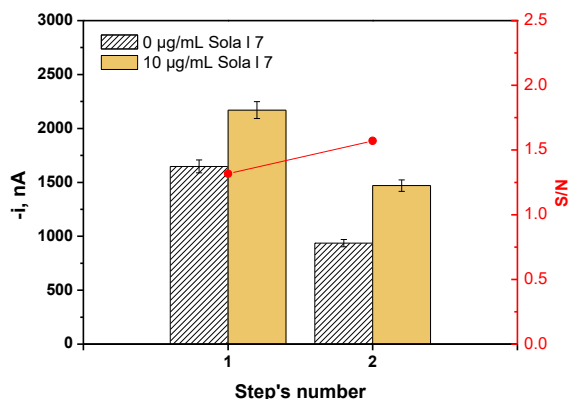


**Figure 19.** Amperometric responses obtained in the optimization of the number of steps. In the one step, the target ( $10 \mu\text{g mL}^{-1}$ ) and det-Ab-HRP (1/50) were incubated at the same time for 30 minutes, whereas in the two steps,  $10 \mu\text{g mL}^{-1}$  of Sola I 7 was incubated firstly in 30 minutes and then 1/50 of anti-solaI7-HRP 30 minutes. Error bars estimated as the standard deviation of three replicates.

Following the optimization of the number of experimental steps, anti-solaI7-HRP dilution and incubation time were also optimized and the results are shown in **Figure 21 A** and **B**, respectively. The dilution factors under investigation were 1:5, 1:10, 1:25, 1:50 and 1:100. The amperometric response was directly dependent with the anti-solaI7-HRP concentration. Examining the **Figure 21 A**, the dilution factor selected as optimum for anti-solaI7-HRP was of 1:50 (S/B of 2.3).. With respect to the incubation time, the best ratio S/B (2.3) and analytical response was obtained with a period of 30 minutes (**Figure 21 B**). It was observed that after 30 minutes of incubation, the ratio S/B (in the presence and absence of the target) decreased in response of non-specific binding sites and it is likely to be a consequence of a steric interference that hinders the antigen-antibody complex.

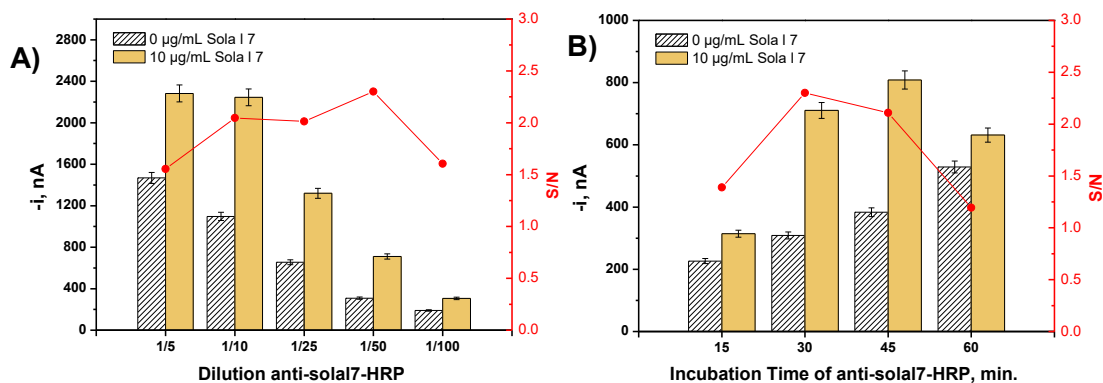


**Figure 20.** Amperometric response obtained in the optimization of the det-Ab-HRP dilutions where 1:50 was the optimal concentration (A) and incubation time of the det-Ab-HRP where 30 minutes was the optimal incubation time (B). Error bars estimated as the standard deviation of three replicates.

The incubation time used in the antigen and antibody reaction is also a relevant variable to qualify the final performance of the magnetoimmunosensor. The obtained results proved to be possible to detect  $10 \mu\text{g mL}^{-1}$  of sola I 7 in only 60 min of reaction, once the HOOC-MBs has been modified with cp-anti-solal7 and blocked with ethanolamine. Such feature confers a great analytical advantage in comparison with many alternative time-consuming techniques.

#### 4.4.1 Analytical characteristics of the immunosensor

Under optimized conditions, a calibration plot for sola I 7 was calculated (**Figure 22**). A linear correlation ( $r = 0.9976$ ) between the amperometric signal and the protein concentration of sola I 7 ranging from  $1 \mu\text{g mL}^{-1}$  and  $10 \mu\text{g mL}^{-1}$ , and with a slope and intercept values of  $81.0696 \pm 1.59 \text{ nA } (\mu\text{g mL}^{-1})^{-1}$  and  $295.3 \pm 4.06 \text{ nA}$ , respectively, were obtained. The LOD and LOQ were accordingly calculated following the **Equation 9** and **10**, respectively, where  $m$  is the slope of the linear calibration plot and  $s_b$  was estimated as the standard deviation of ten amperometric measurements obtained in the absence of target Sola I 7. The LOD and LOQ were  $1.4 \mu\text{g mL}^{-1}$  (which represent  $0.035 \mu\text{g}$  of sola I 7) and  $4.6 \mu\text{g mL}^{-1}$ , respectively.

$$3 \times s_b/m \quad (9)$$

$$10 \times s_b/m \quad (10)$$

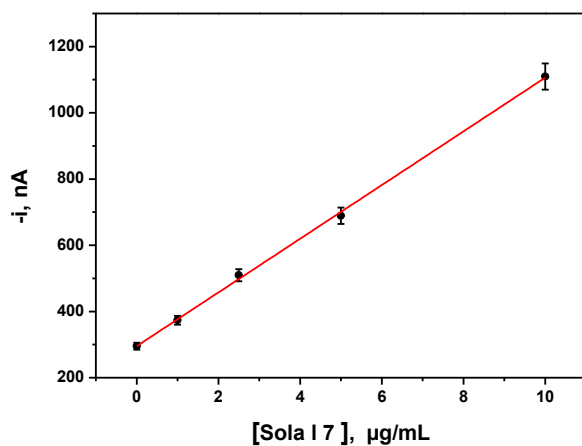


**Figure 21.** Calibration plot designed for sola I 7 (incubation of 25 µL in 0, 1, 2.5, 5 and 10 µg mL<sup>-1</sup> prepared in PBS, pH 7.5). Error bars estimated as the standard deviation of three replicates.

The reliability of the magnetoimmunosensor was evaluated by calculating the RSD for the amperometric current obtained at 5 µg mL<sup>-1</sup> of Sola I 7 with different magnetoimmunosensors (n = 7) developed under the same experimental conditions achieving a good reliability of the modification process in the MBs and amperometric measurement with 3.58 % of RSD.

The lifetime of the modified MBs was evaluated by storing at 4 °C in filtered PBS the cp-anti-solaI7 immobilized on MBs. In **Figure 23** is given the control graph obtained with the respective upper and lower limits – estimated according to the criteria  $\pm 3s$  (9), where  $s$  corresponds to the standard deviation of the average value obtained from 7 measurements.

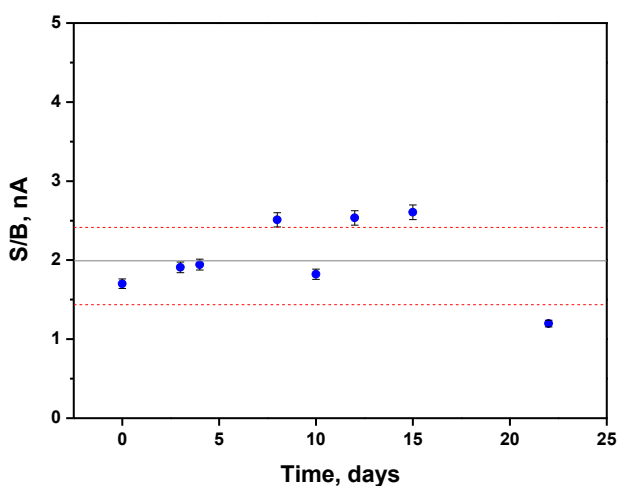


**Figure 22.** Control graph to stability evaluation of cp-anti-solaI7-MBs stored at 4 °C in 50  $\mu$ L of filtrated PBS. Values of amperometric current of signal to blank ratio are represented to 5  $\mu$ g mL<sup>-1</sup> of sola I 7 standard. Error bars estimated as the standard deviation of three replicates.

Observing the **Figure 23**, on could conclude that the cp-anti-solaI7-MBs can be employed for sola I 7 determination as far as 20 days from the day of preparation.

Aiming at evaluating the selectivity of the magnetoimmunosensor amperometric responses, a set of proteins, known as fruit allergens, were tested and compared. All the proteins studied had an association with Sola I 7, namely they all belong to the lipid transfer proteins family but Sina 1 – which is an 2s albumin. Sola I 3 and Sola I 6 are found in tomato seed, Prup 3 presents a similar protein structure to Sola I 7 and can be found in peach. Moreover, Sina 3 can be found in mustard.

The results obtained are presented in the **Figure 24** and shows that it is possible to demonstrate an excellent selective determination of Sola I 7. Such feature represents a huge advantage for the future development of multi-detection platforms. Furthermore, this high selectivity can be attributed to the use of sandwich format with two antibodies with high affinity for Sola I 7.

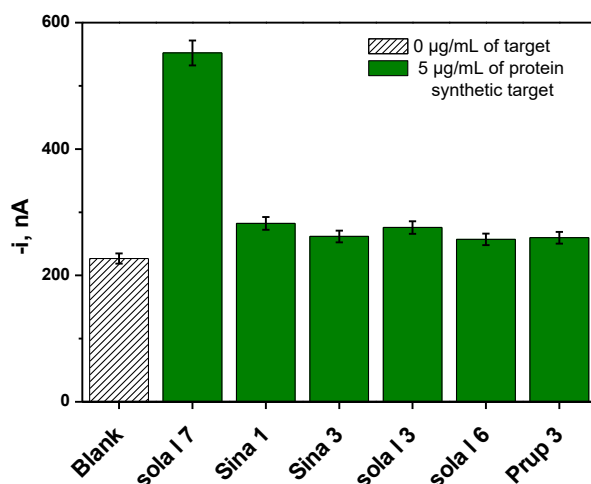


**Figure 23.** Selectivity of the magnetoimmunosensor for sola I 7 detection. Amperometric current values achieved to standards of 5 µl mL<sup>-1</sup> Sola I 7, Sina 1, Sina 3, Sola I 3, Sola I 6, Prup 3. Error bars estimated as the standard deviation of three replicates

#### 4.4.2 Application of immunosensor to detect Sola I 7 in tomato seeds samples

The developed amperometric magnetoimmunosensor was applied in the detection of Sola I 7 in lysed samples of tomato seeds in addition to other fruits containing distinct unknown content of endogenous Sola I 7, as well as in spiked target protein-free samples. For Sola I 7 concentration in the sample extract of tomato seed was obtained by the interpolation of the amperometric current of the sample in the calibration curve of Sola I 7 standard. In a sample of tomato seeds (9000 µg mL<sup>-1</sup>) diluted 1:5000 times (0.05 µg of the lysed sample), it was found 2,37 µg mL<sup>-1</sup> of Sola I 7 protein. The **Figure 25** shows the amperometric currents of all the extracted samples at 25 µg of lysed material in PBS, pH 7.5. These results can be compared with the amperometric response of Sola I 7 standard which the current intensity it is logically similar to the sample of tomato seeds.

Furthermore, the electrochemical current obtained with a sample extract from tomato peel was 2.8 times lower than those obtained from the seeds. As reported by Martín-Pedraza (2016) [31], such behavior was expected because the tomato peel contains very small amounts of Sola I 7.

The samples extracted from apple, mustard seeds, sunflower seeds, corn, peanut, hazelnut and peach – used as negative controls – were also subject to the same protocol and

evaluated with the magnetoimmunosensor. As established in **Figure 25**, the obtained analytical current was smaller than the blank signal, thus confirming the selectivity of the analytical methodology. In the case of corn and hazelnut, the currents were quite higher than the blank—which can be explained by possible sample contaminations or non-specific links.

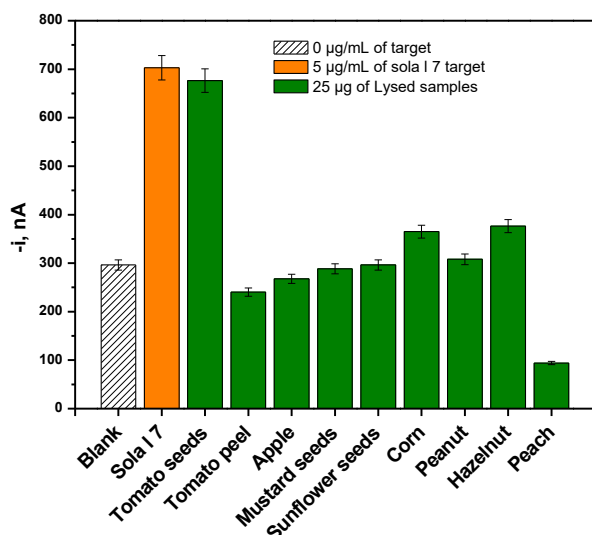


**Figure 24.** Amperometric responses of 9 extracted samples (green) and the Sola I 7 standard (orange). Error bars estimated as the standard deviation of three replicates.

#### 4.5 Dual magnetobiosensor for simultaneous determination of Sola I 7 protein and *sola I 7* DNA

After the successful development of the magnetogenosensor (**Chapter 3**) and the magnetoimmunosensor for Sola I 7 determination, it was proposed the possibility to detect both biomolecules simultaneously in a screen-printed carbon electrode with two working electrodes (SPdCEs). The main aim was to provide a more complete tool of analysis and an accurate determination with the implementation of two types of MBs, *viz.* the HOOC-MBs and Strep-MBs.

One of the foremost potential limitations to take into account when designing electrochemical multidetection platforms is the possible diffusion of the electroactive indicator to the adjacent electrodes, which would lead to inaccurate results [161]. This research effort is intended to show the possibility to evaluate the existence of cross-talking between Sola I 7 protein

and *sola* / 7 DNA mixtures, by measuring the presence/absence of the target molecule in each working electrode (WE). For that purpose, it was considered for SPdCEs with the WE1 and WE2 in 4 different mixtures as can be depicted in **Figure 26**.

The experimental procedure was similar to those described in **Chapter 3** and **Chapter 4** for both displays until the step of transduction of the electrochemical signal. After MBs bearing, the HRP-labelling in the immunocomplex and in the DNA-complex were magnetically captured on the corresponding working electrode (WE1 and WE2) (**Figure 26**).

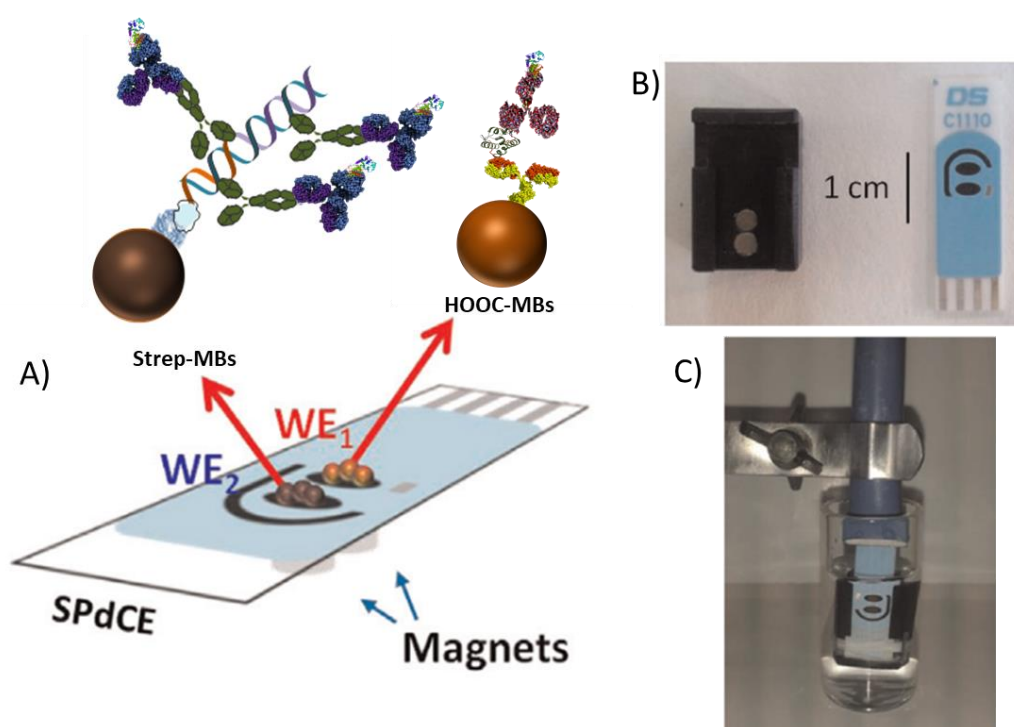


**Figure 25.** Schematic display of the disposable dual magnetobiosensor for the simultaneous determination of *Sola* I7 protein and *sola* / 7 DNA **A**); picture showing the SPdCE and the homemade magnet holding block **B**) and the modified MBs on the SPdCE assembled on the magnet holding block and in the specific cable connector emerged in the electrochemical cell **C**). Relative sizes of the components are not drawn on real scale [162]

The amperometric detection was carried out using the catalytic current of -0.20 V produced by  $H_2O_2$  in the redox reaction using HQ as mediator. As previously mentioned, the use of MBs as immobilization platform makes all the affinity reactions occur on their surface. In this sense, SPdCEs are only used as electrochemical transducer – thus minimizing unspecific adsorptions of the bioreagents on the electrode surfaces and simplifying largely the entire methodology. **Figure 27** shows the amperometric measurements obtained with the dual magnetobiosensor in solutions

containing different Sola I 7 protein and *sola* / 7 DNA mixtures. Accordingly, no significant cross reaction was observed, taking into account the positive S/B value obtained when the mixtures 1 with 2 and 3 with 4 are compared. It must be emphasized that the amperometric signals between 1 and 2 to 3 and 4 decreased approximately from 2.2 to 2.0 S/B in the WE2, and increase 1.36 to 1.7 S/B in the WE1. Nevertheless, such behavior does not represent a major problem for simultaneous detection of Sola I 7 protein and *sola* / 7 DNA sequence. From above, on could conclude that the magnetobiosensor responses endorsed the viability of the dual magnetosensor for the suitable simultaneous determination of both analytes.

**Table 9.** Mixtures containing the immunoassay and the genoassay for Sola I 7 protein and *sola* / 7 DNA simultaneous determination.

Mixtures	[Sola I 7 protein], $\mu\text{g mL}^{-1}$	[ <i>sola</i> / 7 DNA], nM
<b>1</b>	0	0
<b>2</b>	25	0.01
<b>3</b>	0	0.01
<b>4</b>	25	0

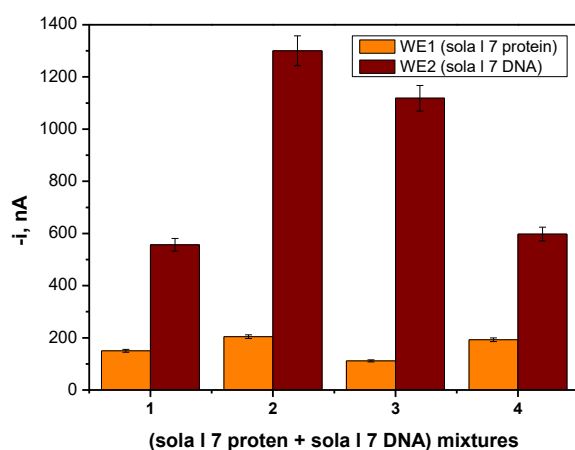


**Figure 26.** Simultaneous amperometric responses measured with the dual magnetobiosensor for mixtures containing different concentrations of Sola I 7 protein and the *sola* / 7 DNA represented in the **Table 9**.  $E_{app} = -0.20$  V vs. Ag pseudo-reference electrode. Error bars were calculated as the standard deviation of three replicates.



## 4.6 Conclusions

The results have proved that the developed magnetoimmunosensor can be applied in the determination of Sola I 7 (a fruit allergen) in real food matrixes with a minimum treatment of the sample (a simple dilution in the pH control solution) and in a overall analysis time of *ca.* 60 minutes, once the cp-anti-solaI7-MBs is prepared. Moreover, the method demonstrated to have high sensitivity. Furthermore, the experimental protocol can be simplified and shortened by carrying out a single incubation stage with the complete immunoreactives. In addition, the use of disposable biosensors allows the integration of the developed methodology in portable and multiplexed systems, which would be of a great advantage for the final implementation in food safety systems.

This research effort provides a novel disposable amperometric magnetobiosensor for the simultaneous determination of two allergens of different nature – namely the *sola* / 7DNA sequence and the Sola I 7 protein. The dual amperometric magnetobiosensor has demonstrated excellent analytical performance for tomato seeds allergen.

## **5 General conclusions and future prospective**

This chapter draws the main conclusions of this master's thesis. In addition, some general recommendations for further research efforts in this field are also presented. Detailed conclusions were given in each specific chapter.

### **5.1 General conclusions**

Attending to the main aim of this master's thesis, two formats of a new electrochemical DNA-based sensor – immunosensor and a dual immuno-DNA-sensor for tomato seeds allergen – have been developed and successfully applied in food samples. The implementation of the developed electrochemical biosensors involved different functionalized MBs as immobilization platforms and SPCEs as transducers.

The research work involved the development of two novel formats for *sola / 7* DNA sequence detection. These DNA magnetobiosensors combined the specific sandwich hybridization format DNA-RNA heteroduplex with the recognition element anti-DNA-RNA. The methodology of labelling was also performed by employing an innovative approach, *viz.* by using protA-HRP and antiIgG-HRP labels in the first and second format, respectively. The first implementation of amperometric magnetoimmunosensor by sandwich assay configurations was also a new approach for *sola / 7* determination.

The developed methodologies can be applied to the analysis of real food samples without laborious pre-treatments (only a simple dilution) and achieving high levels of sensitivity and selectivity. The short analysis time required, the simplicity of the involved experimental procedures, and the easy automation and miniaturization of the employed instrumentation made from the developed electrochemical bioplatfoms promising and attractive analytical tools for the development of user-friendly portable devices for onsite analysis, and with potential important impacts in food quality and control.

### **5.2 Future prospective**

Despite all the scientific work in this area and the results obtained, further research is still needed. As a continuation of the work developed within the scope of this master's thesis it is suggested:

- Incubation time of Sola I 7 in the magnetoimmunosensor assay to increase the sensitivity of the platform;
- Comparison of the sensitivity of these methodologies with conventional methodologies such as ELISA an PCR;
- Calibration curves and analytical characteristics for the dual magnetobiosensor, as well as selectivity studies and application in food samples, so as to complete the methodology; and, finally
- Evaluation of the possibility to increase the sensitivity of the electrochemical biosensors using selected nanomaterials.

## 6 References

- [1] V. R. V. Montiel *et al.*, "Amperometric determination of hazelnut traces by means of Express PCR coupled to magnetic beads assembled on disposable DNA sensing scaffolds," *Sensors Actuators, B Chem.*, vol. 245, pp. 895–902, 2017.
- [2] R. C. Alves, M. F. Barroso, M. B. González-García, M. B. P. P. Oliveira, and C. Delerue-Matos, "New Trends in Food Allergens Detection: Toward Biosensing Strategies," *Crit. Rev. Food Sci. Nutr.*, vol. 56, no. 14, pp. 2304–2319, 2016.
- [3] U. S. Guide *et al.*, *E a Aci Molecular Allergology*. 2016.
- [4] M. Słowianek and I. Majak, "Methods of allergen detection based on DNA analysis," *Biotechnol. Food Sci.*, vol. 75, no. 2, pp. 39–44, 2011.
- [5] C. Kokkinos, A. Economou, and M. I. Prodromidis, "Electrochemical immunosensors: Critical survey of different architectures and transduction strategies," *TrAC - Trends Anal. Chem.*, vol. 79, pp. 88–105, 2016.
- [6] S. Hassan, H. Eissa, and J. Mauzeroll, "Electrochemical Biosensors for Foodborne Contaminants Based on Aptamers and Graphene Materials," 2015.
- [7] S. L. Taylor, "Food allergies and sensitivities.," *J. Am. Diet. Assoc.*, vol. 86, no. 5, pp. 599–600, 1986.
- [8] B. Martín-Fernández, C. L. Manzanares-Palenzuela, M. Sánchez-Paniagua López, N. de-los-Santos-Álvarez, and B. López-Ruiz, "Electrochemical genosensors in food safety assessment," *Crit. Rev. Food Sci. Nutr.*, vol. 57, no. 13, pp. 2758–2774, 2017.
- [9] G. Evtugyn, *Biosensors : Essentials*. 2014.
- [10] M. Rubab, H. M. Shahbaz, A. N. Olaimat, and D.-H. Oh, "Biosensors for rapid and sensitive detection of *Staphylococcus aureus* in food," *Biosens. Bioelectron.*, Jan. 2018.
- [11] J. A. Bird, "Food Allergy Point of Care Pearls," *Immunol. Allergy Clin. North Am.*, vol. 38, no. 2, pp. e1–e8, 2018.
- [12] G. D'Amato *et al.*, "Meteorological conditions, climate change, new emerging factors, and asthma and related allergic disorders. A statement of the World Allergy Organization," *World Allergy Organ. J.*, vol. 8, no. 1, pp. 1–52, 2015.
- [13] G. Du Toit, H. A. Sampson, M. Plaut, A. W. Burks, C. A. Akdis, and G. Lack, "Food allergy: Update on prevention and tolerance," *J. Allergy Clin. Immunol.*, vol. 141, no. 1, pp. 30–40, 2018.
- [14] Y. Shahali and M. Dadar, "Plant food allergy: Influence of chemicals on plant allergens," *Food Chem. Toxicol.*, vol. 115, no. January, pp. 365–374, 2018.
- [15] A. Winberg, C. E. West, Å. Strinnholm, L. Nordström, L. Hedman, and E. Rönmark, "Assessment of allergy to milk, egg, cod, and wheat in Swedish schoolchildren: A population based cohort study," *PLoS One*, vol. 10, no. 7, pp. 1–9, 2015.
- [16] F. S. Agency, E. U. F. Information, C. Regulation, E. U. Fic, and F. I. Regulations, "Questions and Answers on the EU Food Information for Consumers Regulation allergen provisions," pp. 1–20, 2014.
- [17] "Top Allergies Around The World." [Online]. Available: <https://allertrain.com/top-allergies-around-world/>. [Accessed: 06-Jun-2018].
- [18] M. Martens, H. J. Schnoor, H.-J. Malling, and L. K. Poulsen, "Sensitization to cereals and peanut evidenced by skin prick test and specific IgE in food-tolerant, grass pollen allergic patients.," *Clin. Transl. Allergy*, vol. 1, no. 1, p. 15, Dec. 2011.
- [19] J. Aubard, I. De Topologie, and D. Dynamique, "Food Allergy," *Elsevier Saunders*, 2012.
- [20] B. Wüthrich, J. Stäger, and S. G. Johansson, "Celery allergy associated with birch and mugwort pollinosis.," *Allergy*, vol. 45, no. 8, pp. 566–71, Nov. 1990.

- [21] R. Asero *et al.*, "Epidemiology: Features of food allergy in Italian adults attending allergy clinics: A multi-centre study," *Clin. Exp. Allergy*, vol. 39, no. 4, pp. 547–555, 2009.
- [22] R. Asero, M. Piantanida, E. Pinter, and V. Pravettoni, "The clinical relevance of lipid transfer protein," *Clin. Exp. Allergy*, pp. 6–12, 2017.
- [23] E. I. Finkina, D. N. Melnikova, I. V. Bogdanov, and T. V. Ovchinnikova, "Lipid transfer proteins as components of the plant innate immune system: Structure, functions, and applications," *Acta Naturae*, vol. 8, no. 2, pp. 47–61, 2016.
- [24] T. H. Yeats and J. K. Rose, "The biochemistry and biology of extracellular plant lipid-transfer proteins (LTPs)," *Protein Sci*, vol. 17, no. 2, pp. 191–198, 2008.
- [25] I. Giangrieco *et al.*, "Structural features, IgE binding and preliminary clinical findings of the 7 kDa Lipid Transfer Protein from tomato seeds," *Mol. Immunol.*, vol. 66, no. 2, pp. 154–163, Aug. 2015.
- [26] G. Salcedo, R. Sanchez-Monge, A. Diaz-Perales, G. Garcia-Casado, and D. Barber, "Plant non-specific lipid transfer proteins as food and pollen allergens," *Clin. Exp. Allergy*, vol. 34, no. 9, pp. 1336–1341, 2004.
- [27] A. Diaz-Perales *et al.*, "Lipid-transfer proteins as potential plant panallergens: Cross-reactivity among proteins of Artemisia pollen, Castanea nut and Rosaceae fruits, with different IgE-binding capacities," *Clin. Exp. Allergy*, vol. 30, no. 10, pp. 1403–1410, 2000.
- [28] C. M. Kronfel, H. Cheng, B. K. Hurlburt, R. J. Simon, and S. J. Maleki, "Epitope Mapping for the Non-Specific Lipid Transfer Proteins (nsLTP) Among Peanut Allergic Patients," *J. Allergy Clin. Immunol.*, vol. 141, no. 2, p. AB239, Feb. 2018.
- [29] A. Palacin, J. Bartra, R. Muñoz, A. Diaz-Perales, A. Valero, and G. Salcedo, "Anaphylaxis to wheat flour-derived foodstuffs and the lipid transfer protein syndrome: a potential role of wheat lipid transfer protein Tri a 14.," *Int. Arch. Allergy Immunol.*, vol. 152, no. 2, pp. 178–83, 2010.
- [30] V. Pravettoni *et al.*, "Tomato allergy: Detection of IgE-binding lipid transfer proteins in tomato derivatives and in fresh tomato peel, pulp, and seeds," *J. Agric. Food Chem.*, vol. 57, no. 22, pp. 10749–10754, 2009.
- [31] L. Martín-Pedraza *et al.*, "Two nonspecific lipid transfer proteins (nsLTPs) from tomato seeds are associated to severe symptoms of tomato-allergic patients," *Mol. Nutr. Food Res.*, vol. 60, no. 5, pp. 1172–1182, 2016.
- [32] R. Y. Yada, *Proteins in Food Processing*. Elsevier, 2018.
- [33] K. O. Ivens, J. L. Baumert, R. L. Hutkins, and S. L. Taylor, "Effect of proteolysis during Cheddar cheese aging on the detection of milk protein residues by ELISA," *J. Dairy Sci.*, vol. 100, no. 3, pp. 1629–1639, Mar. 2017.
- [34] J. Costa, P. Ansari, I. Mafra, M. B. P. P. Oliveira, and S. Baumgartner, "Development of a sandwich ELISA-type system for the detection and quantification of hazelnut in model chocolates," *Food Chem.*, vol. 173, pp. 257–265, Apr. 2015.
- [35] M. Montserrat *et al.*, "Detection of peanut (*Arachis hypogaea*) allergens in processed foods by immunoassay: Influence of selected target protein and ELISA format applied," *Food Control*, vol. 54, pp. 300–307, Aug. 2015.
- [36] M. Besler, H. Steinhart, and A. Paschke, "Stability of food allergens and allergenicity of processed foods," *J. Chromatogr. B Biomed. Sci. Appl.*, vol. 756, no. 1–2, pp. 207–228, May 2001.
- [37] L. Monaci and A. Visconti, "Immunochemical and DNA-based methods in food allergen analysis and quality assurance perspectives," *Trends Food Sci. Technol.*, vol. 21, no. 6, pp. 272–283, Jun. 2010.
- [38] "Evaluation of Allergenicity of Genetically Modified Foods Report of a Joint FAO/WHO Expert Consultation on Allergenicity of Foods Derived from Biotechnology."
- [39] M. Hayes, P. Rougé, A. Barre, C. Herouet-Guichenev, and E. L. Roggen, "In silico tools for exploring potential human allergy to proteins," *Drug Discov. Today Dis. Model.*, vol. 17–18, pp. 3–11, Dec. 2015.
- [40] A. Hulanicki, S. Glab, and F. Ingman, "Chemical sensors: definitions and classification," *Pure Appl. Chem.*, vol. 63, no. 9, pp. 1247–1250, Jan. 1991.

- [41] E. Simon, "Biological and chemical sensors for cancer diagnosis," *Meas. Sci. Technol.*, vol. 21, no. 11, p. 112002, Nov. 2010.
- [42] Y.-H. P. Hsieh, "Immunoassays," Springer, Boston, MA, 2010, pp. 301–316.
- [43] M. Kumar, "Biosensore and medicine," no. September 2014, 2016.
- [44] P. Skládal, "Piezoelectric biosensors," *TrAC Trends Anal. Chem.*, vol. 79, pp. 127–133, May 2016.
- [45] K. Mosbach, "Thermal biosensors," *Biosens. Bioelectron.*, vol. 6, no. 3, pp. 179–182, Jan. 1991.
- [46] V. Nabaei, R. Chandrawati, and H. Heidari, "Magnetic biosensors: Modelling and simulation," *Biosens. Bioelectron.*, vol. 103, pp. 69–86, Apr. 2018.
- [47] P. Damborský, J. Švitel, and J. Katrlík, "Optical biosensors.," *Essays Biochem.*, vol. 60, no. 1, pp. 91–100, 2016.
- [48] D. R. Thévenot, K. Toth, R. A. Durst, and G. S. Wilson, "Electrochemical biosensors: Recommended definitions and classification," *Biosens. Bioelectron.*, vol. 16, no. 1–2, pp. 121–131, 2001.
- [49] H. A. Abdulbari and E. A. M. Basheer, "Electrochemical Biosensors: Electrode Development, Materials, Design, and Fabrication," *ChemBioEng Rev.*, vol. 4, no. 2, pp. 92–105, Apr. 2017.
- [50] H. Törer, E. B. Aydın, and M. K. Sezgintürk, "A label-free electrochemical biosensor for direct detection of RACK 1 by using disposable, low-cost and reproducible ITO based electrode," *Anal. Chim. Acta*, vol. 1024, pp. 65–72, Sep. 2018.
- [51] A. K. M. Kafi, M. Naqshabandi, M. M. Yusoff, and M. J. Crossley, "Improved peroxide biosensor based on Horseradish Peroxidase/Carbon Nanotube on a thiol-modified gold electrode," *Enzyme Microb. Technol.*, vol. 113, pp. 67–74, Jun. 2018.
- [52] F. Pittino, P. Palestri, P. Scarbolo, D. Esseni, and L. Selmi, "Models for the use of commercial TCAD in the analysis of silicon-based integrated biosensors," *Solid. State. Electron.*, vol. 98, pp. 63–69, Aug. 2014.
- [53] G. Yammouri, J. Mandli, H. Mohammadi, and A. Amine, "Development of an electrochemical label-free biosensor for microRNA-125a detection using pencil graphite electrode modified with different carbon nanomaterials," *J. Electroanal. Chem.*, vol. 806, pp. 75–81, Dec. 2017.
- [54] T. B. Goriushkina *et al.*, "Amperometric biosensor based on glycerol oxidase for glycerol determination," *Sensors Actuators B Chem.*, vol. 144, no. 2, pp. 361–367, Feb. 2010.
- [55] M. Willander, A. Tahira, and Z. H. Ibupoto, "Potentiometric Biosensors Based on Metal Oxide Nanostructures," in *Reference Module in Chemistry, Molecular Sciences and Chemical Engineering*, Elsevier, 2017, pp. 444–450.
- [56] O. O. Soldatkin *et al.*, "Conductometric enzyme biosensor for patulin determination," *Sensors Actuators B Chem.*, vol. 239, pp. 1010–1015, Feb. 2017.
- [57] S. Xie, Y. Tang, D. Tang, and Y. Cai, "Highly sensitive impedimetric biosensor for Hg<sup>2+</sup> detection based on manganese porphyrin-decorated DNA network for precipitation polymerization," *Anal. Chim. Acta*, vol. 1023, pp. 22–28, Sep. 2018.
- [58] A. Poghosian *et al.*, "Field-effect biosensor using virus particles as scaffolds for enzyme immobilization," *Biosens. Bioelectron.*, vol. 110, pp. 168–174, Jul. 2018.
- [59] M. Sánchez-Paniagua López, E. Redondo-Gómez, and B. López-Ruiz, "Electrochemical enzyme biosensors based on calcium phosphate materials for tyramine detection in food samples," *Talanta*, vol. 175, pp. 209–216, Dec. 2017.
- [60] V. Ruiz-Valdepeñas Montiel *et al.*, "Electrochemical detection of peanuts at trace levels in foods using a magnetoimmunosensor for the allergenic protein Ara h 2," *Sensors Actuators, B Chem.*, vol. 236, pp. 825–833, 2016.
- [61] P. Pang *et al.*, "Ultrasensitive enzyme-free electrochemical immunosensor for microcystin-LR using molybdenum disulfide/gold nanoclusters nanocomposites as platform and Au@Pt core-shell nanoparticles as

- signal enhancer," *Sensors Actuators B Chem.*, vol. 266, pp. 400–407, 2018.
- [62] N. F. D. Silva, J. M. C. S. Magalhães, C. Freire, and C. Delerue-Matos, "Electrochemical biosensors for Salmonella: State of the art and challenges in food safety assessment," *Biosens. Bioelectron.*, vol. 99, no. August 2017, pp. 667–682, 2018.
- [63] J. M. Pingarrón Carrazón and P. Sánchez Batanero, *Química electroanalítica: fundamentos y aplicaciones*. Editorial Síntesis, 1999.
- [64] L. Tedeschi, C. Domenici, A. Ahluwalia, F. Baldini, and A. Mencaglia, "Antibody immobilisation on fibre optic TIRF sensors," *Biosens. Bioelectron.*, vol. 19, no. 2, pp. 85–93, Nov. 2003.
- [65] A. Sassolas, L. J. Blum, and B. D. Leca-Bouvier, "Immobilization strategies to develop enzymatic biosensors," *Biotechnol. Adv.*, vol. 30, no. 3, pp. 489–511, 2012.
- [66] C. Bonnet, S. Andreescu, and J.-L. Marty, "Adsorption: an easy and efficient immobilisation of acetylcholinesterase on screen-printed electrodes," *Anal. Chim. Acta*, vol. 481, no. 2, pp. 209–211, Apr. 2003.
- [67] H. Shi *et al.*, "Amperometric choline biosensors prepared by layer-by-layer deposition of choline oxidase on the Prussian blue-modified platinum electrode," *Talanta*, vol. 70, no. 4, pp. 852–858, Nov. 2006.
- [68] J. Zhang, D. Shan, and S. Mu, "Improvement in selectivity and storage stability of a choline biosensor fabricated from poly(aniline-co-o-aminophenol)," *Front. Biosci.*, vol. 12, pp. 783–90, Jan. 2007.
- [69] A. P. Girard-Egrot, S. Godoy, and L. J. Blum, "Enzyme association with lipidic Langmuir–Blodgett films: Interests and applications in nanobioscience," *Adv. Colloid Interface Sci.*, vol. 116, no. 1–3, pp. 205–225, Nov. 2005.
- [70] P. Salazar, ... M. M.-P. science: research, and U. 2016, "Polydopamine-modified surfaces in biosensor applications," *researchgate.net*, 2016.
- [71] N. C. and P. V. Kamat\*, "Improving the Photoelectrochemical Performance of Nanostructured TiO<sub>2</sub> Films by Adsorption of Gold Nanoparticles†," 2000.
- [72] Y. CHEN, J. WANG, and Z.-M. LIU, "Graphene and Its Derivative-based Biosensing Systems," *Chinese J. Anal. Chem.*, vol. 40, no. 11, pp. 1772–1779, Nov. 2012.
- [73] X. Sun *et al.*, "An Amperometric Immunosensor Based on Multi-Walled Carbon Nanotubes-Thionine-Chitosan Nanocomposite Film for Chlorpyrifos Detection," *Sensors*, vol. 12, no. 12, pp. 17247–17261, Dec. 2012.
- [74] L. Zhu, R. Yang, J. Zhai, and C. Tian, "Bienzymatic glucose biosensor based on co-immobilization of peroxidase and glucose oxidase on a carbon nanotubes electrode," *Biosens. Bioelectron.*, vol. 23, no. 4, pp. 528–535, Nov. 2007.
- [75] M. Hanko, N. Bruns, J. C. Tiller, and J. Heinze, "Optical biochemical sensor for determining hydroperoxides in nonpolar organic liquids as archetype for sensors consisting of amphiphilic conetworks as immobilisation matrices," *Anal. Bioanal. Chem.*, vol. 386, no. 5, pp. 1273–1283, Oct. 2006.
- [76] M. F. Desimone, S. B. Matiacevich, M. del P. Buera, and L. E. Díaz, "Effects of relative humidity on enzyme activity immobilized in sol–gel-derived silica nanocomposites," *Enzyme Microb. Technol.*, vol. 42, no. 7, pp. 583–588, Jun. 2008.
- [77] M. B. Fritzen-Garcia *et al.*, "Carbon paste electrode modified with pine kernel peroxidase immobilized on pegylated polyurethane nanoparticles," *Sensors Actuators B Chem.*, vol. 139, no. 2, pp. 570–575, Jun. 2009.
- [78] X. Yu, D. Chattopadhyay, I. Galeska, F. Papadimitrakopoulos, and J. F. Rusling, "Peroxidase activity of enzymes bound to the ends of single-wall carbon nanotube forest electrodes," *Electrochem. commun.*, vol. 5, no. 5, pp. 408–411, May 2003.
- [79] R. K. Mendes, R. F. Carvalhal, and L. T. Kubota, "Effects of different self-assembled monolayers on enzyme immobilization procedures in peroxidase-based biosensor development," *J. Electroanal. Chem.*, vol. 612, no. 2, pp. 164–172, Jan. 2008.

- [80] B. Esteban Fernández de Ávila, "Bioplataformas electroanalíticas para (multi)detección de marcadores, factores de virulencia y bacterias de relevancia clínica y alimentaria," 2014.
- [81] E. Zacco, M. . Pividori, X. Llopis, M. del Valle, and S. Alegret, "Renewable Protein A modified graphite-epoxy composite for electrochemical immunosensing," *J. Immunol. Methods*, vol. 286, no. 1–2, pp. 35–46, Mar. 2004.
- [82] J. D. Moore *et al.*, "Chemical and biological characterisation of a sensor surface for bioprocess monitoring," *Biosens. Bioelectron.*, vol. 26, no. 6, pp. 2940–2947, Feb. 2011.
- [83] L. Häußling, W. Knoll, H. Ringsdorf, F.-J. Schmitt, and J. Yang, "Surface functionalization and surface recognition: Plasmon optical detection of molecular recognition at self assembled monolayers," *Makromol. Chemie. Macromol. Symp.*, vol. 46, no. 1, pp. 145–155, Jun. 1991.
- [84] M. Hasanzadeh, N. Shadjou, and M. de la Guardia, "Non-invasive diagnosis of oral cancer: The role of electro-analytical methods and nanomaterials," *TrAC - Trends Anal. Chem.*, vol. 91, pp. 125–137, 2017.
- [85] E. Zacco, M. I. Pividori, S. Alegret, R. Galve, and M. P. Marco, "Electrochemical magnetoimmunosensing strategy for the detection of pesticides residues," *Anal. Chem.*, vol. 78, no. 6, pp. 1780–1788, 2006.
- [86] F. Lucarelli, G. Marrazza, A. P. . Turner, and M. Mascini, "Carbon and gold electrodes as electrochemical transducers for DNA hybridisation sensors," *Biosens. Bioelectron.*, vol. 19, no. 6, pp. 515–530, Jan. 2004.
- [87] E. Paleček and M. Fojta, "Magnetic beads as versatile tools for electrochemical DNA and protein biosensing," *Talanta*, vol. 74, no. 3, pp. 276–290, 2007.
- [88] S. Amaya-González, N. de-los-Santos-Álvarez, A. J. Miranda-Ordieres, and M. J. Lobo-Castañón, "Aptamer Binding to Celiac Disease-Triggering Hydrophobic Proteins: A Sensitive Gluten Detection Approach," *Anal. Chem.*, vol. 86, no. 5, pp. 2733–2739, Mar. 2014.
- [89] S. Trashin, M. de Jong, T. Breugelmans, S. Pilehvar, and K. De Wael, "Label-Free Impedance Aptasensor for Major Peanut Allergen Ara h 1," *Electroanalysis*, vol. 27, no. 1, pp. 32–37, Jan. 2015.
- [90] C. Ocaña, A. Hayat, R. K. Mishra, A. Vasilescu, M. del Valle, and J.-L. Marty, "Label free aptasensor for Lysozyme detection: A comparison of the analytical performance of two aptamers," *Bioelectrochemistry*, vol. 105, pp. 72–77, Oct. 2015.
- [91] V. Urbanova, M. Magro, A. Gedanken, D. Baratella, F. Vianello, and R. Zboril, "Nanocrystalline Iron Oxides, Composites, and Related Materials as a Platform for Electrochemical, Magnetic, and Chemical Biosensors," *Chem. Mater.*, vol. 26, no. 23, pp. 6653–6673, Dec. 2014.
- [92] V. R.-V. Montiel *et al.*, "Sensitive and selective magnetoimmunosensing platform for determination of the food allergen Ara h 1," *Anal. Chim. Acta*, vol. 880, pp. 52–59, Jun. 2015.
- [93] V. Ruiz-Valdepeñas Montiel *et al.*, "Electrochemical magnetoimmunosensing platform for determination of the milk allergen  $\beta$ -lactoglobulin," *Talanta*, vol. 131, pp. 156–162, Jan. 2015.
- [94] V. Ruiz-Valdepeñas Montiel, S. Campuzano, R. M. Torrente-Rodríguez, A. J. Reviejo, and J. M. Pingarrón, "Electrochemical magnetic beads-based immunosensing platform for the determination of  $\alpha$ -lactalbumin in milk," *Food Chem.*, vol. 213, pp. 595–601, Dec. 2016.
- [95] M. Čadková *et al.*, "Magnetic beads-based electrochemical immunosensor for monitoring allergenic food proteins," *Anal. Biochem.*, vol. 484, pp. 4–8, Sep. 2015.
- [96] J. P. Metters, R. O. Kadara, and C. E. Banks, "New directions in screen printed electroanalytical sensors: an overview of recent developments," *Analyst*, vol. 136, no. 6, p. 1067, Feb. 2011.
- [97] A. Hayat, S. Andreescu, and J.-L. Marty, "Design of PEG-aptamer two piece macromolecules as convenient and integrated sensing platform: Application to the label free detection of small size molecules," *Biosens. Bioelectron.*, vol. 45, pp. 168–173, Jul. 2013.
- [98] A. Hayat, W. Haider, M. Rolland, and J.-L. Marty, "Electrochemical grafting of long spacer arms of hexamethyldiamine on a screen printed carbon electrode surface: application in target induced ochratoxin A electrochemical aptasensor," *Analyst*, vol. 138, no. 10, p. 2951, May 2013.



- [99] X. Niu *et al.*, "Fabrication of graphene and gold nanoparticle modified acupuncture needle electrode and its application in rutin analysis," *Sensors Actuators B. Chem.*, 2017.
- [100] R. Huang, N. He, and Z. Li, "Recent progresses in DNA nanostructure-based biosensors for detection of tumor markers," *Biosens. Bioelectron.*, vol. 109, pp. 27–34, Jun. 2018.
- [101] S. M. Douglas, I. Bachelet, and G. M. Church, "A Logic-Gated Nanorobot for Targeted Transport of Molecular Payloads," *Science (80-. J.)*, vol. 335, no. 6070, pp. 831–834, Feb. 2012.
- [102] F. Kuralay, S. Campuzano, and J. Wang, "Greatly extended storage stability of electrochemical DNA biosensors using ternary thiolated self-assembled monolayers," *Talanta*, vol. 99, pp. 155–160, 2012.
- [103] A. Abi, M. Lin, H. Pei, C. Fan, E. E. Ferapontova, and X. Zuo, "Electrochemical switching with 3D DNA tetrahedral nanostructures self-assembled at gold electrodes," *ACS Appl. Mater. Interfaces*, vol. 6, no. 11, pp. 8928–8931, Jun. 2014.
- [104] R. P. Goodman, M. Heilemann, S. Doose, C. M. Erben, A. N. Kapanidis, and A. J. Turberfield, "Reconfigurable, braced, three-dimensional DNA nanostructures," *Nat. Nanotechnol.*, vol. 3, no. 2, pp. 93–96, Feb. 2008.
- [105] S. Dong *et al.*, "Electrochemical DNA Biosensor Based on a Tetrahedral Nanostructure Probe for the Detection of Avian Influenza A (H7N9) Virus," *ACS Appl. Mater. Interfaces*, vol. 7, no. 16, pp. 8834–8842, 2015.
- [106] D. Zeng *et al.*, "A novel ultrasensitive electrochemical DNA sensor based on double tetrahedral nanostructures," *Biosens. Bioelectron.*, vol. 71, pp. 434–438, 2015.
- [107] T. Hou, W. Li, X. Liu, and F. Li, "Label-Free and Enzyme-Free Homogeneous Electrochemical Biosensing Strategy Based on Hybridization Chain Reaction: A Facile, Sensitive, and Highly Specific MicroRNA Assay," *Anal. Chem.*, vol. 87, no. 22, pp. 11368–11374, 2015.
- [108] V. Ruiz-Valdepen *et al.*, "Disposable Amperometric Polymerase Chain Reaction-Free Biosensor for Direct Detection of Adulteration with Horsemeat in Raw Lysates Targeting Mitochondrial DNA," 2017.
- [109] S. Moura-Melo *et al.*, "Targeting Helicase-Dependent Amplification Products with an Electrochemical Genosensor for Reliable and Sensitive Screening of Genetically Modified Organisms," *Anal. Chem.*, vol. 87, no. 16, pp. 8547–8554, 2015.
- [110] Q. Pu *et al.*, "Universal ratiometric electrochemical biosensing platform based on mesoporous platinum nanocomposite and nicking endonuclease assisted DNA walking strategy," *Biosens. Bioelectron.*, vol. 94, pp. 719–727, Aug. 2017.
- [111] S. Campuzano, P. Yáñez-Sedeño, and J. M. Pingarrón, "Electrochemical genosensing of circulating biomarkers," *Sensors (Switzerland)*, vol. 17, no. 4, pp. 1–20, 2017.
- [112] Y. Wang *et al.*, "A colorimetric biosensor using Fe<sub>3</sub>O<sub>4</sub> nanoparticles for highly sensitive and selective detection of tetracyclines," *Sensors Actuators B Chem.*, vol. 236, pp. 621–626, Nov. 2016.
- [113] Y. Zhang *et al.*, "Ultrasensitive electrochemical biosensor for silver ion based on magnetic nanoparticles labeling with hybridization chain reaction amplification strategy," *Sensors Actuators, B Chem.*, vol. 249, pp. 431–438, 2017.
- [114] M. Bäcker *et al.*, "Tobacco mosaic virus as enzyme nanocarrier for electrochemical biosensors," *Sensors Actuators, B Chem.*, vol. 238, pp. 716–722, 2017.
- [115] M. Prado, I. Ortea, S. Vial, J. Rivas, P. Calo-Mata, and J. Barros-Velázquez, "Advanced DNA- and Protein-based Methods for the Detection and Investigation of Food Allergens," *Crit. Rev. Food Sci. Nutr.*, vol. 56, no. 15, pp. 2511–2542, 2016.
- [116] M. Paoloni and P. Sale, "or Co," no. March, 2015.
- [117] S. Barreda-García, R. Miranda-Castro, N. de-los-Santos-Álvarez, A. J. Miranda-Ordieres, and M. J. Lobo-Castañón, "Comparison of isothermal helicase-dependent amplification and PCR for the detection of Mycobacterium tuberculosis by an electrochemical genomagnetic assay," *Anal. Bioanal. Chem.*, vol. 408, no. 30, pp. 8603–8610, 2016.

- [118] M. R. Akanda, Y.-L. Choe, and H. Yang, "'Outer-Sphere to Inner-Sphere' Redox Cycling for Ultrasensitive Immunosensors," *Anal. Chem.*, vol. 84, no. 2, pp. 1049–1055, Jan. 2012.
- [119] H. Niu *et al.*, "Highly enhanced electrochemiluminescence based on synergetic catalysis effect of enzyme and Pd nanoparticles for ultrasensitive immunoassay," *Chem. Commun.*, vol. 47, no. 29, p. 8397, Jul. 2011.
- [120] O. Niwa, "Electroanalysis with interdigitated array microelectrodes," *Electroanalysis*, vol. 7, no. 7, pp. 606–613, Jul. 1995.
- [121] G. J. Tsongalis, "Branched DNA Technology in Molecular Diagnostics," *Am. J. Clin. Pathol.*, vol. 126, no. 3, pp. 448–453, Sep. 2006.
- [122] H. Yang, "Enzyme-based ultrasensitive electrochemical biosensors," *Curr. Opin. Chem. Biol.*, vol. 16, no. 3–4, pp. 422–428, Aug. 2012.
- [123] P. R. B. De Oliveira Marques *et al.*, "Double-tagging polymerase chain reaction with a thiolated primer and electrochemical genosensing based on gold nanocomposite sensor for food safety," *Anal. Chem.*, vol. 81, no. 4, pp. 1332–1339, 2009.
- [124] L. Wu *et al.*, "From Electrochemistry to Electroluminescence: Development and Application in a Ratiometric Aptasensor for Aflatoxin B1," *Anal. Chem.*, vol. 89, no. 14, pp. 7578–7585, 2017.
- [125] J. Liu, Q. Huang, X. Wang, Z. Li, and H. Chen, *Application of Quantum Dots in Electrochemical Biosensors*, vol. 22. 2010.
- [126] D. Martín-Yerga, P. Fanjul-Bolado, D. Hernández-Santos, and A. Costa-García, "Enhanced detection of quantum dots by the magnetohydrodynamic effect for electrochemical biosensing," *Analyst*, vol. 142, no. 9, pp. 1591–1600, 2017.
- [127] C. Kokkinos, M. Prodromidis, A. Economou, P. Petrou, and S. Kakabakos, "Quantum dot-based electrochemical DNA biosensor using a screen-printed graphite surface with embedded bismuth precursor," *Electrochem. commun.*, vol. 60, pp. 47–51, 2015.
- [128] Y. ping Wei, X. P. Liu, C. jie Mao, H. L. Niu, J. M. Song, and B. K. Jin, "Highly sensitive electrochemical biosensor for streptavidin detection based on CdSe quantum dots," *Biosens. Bioelectron.*, vol. 103, no. December 2017, pp. 99–103, 2018.
- [129] I. Navarro-González, J. García-Alonso, and M. J. Periago, "Bioactive compounds of tomato: Cancer chemopreventive effects and influence on the transcriptome in hepatocytes," *J. Funct. Foods*, vol. 42, pp. 271–280, Mar. 2018.
- [130] N. Bertin and M. Génard, "Tomato quality as influenced by preharvest factors," *Sci. Hortic. (Amsterdam)*, vol. 233, pp. 264–276, Mar. 2018.
- [131] M. Figueiredo-González, P. Valentão, D. M. Pereira, and P. B. Andrade, "Further insights on tomato plant: Cytotoxic and antioxidant activity of leaf extracts in human gastric cells," *Food Chem. Toxicol.*, vol. 109, pp. 386–392, Nov. 2017.
- [132] K. Kiyota, M. Yoshimitsu, T. Satsuki-Murakami, K. Akutsu, K. Kajimura, and T. Yamano, "Detection of the tomato allergen Sola I 1 and evaluation of its reactivity after heat and papain treatment," *Food Agric. Immunol.*, pp. 1–10, Jul. 2017.
- [133] C. H. Larramendi *et al.*, "Sensitization to tomato peel and pulp extracts in the Mediterranean Coast of Spain: prevalence and co-sensitization with aeroallergens," *Clin. Exp. Allergy*, vol. 0, no. 0, p. 071115150625002–???, Nov. 2007.
- [134] O. Y. Bäessler *et al.*, "Evidence for Novel Tomato Seed Allergens: IgE-Reactive Legumin and Vicilin Proteins Identified by Multidimensional Protein Fractionation–Mass Spectrometry and *in Silico* Epitope Modeling," *J. Proteome Res.*, vol. 8, no. 3, pp. 1111–1122, Mar. 2009.
- [135] M. Geroldinger-Simic *et al.*, "Birch pollen-related food allergy: clinical aspects and the role of allergen-specific IgE and IgG4 antibodies.," *J. Allergy Clin. Immunol.*, vol. 127, no. 3, p. 616–22.e1, Mar. 2011.
- [136] M. Piantanida *et al.*, "Tomato hypersensitivity in peach allergic patients: rPru p3 and rPru p1 positivity is

- predictive of the symptom severity," *Clin. Transl. Allergy*, vol. 1, no. Suppl 1, p. P77, Aug. 2011.
- [137] M. Á. López-Matas *et al.*, "Identification and quantification of tomato allergens: In vitro characterization of six different varieties," *Ann. Allergy, Asthma Immunol.*, vol. 106, no. 3, pp. 230–238, 2011.
- [138] J. Goodman, Richard E. , Davies, "ALLERGEN NOMENCLATURE." [Online]. Available: <http://www.allergen.org/index.php>.
- [139] I. Giangrieco *et al.*, "Structural features, IgE binding and preliminary clinical findings of the 7 kDa Lipid Transfer Protein from tomato seeds," *Mol. Immunol.*, vol. 66, no. 2, pp. 154–163, 2015.
- [140] V. Lollier, S. Denery-Papini, C. Brossard, and D. Tessier, "Meta-analysis of IgE-binding allergen epitopes.," *Clin. Immunol.*, vol. 153, no. 1, pp. 31–9, Jul. 2014.
- [141] A. Wangorsch *et al.*, "Identification of Sola I 4 as Bet v 1 homologous pathogenesis related-10 allergen in tomato fruits," *Mol. Nutr. Food Res.*, vol. 59, no. 3, pp. 582–592, Mar. 2015.
- [142] S. Welter *et al.*, "Pepino mosaic virus Infection of Tomato Affects Allergen Expression, but Not the Allergenic Potential of Fruits," *PLoS One*, vol. 8, no. 6, p. e65116, Jun. 2013.
- [143] M. Bencivenni *et al.*, "Electrospray MS and MALDI imaging show that non-specific lipid-transfer proteins (LTPs) in tomato are present as several isoforms and are concentrated in seeds," *J. Mass Spectrom.*, vol. 49, no. 12, pp. 1264–1271, Dec. 2014.
- [144] S. Santiago-Felipe, L. A. Tortajada-Genaro, R. Puchades, and A. Maquieira, "Recombinase polymerase and enzyme-linked immunosorbent assay as a DNA amplification-detection strategy for food analysis," *Anal. Chim. Acta*, vol. 811, pp. 81–87, Feb. 2014.
- [145] M. S.-P. López, G. F. Cabanillas, M. J. L. Castañón, and B. López-Ruiz, "Development of a genosensor for peanut allergen ARA h 2 detection and its optimization by surface response methodology," *Biosens. Bioelectron.*, vol. 62, pp. 350–356, Dec. 2014.
- [146] M. Volpicella, C. Leoni, I. Fanizza, S. Rinalducci, A. Placido, and L. R. Ceci, "Expression and characterization of a new isoform of the 9 kDa allergenic lipid transfer protein from tomato (variety San Marzano)," *Plant Physiol. Biochem.*, vol. 96, pp. 64–71, 2015.
- [147] A. Ghiani *et al.*, "Impact of Wild Loci on the Allergenic Potential of Cultivated Tomato Fruits," *PLoS One*, vol. 11, no. 5, p. e0155803, May 2016.
- [148] M. Freitas *et al.*, "Highly Monodisperse Fe<sub>3</sub>O<sub>4</sub>@Au Superparamagnetic Nanoparticles as Reproducible Platform for Genosensing Genetically Modified Organisms," *ACS Sensors*, vol. 1, no. 8, pp. 1044–1053, Aug. 2016.
- [149] B. Martín Fernández, C. L. Manzanares Palenzuela, M. Sánchez-Paniagua López, B. López-Ruiz, and G. Frutos Cabanillas, "Diseño de un genosensor electroquímico para la detección indirecta de gluten en alimentos," *An. la Real Acad. Nac. Farm.*, vol. 78, no. 3, pp. 323–343, 2012.
- [150] G.-X. Wang, W.-J. Bao, J. Wang, Q.-Q. Lu, and X.-H. Xia, "Immobilization and catalytic activity of horseradish peroxidase on molybdenum disulfide nanosheets modified electrode," *Electrochem. commun.*, vol. 35, pp. 146–148, Oct. 2013.
- [151] M. Zuker, "Mfold web server for nucleic acid folding and hybridization prediction.," *Nucleic Acids Res.*, vol. 31, no. 13, pp. 3406–15, Jul. 2003.
- [152] B. Rafique, M. Iqbal, T. Mehmood, and M. A. Shaheen, "Electrochemical DNA biosensors: a review," *Sens. Rev.*, p. SR-08-2017-0156, Apr. 2018.
- [153] "National Center for Biotechnology Information Search database." [Online]. Available: [www.ncbi.nlm.nih.gov/blast](http://www.ncbi.nlm.nih.gov/blast).
- [154] B. Xu, D. Zheng, W. Qiu, F. Gao, S. Jiang, and Q. Wang, "An ultrasensitive DNA biosensor based on covalent immobilization of probe DNA on fern leaf-like  $\alpha$ -Fe<sub>2</sub>O<sub>3</sub> and chitosan Hybrid film using terephthalaldehyde as arm-linker," *Biosens. Bioelectron.*, vol. 72, pp. 175–181, Oct. 2015.

- [155] A. Ulianas, L. Y. Heng, S. A. Hanifah, and T. L. Ling, "An Electrochemical DNA Microbiosensor Based on Succinimide-Modified Acrylic Microspheres," *Sensors*, vol. 12, no. 5, pp. 5445–5460, Apr. 2012.
- [156] U. Andjelković, M. Gavrović-Jankulović, T. Martinović, and D. Josić, "Omics methods as a tool for investigation of food allergies," *TrAC Trends Anal. Chem.*, vol. 96, pp. 107–115, Nov. 2017.
- [157] O. Hosu, G. Selvolini, and G. Marrazza, "Recent advances of immunosensors for detecting food allergens," *Curr. Opin. Electrochem.*, vol. 10, pp. 149–156, 2018.
- [158] R. C. Alves *et al.*, "Detection of the peanut allergen Ara h 6 in foodstuffs using a voltammetric biosensing approach," *Anal. Bioanal. Chem.*, vol. 407, no. 23, pp. 7157–7163, Sep. 2015.
- [159] M. Gamella, S. Campuzano, F. Conzuelo, A. J. Reviejo, and J. M. Pingarrón, "Amperometric Magnetoimmunosensors for Direct Determination of D-Dimer in Human Serum," *Electroanalysis*, vol. 24, no. 12, pp. 2235–2243, Dec. 2012.
- [160] B. Esteban-Fernández de Ávila *et al.*, "Ultrasensitive amperometric magnetoimmunosensor for human C-reactive protein quantification in serum," *Sensors Actuators B Chem.*, vol. 188, pp. 212–220, Nov. 2013.
- [161] V. Escamilla-Gómez, D. Hernández-Santos, M. B. González-García, J. M. Pingarrón-Carrazón, and A. Costa-García, "Simultaneous detection of free and total prostate specific antigen on a screen-printed electrochemical dual sensor," *Biosens. Bioelectron.*, vol. 24, no. 8, pp. 2678–2683, Apr. 2009.
- [162] R. M. Torrente-Rodríguez, S. Campuzano, V. Ruiz-Valdepeñas Montiel, M. Gamella, and J. M. Pingarrón, "Electrochemical bioplatfoms for the simultaneous determination of interleukin (IL)-8 mRNA and IL-8 protein oral cancer biomarkers in raw saliva," *Biosens. Bioelectron.*, vol. 77, pp. 543–548, 2016.